From loose grains to resilient dunes

van IJzendoorn, Christa

DOI
10.4233/uuid:2297978b-30e2-48e4-9e6a-e2fb61dcab94

Publication date
2023

Document Version
Final published version

Citation (APA)
van IJzendoorn, C. (2023). *From loose grains to resilient dunes*. [Dissertation (TU Delft), Delft University of Technology]. https://doi.org/10.4233/uuid:2297978b-30e2-48e4-9e6a-e2fb61dcab94

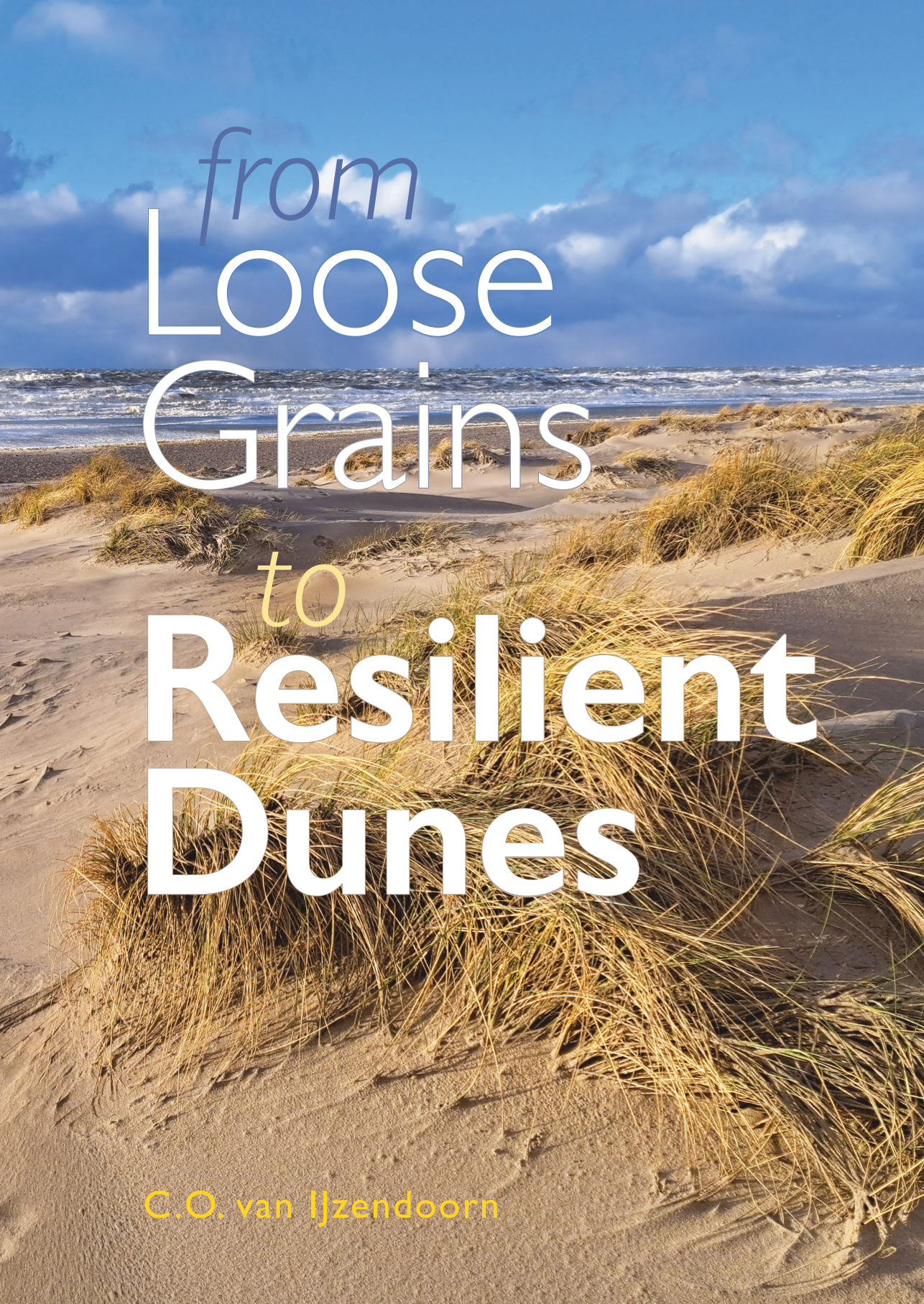
from
Loose
Grains
to
Resilient
Dunes
C.O. van IJzendoorn

From loose grains to resilient dunes

Christa Ottie van IJzendoorn

Author: Christa van IJzendoorn

Book design by the author
Cover design by Christien van IJzendoorn, www.carrotent.com
Figures by the author
Printed by Ridderprint, www.ridderprint.nl

Keywords: coastal dunes, sea level rise, aeolian sediment transport, grain size

PhD thesis Delft University of Technology
ISBN 978-94-6366-695-4
An electronic version of this dissertation is available at:
https://repository.tudelft.nl/.

From loose grains to resilient dunes

Dissertation

for the purpose of obtaining the degree of doctor
at Delft University of Technology,
by the authority of the Rector Magnificus, Prof. dr. ir. T.H.J.J. van der Hagen,
Chair of the Board for Doctorates,
to be defended publicly on
Thursday 22 June 2023 at 15:00 o'clock

by

Christa Ottie VAN IJZENDOORN

Master of Science in Earth Sciences, Utrecht University, the Netherlands
born in 's-Hertogenbosch, the Netherlands

This dissertation has been approved by the promotors.

Composition of the doctoral committee:

Rector Magnificus,	Chairperson
Prof. dr. ir. A.J.H.M. Reniers,	Delft University of Technology, promotor
Dr. ir. S. de Vries,	Delft University of Technology, promotor
Dr. ir. E.C. Hallin,	Delft University of Technology & Lund University, Sweden, co-promotor
Independent members:	
Prof. dr. C.A. Katsman	Delft University of Technology
Prof. dr. G.B. Ruessink	Utrecht University
Prof. dr. I. Delgado-Fernandez	University of Cádiz, Spain
Prof. dr. L.J. Moore	University of North Carolina at Chapel Hill, United States
Reserve member:	
Prof. dr. ir. S.G.J. Aarninkhof	Delft University of Technology

TU Delft Delft University of Technology

NWO

This research is part of the research programme DuneForce with project number 17064 which was (partly) financed by the Dutch Research Council (NWO).

Sand, so much sand, there is sand everywhere
In my hands, in my pants, in my eyes, in my car,
They might need to re-nourish the beaches.

The Author

Contents

Summary

Coastal dune systems provide valuable functions that are threatened by human activity and climate change. Preserving and strengthening coastal dunes through coastal management and the implementation of interventions requires accurate predictions of coastal dune development. The development of coastal dunes is driven by complex interactions between aeolian (wind-driven) and marine processes. The aim of this thesis is to determine how marine and aeolian processes influence coastal dune development on a yearly to decadal scale. Specifically, the effect of sea level rise and aeolian processes related to grain size were addressed.

The effect of sea level rise on coastal dune development was studied by investigating the decadal development of the dune toe. Analysis of coastal profiles showed that the dune toe elevation increases 7-8 times faster than the rate of sea level rise along the Dutch coast (Chapter 3). This indicates that the dune development along the Dutch coast is dominated by other factors than sea level rise on the yearly to decadal time scale. The accompanying Jarkus Analysis Toolbox allows practitioners and students to analyze the Dutch long-term coastal dataset.

Dune growth is caused by aeolian sediment transport, which can be affected by supply-limiting factors such as grain size. To investigate grain size variations in the intertidal area, field measurements were collected with a newly developed sediment sampling device, the sand scraper (Chapter 4). The measurements showed that the largest temporal changes in grain size occurred due to marine processes, and that the bed composition in the intertidal area is heterogenous in both the horizontal and vertical dimension.

The recorded spatial grain size variations inspired grain size scenarios that were created to determine to what extent grain size variations impact aeolian sediment transport. The grain size scenarios were implemented in the aeolian sediment transport model AeoLiS (Chapter 5). Simulations showed that the median grain size can often be used as a representative grain size on time scales of days to years. They also showed that vertical grain size variations are only relevant on a minute time scale, whereas grain size variations in the horizontal dimension have considerable impacts on time scales from minutes to years. Based on the relevance of the bed surface grain size in the upwind part of the domain, it was recommended to include the grain size present in this region in aeolian sediment transport models.

The Adapted Burland Triangle, which can guide the development and application of modeling in the coastal research and engineering field, was presented and applied (Chapter 2). The different research approaches in this dissertation were connected within the framework, and it was used for the identification and prioritization of missing links and knowledge gaps (Chapter 6). The framework contributes to clarifying the purpose of research and engineering projects, and is expected to advance the coastal

research and engineering field as a whole.

In summary, new insights on the impact of sea level rise and aeolian processes related to grain size were presented. The investigation of these processes resulted in a wide range of new research methods that are and will be used beyond the scope of this dissertation. The recommendations on the implementation of grain size will affect future aeolian sediment transport modeling. Additionally, several pathways were presented to improve models and their applicability. Through model application and further research, valuable knowledge and recommendations will be gathered that can help coastal communities to balance the different functions of the coastal dune system.

Samenvatting

Kustduinen bieden waardevolle functies die worden bedreigd door menselijke activiteit en klimaatverandering. Het behouden en versterken van kustduinen door beheer en het uitvoeren van ingrepen, vereist nauwkeurige voorspellingen van kustduinontwikkeling. De ontwikkeling van kustduinen wordt aangedreven door complexe interacties tussen eolische (windgedreven) en mariene processen. Het doel van dit proefschrift is om te bepalen hoe mariene en eolische processen de ontwikkeling van kustduinen op de schaal van jaren en decennia beïnvloeden. Specifiek, werden het effect van zeespiegelstijging en van eolische processen gerelateerd aan korrelgrootte behandeld.

Het effect van zeespiegelstijging op de ontwikkeling van kustduinen werd bestudeerd door de ontwikkeling van de duinvoet te onderzoeken op de schaal van decennia. Analyse van kustprofielen toonde aan dat de hoogte van de duinvoet 7-8 keer sneller toeneemt dan de zeespiegel stijgt langs de Nederlandse kust (Hoofdstuk 3). Dit wijst erop dat de duinontwikkeling langs de Nederlandse kust wordt gedomineerd door andere factoren dan zeespiegelstijging op de schaal van jaren tot decennia. De bijbehorende Jarkus Analyse Toolbox stelt praktijkbeoefenaars en studenten in staat om de Nederlandse, lange termijn kustdataset te analyseren.

Duingroei wordt veroorzaakt door eolisch sedimenttransport. Dit transport kan worden beïnvloed door factoren, zoals korrelgrootte, die de aanvoer van sediment kunnen beperken. Om variaties in de korrelgrootte in het intergetijdengebied te onderzoeken, werden veldmetingen gedaan met een nieuw ontwikkeld apparaat voor sedimentbemonstering, de zandschraper (Hoofdstuk 4). De metingen toonden aan dat de grootste veranderingen in korrelgrootte door de tijd optreden als gevolg van mariene processen. Ook toonden ze aan dat de bodemsamenstelling in het intergetijdengebied heterogeen is in zowel horizontale als verticale dimensie.

De gemeten ruimtelijke variaties in korrelgrootte inspireerden tot korrelgroottescenario's die werden gemaakt om te bepalen in welke mate variaties in korrelgrootte het transport van eolisch sediment beïnvloeden. De korrelgroottescenario's zijn geïmplementeerd in het eolische sedimenttransportmodel AeoLiS (Hoofdstuk 5). Simulaties lieten zien dat op tijdschalen van dagen tot jaren de mediane korrelgrootte vaak gebruikt kan worden als representatieve korrelgrootte. Ze toonden ook aan dat variaties in verticale korrelgrootte alleen relevant zijn op een tijdschaal van minuten, terwijl variaties in korrelgrootte in de horizontale dimensie een aanzienlijke impact hebben op tijdschalen van minuten tot jaren. De korrelgrootte van het bodemoppervlak in het bovenwindse deel van het domein is zeer relevant. Daarom werd aanbevolen om de korrelgrootte die aanwezig is in dit gebied op te nemen in modellen voor eolisch sedimenttransport.

De Aangepast Burland Driehoek, die de ontwikkeling en toepassing van modellering op het gebied van kustonderzoek en -waterbouw kan sturen, werd gepresenteerd en toegepast (Hoofdstuk 2). De verschillende onderzoeksbenaderingen in dit proefschrift

werden binnen het raamwerk met elkaar verbonden en het werd gebruikt voor het identificeren en prioriteren van ontbrekende schakels en kennisleemtes (Hoofdstuk 6). Het raamwerk draagt bij aan het verhelderen van het doel van onderzoeks- en ingenieursprojecten en zal naar verwachting het veld van kustonderzoeks en- waterbouw als geheel vooruit helpen.

Samenvattend werden nieuwe inzichten over de impact van zeespiegelstijging en eolische processen met betrekking tot korrelgrootte gepresenteerd. Het onderzoek naar deze processen resulteerde in een breed scala aan nieuwe onderzoeksmethoden die ook buiten de context van dit proefschrift (zullen) worden gebruikt. De aanbevelingen over de implementatie van korrelgrootte zullen van invloed zijn op toekomstige modellering van eolisch sedimenttransport. Daarnaast werden verschillende aanpakken gepresenteerd om modellen en hun toepasbaarheid te verbeteren. Door toepassing van modellen en verder onderzoek zullen waardevolle kennis en aanbevelingen worden verzameld die kustgemeenschappen kunnen helpen om de verschillende functies van kustduinen te balanceren.

Preface

Studying sediment transport on the coast can be fascinating and challenging. In sediment transport, time scales and spatial scales are intertwined. For example, within seconds, a small sand grain can be picked up by the wind and carried over the beach. The movement of a single sand grain seems unimportant, but over years and decades, many sand grains can build up and form a coastal dune. This larger scale is relevant for humans, as we want to know whether coastal dunes will be able to protect us against flooding during our lifetime. However, investigating the resilience of dunes can be reliant on the understanding of relevant smaller scale processes. Finding the balance between detail and the big picture is a continuous adventure when studying sediment transport. By reading this dissertation, I invite you to join the journey through time and spatial scales that I have gone through in the past four years; from minutes to decades, and from loose grains to resilient dunes.

Christa van IJzendoorn

It's an earthquake, it's a hard wind
It's a record breakin' tide and it is rollin' in
It's a big sea, but it can't touch you and me
It's just a water view
and what a view

Brandi Carlile

1

Introduction

1

1.1. Coastal dunes under pressure

The coastal dune system has large societal importance due to the multitude of functions it provides (Everard et al., 2010; Martínez et al., 2008). Coastal dunes have an ecological function because they provide habitat for unique and protected species (e.g., Everard et al., 2010; Van Der Meulen & Udo De Haes, 1996). Beaches and dunes fulfill a recreational function as they are popular destinations for vacation and are intensively used as leisure zones (e.g., De Ruyck et al., 1997; Sytnik & Stecchi, 2015). Additionally, coastal dunes often provide a flood protection function by preventing low-lying hinterlands being flooded by the sea (e.g., Coch & Wolff, 1992).

Accommodating the different functions of the coastal dune system can be challenging, as they can have negative effects on each other. For instance, recreation is associated with urban development (Figure 1.1) (Nordstrom et al., 2000; Poppema et al., 2021), vehicle traffic and trampling (Schlacher et al., 2016). These activities can result in the destruction of vegetation and deterioration of coastal dunes (Biel et al., 2017; Delgado-Fernandez, O'Keeffe, & Davidson-Arnott, 2019). Consequently, recreation can negatively affect the ecological and flood defense function of the coastal dunes. Similarly, coastal stabilization for flood protection with invasive vegetation species can result in reduced biodiversity. Thus, management geared towards flood protection can negatively affect the ecological function of the dunes. In turn, protection of the ecological function of coastal dunes might require the enforcement of beach or dune closures that affect the recreational function (Melvin et al., 1991).

The functions provided by the coastal dune system are threatened by growing human activity and climate change (Nordstrom et al., 2000; Defeo et al., 2009). Urbanization and tourism in the coastal zone increase due to population growth and increased wealth, exacerbating their deteriorating impact on dunes (Nordstrom et al., 2000). Additionally, sea level rise (Katsman et al., 2011; Slangen et al., 2014) and changes in wave climate (Semedo et al., 2012) resulting from climate change can increase the erosive effects of marine processes (Ranasinghe, 2016; Hemer et al., 2013). This can lead to beach and dune erosion, reducing the size of the coastal dune system, and reducing the space available for habitat, flood protection and recreation (Figure 1.1). This process is known as coastal squeeze (Pontee, 2013).

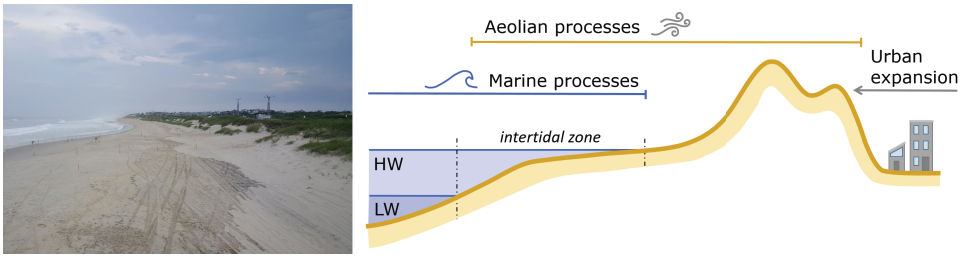

Figure 1.1: On the left, coastal dunes near Duck, North Carolina, USA. On the right, the overlap between marine and aeolian processes in the intertidal zone. The high water (HW) and low water (LW) line indicate the upper and lower boundary of the intertidal zone. Urban development and expansion on the landward side of the coastal dunes puts pressure on the coastal system.

To provide space for the different coastal dune functions, nature-based solutions are implemented that preserve and strengthen the coastal zone (e.g., de Vriend et al., 2015; Slinger et al., 2021). Coastal dunes are increasingly being discussed as a long-term building with nature approach in coastal management and engineering projects (Martínez et al., 2013; Delgado-Fernandez, Davidson-Arnott, & Hesp, 2019). For example, notches are dug in foredunes to encourage sediment flux to the back dunes and enhance the flood safety function and biodiversity (Ruessink et al., 2018; Delgado-Fernandez, Davidson-Arnott, & Hesp, 2019). Furthermore, artificial dunes are created (Kroon et al., 2022) and dune fields are restored (Rozé & Lemauviel, 2004; Kurtböke et al., 2007; Darke et al., 2016; Pickart et al., 2021) to increase flood safety as well as space for recreation and ecology. However, the development and the related effectiveness of these relatively new measures is uncertain due to the complexity of the sediment transport processes that determine the evolution of the coastal dune system on a yearly to decadal time scale.

Therefore, coastal management, as well as design and implementation strategies, need accurate predictions of coastal dune development on a yearly to decadal time scale. These predictions can provide insight into the expected pressures in the coastal zone, and determine locations where measures might be necessary. Additionally, the predictions can be used to determine the most efficient implementation of measures, and provide information about their future development. Eventually, the insights into coastal dune development gained from the predictions can result in improved long term planning and decision making, allowing for multi-function use of the coastal zone in the future.

1.2. Predicting coastal dune development

1.2.1. Multi-scale aeolian and marine processes

Coastal dune development is driven by a complex interplay of marine and aeolian processes (Figure 1.1 and 1.2). In the marine zone, sediment transport is driven by waves, tides, swash and storm surges, which shape the shoreface, beach and dunes (e.g. Wright & Short, 1984). Additionally, the process of sea level rise affects sediment transport that occurs along the coast (Cazenave & Cozannet, 2014; Reeves et al., 2021). In the aeolian part of the coastal zone, sediment transport is forced by the wind (e.g. Bagnold, 1937b; Bauer et al., 2009; Delgado-Fernandez, 2011) and bed properties like grain size soil moisture and shells affect how much sediment is available for transport by the wind.

Sediment transport can have both accretive and erosive effects on coastal dune development (Figure 1.2). The wind can initiate aeolian sediment transport that supplies sediment towards the dunes, resulting in dune growth (de Vries et al., 2012). Marine processes can cause dune erosion (e.g., Vellinga, 1982) but they can also result in marine accretion (Cohn et al., 2018). This marine accretion can promote aeolian sediment transport as it provides sediment that is available to be picked up by the wind. Additionally, alongshore sediment transport is a marine sediment transport process caused by wave-driven currents that can result in both erosion and accretion (Van Rijn, 2014; Hallin, Almström, et al., 2019).

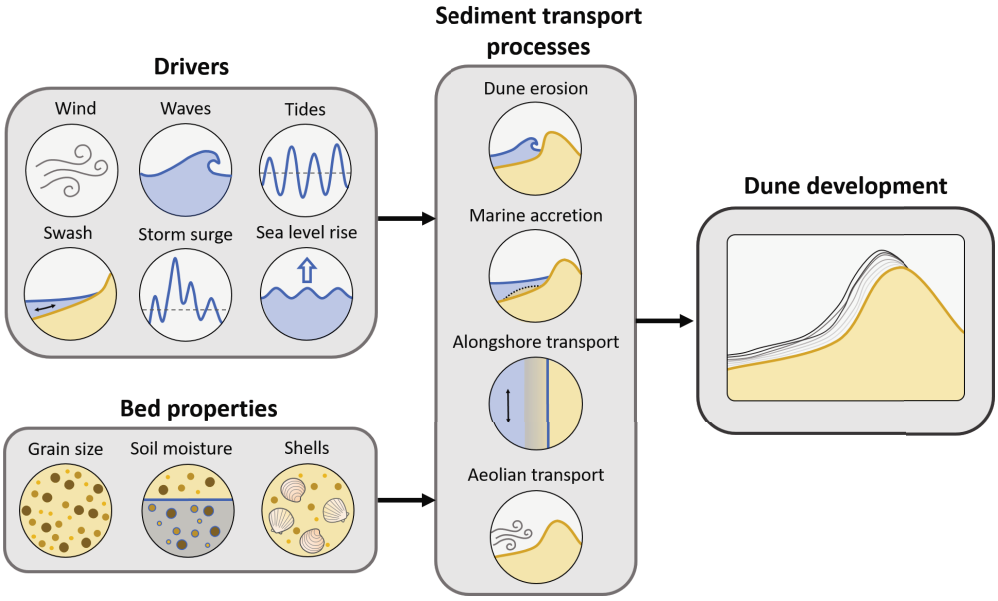

Figure 1.2: Physical drivers and bed properties determine sediment transport that impacts coastal dune development.

The sediment transport processes that affect dune development on a yearly to decadal scale are caused by drivers that act across temporal and spatial scales (Figure 1.3, left pane). For example, sea level rise occurs over decades to centuries, which affects the water level across the world and translates into local water level variations (Katsman et al., 2011; Slangen et al., 2014; Carson et al., 2016). Wind variations occur at shorter time scales (from seconds to minutes) and can show variations due to turbulence (Baas, 2006; Wiggs & Weaver, 2012), topographic steering (Walker et al., 2006; de Winter et al., 2020) and weather systems (Beaucage et al., 2007; Li & Hong, 2015), which cover millimeters to kilometers.

The temporal and spatial variations in the drivers, result in similar variations in the sediment transport processes (Figure 1.3, right pane). Erosion and accretion can occur as short, episodic bursts as well as gradual, long term changes. For instance, marine processes occurring during a storm event can cause considerable dune erosion within a few hours (e.g. Vellinga, 1982; W. Zhang et al., 2015; Splinter et al., 2018; Cohn, Ruggiero, et al., 2019). Similarly, weather events with strong winds can result in dune growth, although the transport volumes are usually lower than those of dune erosion (Castelle et al., 2017; Keijsers et al., 2014). The aggregated effect of the spatially and temporally varying sediment transport processes determines coastal dune development at a yearly to decadal scale (Hovenga et al., 2021). Namely, the net balance between erosion and accretion caused by marine and aeolian processes determines whether dune erosion or growth occurs on the long term (Houser et al., 2015; George et al., 2021). For example, while dune erosion events and aeolian sediment transport events

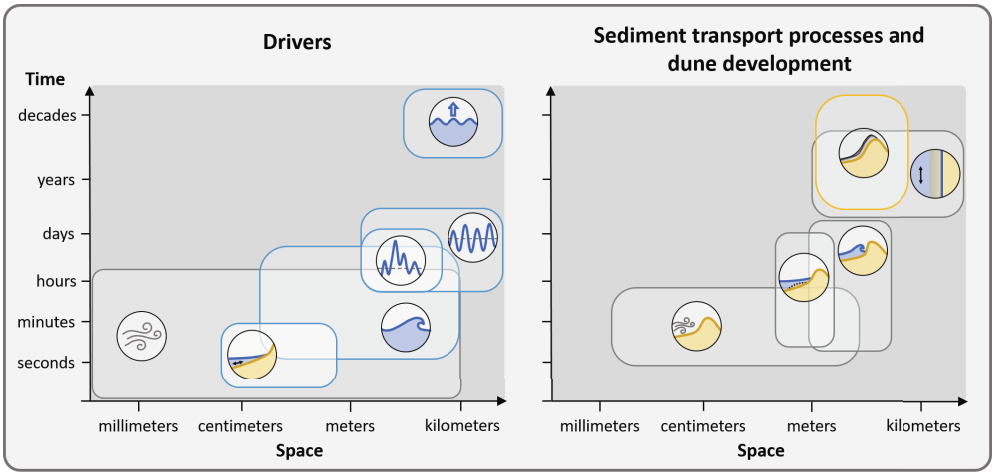

Figure 1.3: An indication of the temporal and spatial scales at which physical drivers, sediment transport processes and coastal dune development occur. Icons correspond to those in Figure 1.2. Adapted from De Vriend (1991).

take place along the Dutch coast (Keijsers et al., 2014), dune growth has been found to be a gradual process with a linear trend over several decades (de Vries et al., 2012).

The dune development trend over years to decades is the relevant time scale for coastal management. To predict coastal dune development at this time scale, an understanding of both the impact of marine processes and the impact of aeolian processes is needed. Since these processes act on a large range of time scales, from minutes to centuries, it is important to determine which processes are relevant for the yearly to decadal scale predictions of dune development. Specifically, short term processes that are relevant on the long term should be well-represented on the yearly to decadal scale. Similarly, long-term processes that affect the short term processes and can impact the overall development of coastal dunes should be taken into account. In this thesis, both short term processes and long term processes are discussed with the aim to integrate them to provide yearly to decadal dune development predictions.

This thesis focuses on the links between the aeolian and marine processes that affect the magnitude of aeolian sediment transport towards the dunes. Short term, erosive, marine processes are excluded because there is a range of tools available to predict their effect on the coastal zone (e.g., Kriebel & Dean, 1985; Roelvink et al., 2009). On the long term, aeolian sediment transport towards the dunes depends on sediment supply by marine processes (Houser, 2009). Despite the collection of long term dune development datasets, the effect of long term marine processes on sediment availability has been underexposed. In this thesis, the process of sea level rise, which affects sediment availability and morphology on a temporal scale of years to decades is investigated. Additionally, the prediction of aeolian sediment transport on a time scale of minutes to days remains underdeveloped (Barchyn et al., 2014), where a key factor for predicting aeolian sediment transport towards the dunes is sediment availability (de

Vries, Arens, et al., 2014).

Below, the effect of the long term marine process of sea level rise on the sediment availability for aeolian sediment transport is described. Subsequently, short term variations in sediment availability for aeolian transport are discussed, specifically, those caused by grain size.

1.2.2. Long-term marine processes: Sea level rise

The relevance of long term marine processes on yearly to decadal dune development depends on the effect they have on erosion and accretion. For example, numerous studies have investigated the coastline response to sea level rise (Ranasinghe et al., 2012; Vousdoukas et al., 2020), but it remains uncertain how sea level rise is impacting coastal dune development. With sea level rise, the vertical extent of marine processes is altered (Figure 1.4), which influences the sediment budget of sandy beaches. Most predictions of coastline change due to sea level rise are based on variations of the Bruun rule (Bruun, 1962). The Bruun Rule assumes that with rising sea level the beach is eroded and that the eroded sediment is moved to the offshore part of the coastal profile. This rule can be extended to coastal dunes, implying that coastal dunes are expected to erode as sea level rises (Rosati et al., 2013). However, coastal profile measurements have not yet been used to compare coastal dune development to sea level rise rates.

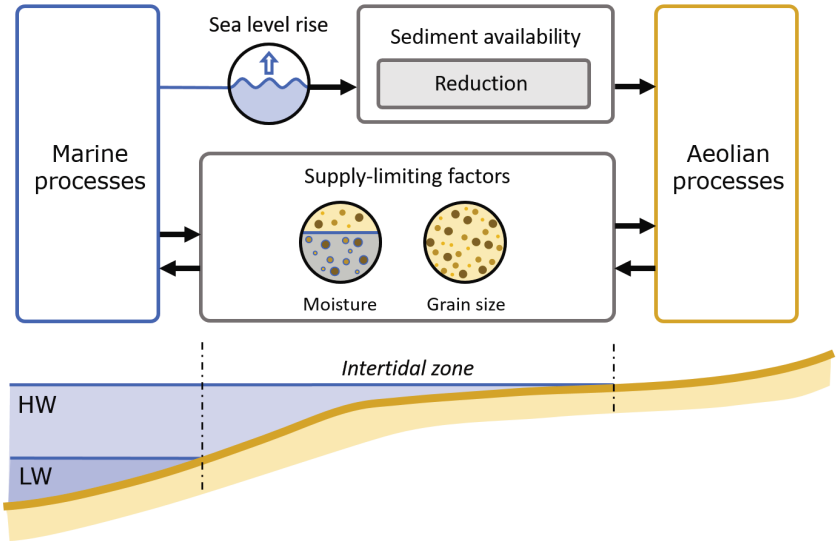

Figure 1.4: Long term marine processes like sea level rise can affect sediment availability for aeolian sediment transport. Supply-limiting factors like moisture content and grain vary in time and space, impact the marine and aeolian processes, and are impacted by the marine and aeolian processes.

1.2.3. Short-term aeolian processes: Supply-limited aeolian sediment transport

Predictions of aeolian sediment transport can deviate from measured sediment transport due to variations in sediment availability caused by supply-limiting factors, such as shells, moisture content, grain size and vegetation. Aeolian sediment transport towards the dunes can be calculated using Bagnold-type sediment transport equations where the transport has a cubic relation to the wind velocity (Bagnold, 1937b; Sherman & Li, 2012). However, these sediment transport equations do not fully take into account the various temporally and spatially varying supply-limiting factors that reduce the uptake of the sediment by the wind (Davidson-Arnott & Law, 1990). Thus, calculated aeolian sediment transport often overestimates measured sand deposition (Delgado-Fernandez, 2010).

Considerable variations in the supply-limiting factors occur in the intertidal zone, so considerable variations in sediment availability for aeolian transport can be expected in this zone. The intertidal zone, located between the mean low water and high water line, is intermittently exposed to aeolian and marine processes that impact the supply-limiting factors (Figure 1.4). In turn, the supply-limiting factors that occur in the intertidal area can directly impact aeolian sediment transport towards the dunes. For instance, de Vries, Arens, et al. (2014) showed an increase and decrease in tidal elevation (i.e. a marine process) resulting in varying moisture content (i.e. a supply-limiting factor) in the intertidal zone had a clear impact on the magnitude of aeolian sediment transport. Thus, variations in supply-limiting factors can result in variations in sediment availability and can affect aeolian transport.

Specifically, soil moisture and grain size are supply-limiting factors that are continuously altered in the intertidal zone (Figure 1.4). Both soil moisture and grain size are dynamic factors because they are intermittently affected by the marine and aeolian processes. Soil moisture content in the intertidal zone depends on tidal elevation and waves, which has been described by several studies (e.g., Brakenhoff et al., 2017). Waves and currents can move sediment underwater and affect the grain size present in the intertidal zone (Gallagher et al., 2016). Additionally, the removal and deposition of sediment by aeolian processes can impact the grain size present at the bed surface (Bagnold, 1937b; Bauer et al., 2009). This, combined with the fact that the soil moisture and grain size have a reciprocal effect on the marine and aeolian processes, demonstrates the complexity of the interactions in the intertidal zone.

1.2.4. Short-term aeolian processes: Grain size variability

Contrary to soil moisture dynamics, field data showing the grain size variability occurring in the intertidal zone are limited. Several studies have shown that beaches show a cross-shore gradient in grain size (e.g., Çelikoglu et al., 2006; Stauble & Cialone, 1997), often with a fining grain size in landward direction. Additionally, longshore variations can occur where adjacent stretches of coast show significant variations in grain size (Hallin, Almström, et al., 2019). In the vertical dimension, Gallagher et al. (2016) showed vertical variability on a centimeter to decimeter scale. Erosion of surface sediment layers may expose underlying layers and affect aeolian sediment transport. However, mm-scale, hourly variations in grain size in the intertidal zone have not yet been demonstrated with field data.

In aeolian sediment transport modeling, it is often assumed that only one grain size fraction is present on the beach and the grain size is spatially invariant (Hoonhout & de Vries, 2016; van der Wal, 2000b). On the contrary, measurements have shown that the sediment at the beach surface consists of a grain size distribution with many different grain sizes, and that this distribution varies spatially. The grain size distribution and the spatial grain size variability are expected to affect the aeolian sediment transport magnitude, as grain size alters the transport rate, threshold velocity, and bed roughness (Bagnold, 1937b). However, the extent to which the grain size distribution and the spatial variability impact the aeolian sediment transport magnitude have not yet been quantified.

1.2.5. Spatial and temporal integration of marine and aeolian processes in sediment transport modeling

Since both marine and aeolian processes can affect predictions of coastal dune development, these processes need to be integrated to get predictions on a yearly to decadal time scale. In sediment transport modeling, insights gained on marine and aeolian processes can be combined. Different marine sediment transport models (e.g., XBEACH by Roelvink et al., 2009) and aeolian sediment transport models are available (e.g., SAFE-HILL by Van Dijk et al., 1999, CDM by Durán & Moore, 2013, AeoLiS by Hoonhout & de Vries, 2016 and Duna by Roelvink & Costas, 2019). Recently, efforts have been made to couple marine, aeolian and ecological models into coupled-models like Windsurf to predict coastal dune development (Roelvink & Costas, 2019; Cohn, Hoonhout, et al., 2019; Itzkin et al., 2022). These sediment transport models and modeling frameworks provide the opportunity to implement and integrate the knowledge on short and long term processes. By including short-term and long-term sediment transport processes time scales can be aggregated. Additionally, drivers and sediment transport processes can be included or excluded based on their relevance on specific temporal and spatial scales that are addressed with each model and application. To promote their integration, the insights gained in this dissertation will be discussed within the context of their relevance for sediment transport modeling efforts.

In summary, data on grain size variability in the intertidal zone and its impact on aeolian sediment transport towards the dunes are needed to improve the understanding of short term aeolian sediment transport processes. Additionally, studying the effect of sea level rise is needed to increase understanding of its effect on coastal dune development. Coastal sediment transport models provide the opportunity to integrate these kinds of short and long term processes to work towards accurate coastal dune development predictions.

1.3. Research objectives

A thorough understanding is needed of both the impact of marine and aeolian processes on aeolian sediment transport towards the dunes. **The main aim of this thesis is to determine how marine and aeolian processes influence coastal dune development on a yearly to decadal scale.** At the end of this thesis, it is discussed how the gained knowledge on the marine and aeolian processes can be integrated in aeolian sediment transport modeling to work towards accurate coastal dune development predictions. Below, each research objective related to sea level rise and grain size variability is listed, including a short explanation of the approach.

1. Investigate the link between sea level rise and coastal dune development at a decadal scale

The effect of sea level rise has often been studied based on the Bruun Rule (Vitousek et al., 2017; Ranasinghe et al., 2012; Vousdoukas et al., 2020). Some studies investigate the effect of sea level rise based on historical field data (Hesp, 2013). In this thesis, the link between long term dune development and sea level rise is investigated. The Jarkus dataset is collected along 200+ km of the Dutch coast and consists of coastal transects measured yearly since 1965. This dataset provides the ability to study the decadal trends in dune development and comparing them to sea level rise rates along the Dutch coast.

2. Measure the extent of grain size variability due to marine and aeolian processes in the intertidal zone

The grain size present on the beach can be influenced by both marine (e.g., Gallagher et al., 2016) and aeolian (Bauer, 1991; van der Wal, 2000a) processes. In the intertidal zone, these effects can occur intermittently (de Vries, Arens, et al., 2014) on an hourly scale. To measure the variations caused by the marine and aeolian processes a new sand scraper sampling technique is presented. The measurements collected with the sand scraper can give insights into the range of detailed spatial variations in grain size that occur on the beach.

1

3. Determine the extent to which the grain size distribution and spatial grain size variability impact the aeolian sediment transport magnitude

A numerical modeling study is set up to test the effects of grain size variations on the aeolian sediment transport magnitude. Different scenarios with varying grain size distributions and spatial gradients are used as input to simulate aeolian sediment transport on time scales of minutes to years. These scenarios give new insights into the quantitative impact of grain size variations across temporal scales.

1.4. Outline

The content of each chapter and the relation between the different chapters is shown in Figure 1.5. Chapter 2 introduces the methods that are used to achieve the research objectives. Subsequently, each of the research objectives is addressed in an individual chapter. Chapter 3 (blue in Figure 1.5) investigates the relation between sea level rise and decadal dune development by analyzing the long term development of the dune toe as retrieved from a long term dataset containing measured coastal profiles of the Dutch coast. Together, Chapter 4 and 5 (yellow in Figure 1.5) focus on the short term aeolian processes related to grain size variability. Chapter 4 presents field measurements that show grain size variability due to marine and aeolian processes in the intertidal zone. Spatial gradients and the range in grain size variability, found in the measurements in Chapter 4, are used as inspiration for aeolian sediment transport simulations that are executed in Chapter 5. These aeolian sediment transport simulations are used to determine the quantitative impact of (spatial) grain size variations for aeolian sediment transport. Subsequently, Chapter 6 presents a synthesis of the findings presented in this dissertation. The conclusions and a perspective for future work are given in Chapter 7.

Chapters 3 and 4 are based on published journal articles. Chapter 5 is based on a submitted manuscript, and excerpts from a conference article were used as the basis for Chapter 1 and 6.

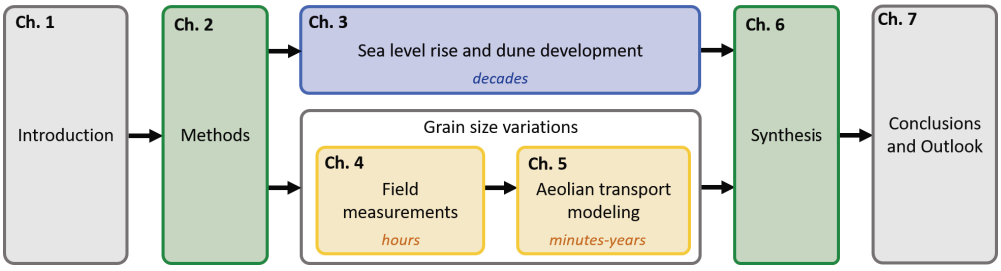

Figure 1.5: Schematization of the content of the chapters in this dissertation and their coherence

2

Methods

The research objectives of this dissertation (Section 1.3) were addressed with a wide range of research methods, including data-analysis of long-term coastal profile measurements (Section 2.1), field measurements (Section 2.2), and the use of a numerical model (Section 2.3). For all of these methods, new developments were made in the context of this dissertation. Here, these new methodologies are introduced. Also, a framework is presented (Section 2.4) that was used to discuss how new insights from this dissertation can be incorporated into modeling and the broader field of coastal research and engineering (Section 2.5).

2.1. Jarkus Analysis Toolbox

Along the Dutch coast, coastal profiles that are spaced about 250-500 m apart have been measured yearly since 1965. These profiles are collected in the Jarkus dataset which is one of the most elaborate coastal datasets in the world. For the analysis of the Dutch coastal profiles, the Python-based open-source Jarkus Analysis Toolbox (JAT) was developed. The main purpose of the JAT is to provide stakeholders (e.g. scientists, engineers and coastal managers) and students with the techniques to study the spatial and temporal variations in characteristic parameters like dune height, dune volume, dune toe, beach slope and closure depth. Different available definitions for extracting these characteristic parameters were collected and implemented in the JAT. In Chapter 3, the JAT is used for the extraction of the dune toe. The full documentation of the JAT is available on Read the docs (`https://jarkus-analysis-toolbox.readthedocs.io/en/latest/`) and the source code can be found on Github (`https://github.com/christavanijzendoorn/JAT`). Additionally, the extracted parameters for the entire Jarkus dataset were made available through the 4TU repository (`https://doi.org/10.4121/14514213.v1`).

2.2. Sand scraper

Field measurements to study spatial and temporal grain size variability on the beach were collected with a new sand scraper device that was specifically designed for this

purpose. In Chapter 4, the sand scraper is used to study grain size variations in the intertidal zone on the time scale of a tidal cycle. The device was inspired by a surface sediment sampler used for moisture content measurements by Wiggs et al. (2004). The sand scraper provides a detailed way of measuring the grain size variations at the bed surface. It was created to scrape smooth beach surfaces (e.g. the intertidal area) layer by layer to study vertical grain size variations at a resolution of 2 mm down to 50 mm depth. Documentation that allows the reproduction of the device was made available online. Designs, drawings, photos, and the manual of the device are available on the 4TU repository (https://doi.org/10.4121/17121269.v2).

2.3. AeoLiS

As a process-based model, AeoLiS can be used to study physical processes and simulate aeolian sediment transport on the scale of engineering applications (Hoonhout & de Vries, 2016, 2019). The model was developed to simulate aeolian sediment transport in supply-limited situations due to, for instance, soil moisture content and sediment sorting. Other important aspects like marine, vegetation and wind field dynamics are also (being) implemented in the model. In Chapter 5, AeoLiS is used to study the effect of grain size variations on aeolian sediment transport simulations. This approach requires the assignment of an initial bed composition that includes horizontal and vertical grain size variations to the model domain. Thus, the AeoLiS model was extended with the capability to input spatially varying grain sizes both in the horizontal and vertical dimension. The version of AeoLiS that includes this capability was made available on the 4TU repository (https://doi.org/10.4121/22215562).

2.4. The Adapted Burland Triangle (ABT)

To connect the different approaches in this dissertation, an adaptation of the Burland Triangle (ABT) is adopted (Figure 2.1). The Burland Triangle provides guidance on the utilization and the role of modeling in the field of geotechnical engineering (Burland, 1987). Here, the Burland Triangle is adapted for a coastal research and engineering context. Coastal research and engineering require an understanding of the physical properties of a coastal system, the definition of observed behavior, and the application of this knowledge through modeling. In the center, these three aspects are connected by experience (Barbour & Krahn, 2004). Experience is a broad term that includes knowledge, precedent and everything that has been learned, perceived, and discovered within the coastal science and engineering field; from the most detailed scientific study to a failed attempt at applying the first version of a model.

In a coastal context, the physical properties component of the Adapted Burland Triangle (ABT) can be defined as the characteristics of a coastal system that can be used as model input parameters. For instance, physical properties can be the average wave height, the median grain size, or the beach state (Wright & Short, 1984) of a coastal stretch. These characteristics can be recorded by exploration and description of a system. The observed behavior of the coastal system can be obtained by conducting observations, measurements and lab and field testing. For example, lab tests can show

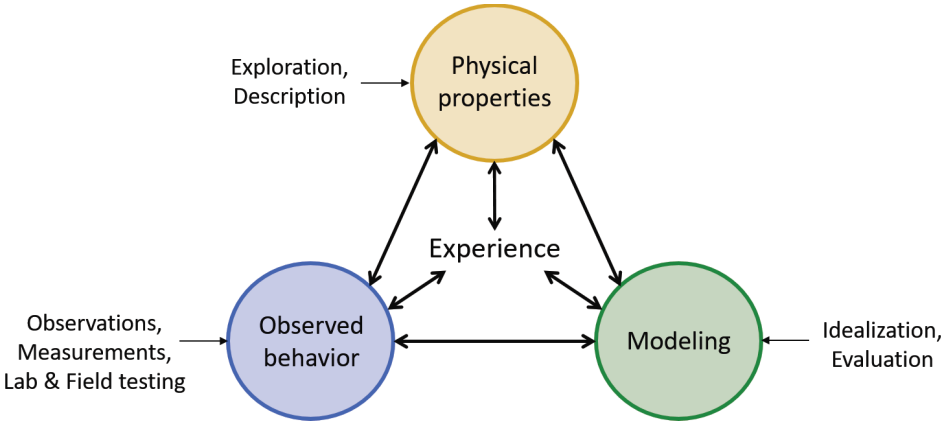

Figure 2.1: The Adapted Burland Triangle modified for a coastal research and engineering context. Adapted from Burland (1987).

the behavior of waves on beaches with varying slopes (De Bakker et al., 2016) or lidar measurements in the field can show sand bar behavior (Phillips et al., 2019).

The physical properties are hard to distinguish from the observed behavior in coastal systems due to the morphodynamic feedback loop that occurs. In the morphodynamic feedback loop, the behavior of the system continuously affects the state of the system and vice versa. The physical properties component is a static description of the system and its drivers, whereas the observed behavior contains a time component that allows for the recording and description of sediment transport processes and morphological development of the coastal system. For instance, profile measurements in a coastal system can reveal a physical property like the beach state, and a time series of profile measurements can show the temporal behavior of the foreshore and dunes. The close interaction between properties and behavior makes investigating and understanding the coastal system challenging. However, it is also a reason that modeling of coastal systems is a suitable approach, since it gives the ability to deal with complexity, and use simplification or full representation of processes where necessary.

Modeling has a close connection to the other two components of the ABT. Through idealization and evaluation, information gained on physical properties and observed behavior can lead to development of a model. For example, Palmsten and Holman (2012) found an appropriate runup statistic for quantifying dune erosion based on laboratory tests, and Bruun (1962) formulated a simple equation for the effect of sea level rise on the coast based on the expected continuity of mass. Physical properties can be input parameters for modeling, and in turn modeling can be used to determine the sensitivity of different physical properties on modeling outcomes. There is also a strong connection between observed behavior and modeling as verification based on expected behavior and validation based on measured behavior can be used to test models. Additionally, behavior that is predicted by models might give new insights in coastal processes. For example, McCarroll et al. (2021) used a model to create a parameterization for the bypassing of sediment past rocky headlands.

2.5. Guiding coastal model application with the ABT

There are many different types of models that are related to coastal systems. For example, there are relatively simple empirical relations like the Bruun Rule (Bruun, 1962), conceptual models like the active bed surface layer by Uphues et al. (2022), and more complex numerical models like AeoLiS (Hoonhout & de Vries, 2016) and XBeach (Roelvink et al., 2009). These models are applied across temporal and spatial scales and used for different purposes.

A division between the different applications of models was presented by Barbour and Krahn (2004). They divide model application into the categories interpretation, design and prediction. The use of straightforward, explicit terms in this categorization makes it appropriate for the coastal context, where different fields converge. In coastal literature, each model application category has countless examples.

Interpretation with a model was used by de Vries, van Thiel de Vries, et al. (2014), who applied a simple model concept to simulate aeolian sediment transport that is dependent on wind speed and sediment supply. Similarly, Srisuwan et al. (2015) developed a model to replicate beach profile evolution and associated changes in grain size composition. **Prediction** of coastal erosion has been done by applying the Bruun Rule (Vousdoukas et al., 2020), and Windsurf has been used to predict dune development (Itzkin et al., 2022). **Design** of coastal interventions often requires the use of models like XBeach. For example, for the exploration of different coastal flood protection options (Muller et al., 2018).

In an ideal scenario, applied models are robust, accurate and validated. However, as Thieler et al. (2000) indicate, models are often used beyond their capabilities. They emphasize that, for the purpose of application, understanding model limitations is crucial. Similarly, Barchyn et al. (2014) discuss that issues in aeolian sediment transport modeling arise because measurements and modeling are disconnected. In these cases, the output of models cannot be tested and model input cannot be measured. For example, this occurs when measurements and modeling are compared on distinctly different temporal and spatial scales (Figure 1.3).

Modeling is a crucial aspect of solving coastal challenges, as it improves understanding of coastal processes, and provides input on design and decision making. I believe that the ABT can structure the model application and development process. For example, I envision that the ABT can be used as a framework to discuss existing knowledge and experience on physical properties and behavior of a specific coastal system to determine model suitability. Also, the framework can be used to discuss model development projects in which a stronger connection with the observed behavior and physical properties components could improve the quality of the project. In this way, the framework provided by the ABT connects the acquirement of additional process knowledge more closely to its function in modeling. This prevents a disconnect between measurements and modeling as raised by Barchyn et al. (2014), provided that there is specific attention for the temporal and spatial scales at which each component of the ABT is discussed.

In Chapter 6, the ABT will be used to discuss the relation between the different aspects of the research presented in this dissertation. Additionally, it will be used to discuss the expected implementation of new insights into modeling and the broader field of coastal

research and engineering. Overall, I anticipate that the ABT can be used to clarify the purpose of research and engineering projects, to identify and prioritize missing links, and that it ultimately will benefit and advance the coastal research and engineering field as a whole.

3

Sea level rise outpaced by vertical dune toe translation

Sea level rise is a long term marine process that can alter sediment availability and coastal dune development. It remains uncertain how sea level rise impacts coastal dune development. The location of the dune toe in the coastal profile can be used as a proxy for the development of coastal dunes. In this chapter, the effect of sea level rise on coastal dune development is studied by investigating the decadal development of the dune toe.

Chapter highlights:

- The dune toe is extracted from 27.000 coastal profiles along the Dutch coast.
- The dune toe moves seaward and upward.
- The dune toe elevation increases 7.6 times faster than sea level rise.
- Decadal behavior of the Dutch coast deviates from expectations based on the sea level rise rate.

This chapter has been published as:
C.O. van IJzendoorn, S. de Vries, C. Hallin, P.A. Hesp (2021). Sea level rise outpaced by vertical dune toe translation on prograding coasts. *Scientific Reports* 11, 12792.

Abstract

Sea level is rising due to climate change and is expected to influence the development and dynamics of coastal dunes. However, the anticipated changes to coastal dunes have not yet been demonstrated using field data. Here, we provide evidence of dune translation that is characterized by a linear increase of the dune toe elevation on the order of 13-15 mm/yr during recent decades along the Dutch coast. This rate of increase is a remarkable 7-8 times greater than the measured sea level rise. The observed vertical dune toe translation coincides with seaward movement of the dune toe (i.e., progradation), which shows similarities to prograding coasts in the Holocene both along the Dutch coast and elsewhere. Thus, we suspect that other locations besides the Dutch coast might also show such large ratios between sea level rise and dune toe elevation increase. This phenomenon might significantly influence the expected impact of sea level rise and climate change adaptation measures.

3.1. Introduction

Coastal Coastal dunes are of vital importance for coastal protection and flood safety, have high geomorphological, ecological and intrinsic values, and are an important recreational resource along large parts of the world's coasts. Climate change, and its associated sea level rise (SLR), is an important driver for the development of coastal dunes. Numerous studies have investigated the coastline response to sea-level rise (Atkinson et al., 2018; Dean & Houston, 2016; Houston, 2015; Ranasinghe et al., 2012; Vitousek et al., 2017; Vousdoukas et al., 2020; Bruun, 1962; Davidson-Arnott, 2005), but it remains uncertain how SLR is impacting coastal dunes. Most predictions of coastline change due to SLR (Ranasinghe et al., 2012; Vitousek et al., 2017; Vousdoukas et al., 2020) are based on variations of the Bruun rule (Bruun, 1962). The Bruun Rule assumes that with rising sea level the beach is eroded and that the eroded sediment is moved to the offshore part of the coastal profile(Bruun, 1962). Work that expands on the Bruun rule predicts that, with SLR, the beach and dune will maintain their shape while moving landward and upward (Davidson-Arnott, 2005; Rosati et al., 2013). This implies that the dune toe will show the same behaviour. Here, the dune toe is defined as the boundary between the backshore limit (commonly around the high spring tide limit) and the seaward edge of the dunes.

The dune toe is a key parameter to describe the dune profile and is part of the spatially and temporally varying beach-dune system typically moving seawards during accretionary periods, and landwards during storms and erosion events (Castelle et al., 2015; Cohn, Ruggiero, et al., 2019; Dodet et al., 2019; S. G. Davidson et al., 2020). With SLR, the vertical extent of marine processes is altered, which influences the sediment budget of sandy beaches. Thus, it can be expected that SLR influences both the horizontal and the vertical dune toe position (Hesp, 2013). In this research, we present a unique study that compares the response of coastal dunes to sea level rise by tracking the horizontal and vertical dune toe position in an extensive dataset with measured coastal profiles.

In the Netherlands, coastal dune-beach-nearshore profiles have been measured yearly since 1965 (i.e., the Jarkus dataset). This is the largest dataset of measured

coastal profiles in the world and it has been used to analyse decadal morphological development in several previous studies (de Vries et al., 2012; Keijsers et al., 2014; Arens & Wiersma, 1994). However, the vertical translation of the dune toe has not previously been investigated. Traditionally, the vertical location of the dune toe in the Netherlands has been defined as a temporal constant, namely as the point in a beach-dune profile at 3 meters elevation above NAP (Normaal Amsterdams Peil – the Dutch fixed reference datum) (Ruessink & Jeuken, 2002). This traditional method to identify the dune toe location is easy to apply and suitable for short-term applications. However, it cannot be used to track the changes in the dune toe elevation that occur due to longer-term natural variations of the dune profile. More advanced methods include defining the dune toe position as the location of maximum slope change that occurs landward of the shoreline (Stockdon et al., 2007; Elko et al., 2002; Houser, 2013; Pellón et al., 2020; Splinter et al., 2018) or calculating the dune toe position based on the sediment volume between +1 and +5 m NAP (Guillén et al., 1999). Alternatively, in natural dune systems, the dune toe can be based on the seaward extent of dune vegetation (Hesp, 2013; Miot da Silva & Hesp, 2010) since the vegetation cannot grow seawards of the high spring tide line and semi-regular tidal inundation. The application of the different dune toe identification methods depends on the context in which they are used, the available data and the preference of the user (Wernette et al., 2018; Smith et al., 2020).

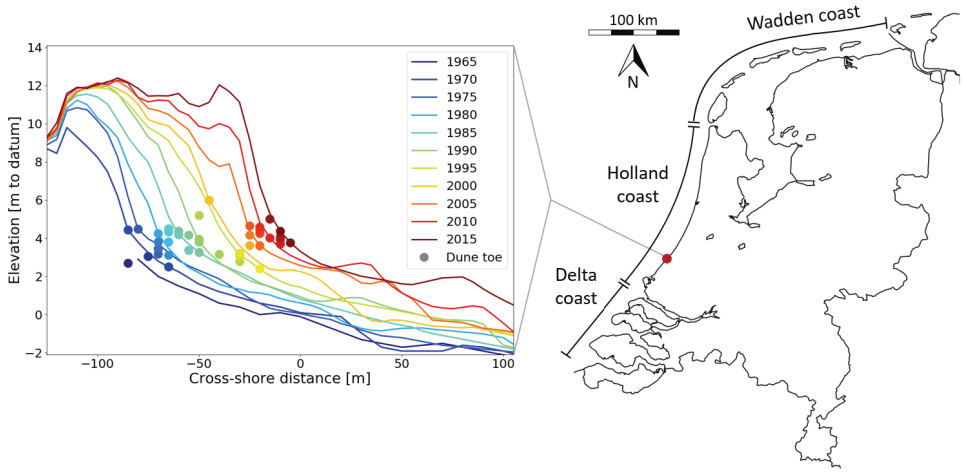

Figure 3.1: **Example of dune toe identification for a transect (ID. 9010235) along the Holland Coast.** Colored lines show the profiles measured between 1965 and 2005, for clarity displayed with a 5-year interval, revealing the morphological development through time. Colored dots represent the extracted dune toe position for each year in the period from 1965 (dark blue) to 2017 (dark red). For some years an indication of the dune toe is missing because the algorithm was not able to extract a dune toe from the corresponding profile. The map in this figure was created using basemap 1.2.0 (`https://matplotlib.org/basemap/index.html`).

Recently, new semi-automated methods have become available that can systematically extract the dune toe position from coastal profiles (Mitasova et al., 2011; Hardin et al., 2012; Wernette et al., 2016; Beuzen et al., 2019; Diamantidou et al., 2020; Itzkin et al., 2020). These new methods strive towards providing a generic derivation of a dynamic dune toe. A generic definition of the dune toe, consistent through space and time, makes it possible to track temporal and spatial variations in the dune toe position on an unprecedented scale using large datasets. It should be noted that the available methods have varying degrees of subjectivity depending on user input (Wernette et al., 2018). The results presented in this research were obtained by analysing dune toes extracted with the second derivative method (Diamantidou et al., 2020) from the Dutch Jarkus dataset. Additionally, the machine learning method of pybeach (Beuzen et al., 2019) was used to verify that a different extraction method gives similar results. The second derivative method was developed and tested by Diamantidou et al. (2020) using the Jarkus dataset. A comparison with in situ visual observations showed that the method selects the dune toe consistently (Diamantidou et al., 2020). An example of measured profiles and derived dune toes is presented in Figure 3.1.

3.2. Increase in elevation and seaward movement of the dune toe

Between 1980 and 2017, the derived dune toe elevation along the Holland coast shows a linear increase in time of 13.9 mm/y (r^2 = 0.51) and along the Delta coast, an increase of 15.1 mm/y (r^2 = 0.69) (Figure 3.2). The derived dune toe position along the Holland and Delta coast also shows seaward movement of 1.26 m/yr (r^2 = 0.92) and 0.91 m/yr (r^2 = 0.97), respectively. At the Wadden coast, no significant trend in the data was found. The regional morphological variability associated with the tidal inlets in this area likely dominates the decadal changes in the dune toe position. The trends shown in Figure 3.2 are based on nearly 27.000 dune toe positions spread over 816 different transects. The derived dune toe elevations for both the Holland and Delta coast vary within a range of 2-4 m +NAP, which includes the commonly assumed value of 3 m +NAP. Similar results are found using dune toes derived with the machine learning method of pybeach (Figure A.1 in Appendix A).

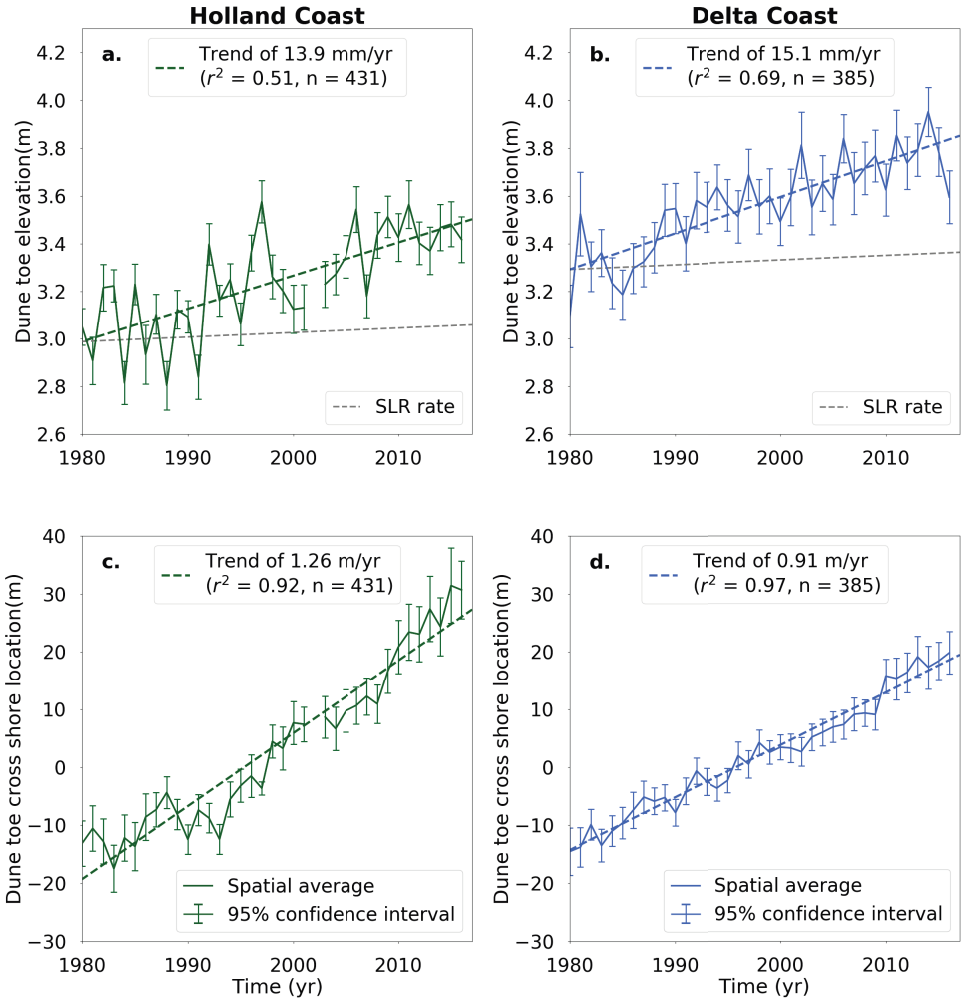

Figure 3.2: **Trends in the dune toe position along the Holland coast (a and c) and Delta coast (b and d).** The trend in dune toe elevation (a and b), and the trend in cross-shore dune toe location (c and d) are shown. In each subplot, the spatial average of all transects along the coast is represented by the solid line. The vertical bars along this line show the 95% confidence interval for each year. The overall trend in the spatial average is represented by the dashed line. In each subplot, the rate (in m/yr), r-squared value and number of transect locations (n) of this trend are given in the upper left corner. The grey dashed lines in subplots a and b show the development of the dune toe elevation if it had increased at the same rate as sea level rise (SLR).

3.3. Physical processes explain regional variations in dune toe position

Alongshore variations in the dune toe elevation are probably related to alongshore variations in waves and tides. Other mechanisms which might be related are, e.g., geological framework, grain size variations and vegetation dynamics; however, these are relatively uniform along the Dutch coast. The dune toe elevations along the Delta coast are overall higher than along the Holland coast (Figure 3.3), which is expected based on the higher mean high water levels along the Delta coast which lead to higher extreme water levels. Along the Delta coast, the dune toe elevation increases by approximately 1.0 m in a southward direction, while the mean high water also shows an increase in elevation in that direction. A similar relation is visible for the southern part of the Holland coast. However, along the entire Dutch coast, dune toe elevations are between 0.5 and 3.0 metres higher than the mean high water. This difference may be explained by the variations in wave exposure that are superimposed on the tides. For instance, dune toe elevations peak in the centre of the islands along the Delta and Wadden coast, where waves arrive perpendicular to the coast. In contrast, dune toe elevations are lower near the edges of the islands, where wave exposure is expected and likely to be less.

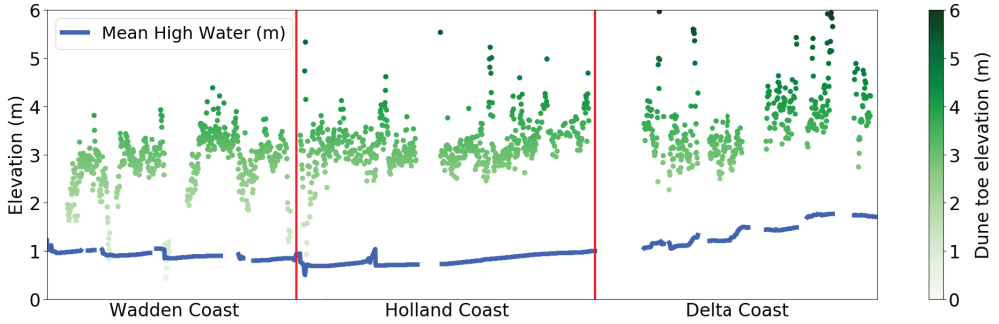

Figure 3.3: **Alongshore variation of the temporally averaged dune toe elevation (m) for the period between 1980 and 2017.** Each dot (in green) represents the average value for a transect along the Dutch coast. The blue line shows the alongshore variation in the mean high water as included in the Jarkus dataset

These findings are in line with the common assumption that the vertical location of the dune toe is mostly dependent upon marine processes. For instance, the dune toe position has been related to the maximum total water level (TWL) that occurs every ten years (Pellón et al., 2020). The TWL is made up of the measured tide level, setup and swash (Ruggiero et al., 1996). The factors influencing the TWL, and thus possibly the dune toe elevation, can be summarized as 1) waves, 2) astronomical and meteorological tides and 3) mean sea level. The spatial and temporal resolution of water level and wave height data was not sufficient to correlate the TWL to the dune toe elevation in this study. Still, in Figure 3.3, we probably see the effect of waves and tides causing alongshore variation in dune toe elevation. We cannot see the effect of mean sea level

because that does not have significant variations on this spatial scale. Temporal variations in sea level might, however, be linked to the increase of the dune toe elevation through time.

3.4. Dune translation outpaces sea level rise

The SLR trend along the Dutch coast is linear and consistent at a rate of 1.9 mm per year (Figure 3.4) (CBS; PBL; RIVM; WUR, 2016). Conceptual models based on the Bruun Rule assume a 1:1 ratio between sea level rise and dune toe elevation increase (Davidson-Arnott, 2005; Hallin, Larson, & Hanson, 2019). Our results show that this assumption is not valid for the Holland and Delta coast. SLR is significantly slower than the increase in dune toe elevation (Figure 3.2), namely 1.9 mm/yr SLR compared to 13.9 - 15.1 mm/yr dune toe elevation increase. We may define this difference between the rate in dune toe elevation increase and SLR as the Dune Translation Index (DTI). The DTI is derived by dividing the rate of dune toe change by the mean SLR, which in the case of the Holland coast results in a DTI of 7.33, and for the Delta coast, a DTI of 7.95. Thus, for the Holland and Delta coast together, the mean DTI is estimated to be 7.6. At this moment, we cannot fully explain the physics behind the DTI. However, as additional data from other coasts become available, the DTI provides a means by which to compare the relationship between SLR and vertical dune toe translation for different surfzone-beach types and various retrogradation to progradation (i.e., landward to seaward movement) rates.

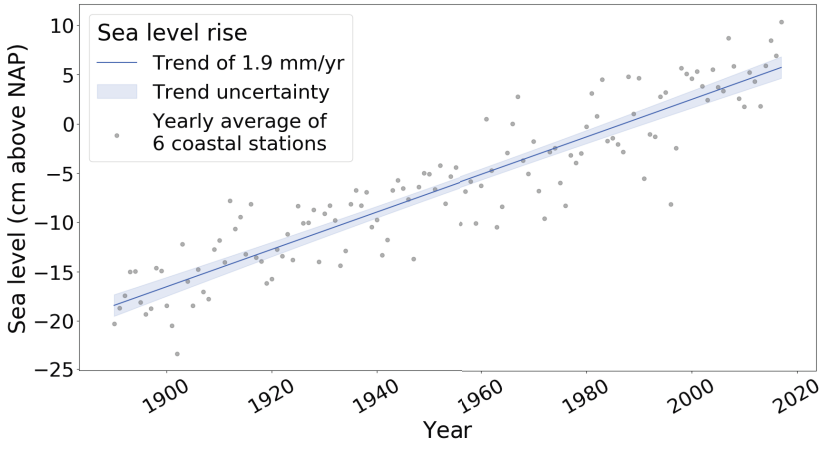

Figure 3.4: **Sea level rise along the Dutch coast measured at 6 different coastal stations from 1880 to 2019** (CBS; PBL; RIVM; WUR, 2016). Each grey dot represents the yearly averaged value of the 6 coastal station. The solid blue line represents the trend in these yearly averaged values and the uncertainty of this trend is represented by the blue shading. This uncertainty was calculated as the trend ± 2 standard deviations.

3.5. Similarities to Holocene transgression

The contemporary behaviour of the dune toe position along the Dutch coast is similar to its documented seaward movement during sea level rise in the Holocene (Beets et al., 1992) and to Holocene coastal barrier development at other locations. At a millennium scale, several studies of coastal barriers show that as the Holocene sea level was rising in the 8000 to 5000 years BP period, where there was sufficient sediment supply, barriers (dunes, beaches and shoreface) prograded seawards in concert with the backshore/dune contact rising vertically (Rodriguez & Meyer, 2006; Martinho et al., 2010; Costas et al., 2016). This same increase in elevation and progradation of the coastal profile also occurred along the Dutch coast during the Holocene (Beets et al., 1992). The progradation of the profile was linked to the supply of sediment from offshore (i.e., shoreface feeding) (Stive & de Vriend, 1995) while rising sea level caused the dune toe elevation to increase. Currently, the dune toe is increasing in elevation and prograding along the Holland and Delta coast (Figure 3.2). Based on this study, it is uncertain whether the entire dune is prograding in relation to sea level rise simultaneously with the dune toe. This depends on the behaviour of the dune crest and the associated profile shape. Milder dune slopes will develop over time if dune crests are less mobile than the dune toe. Since this is the first study of its kind, it remains unclear if the contemporary changes in the dune toe position along the Dutch coast also occur at other locations. If that is the case, we might expect other locations where the dune toe elevation increase outpaces SLR.

3.6. Vertical dune toe translation 7-8 times faster than SLR

The DTI of 7.6 shows that vertical dune toe translation (14-15 mm/yr) outpaces SLR (1.9 mm/yr) along the Dutch coast with a remarkable rate compared to the 1:1 ratio predicted by models based on the Bruun Rule (Bruun, 1962). Additionally, the progradation of the dune toe deviates from the seaward movement assumed by the Bruun rule. Initially, when trying to explain the high DTI, it should be considered that this is the first time this extensive dataset has been utilized to determine the relationship between contemporary dune toe elevation and SLR. Thus, the DTI of 7.6 might be the natural rate of change for the surfzone-beach systems typical for the Dutch coast over the past decades. However, the dune toe development cannot continue like this indefinitely because the vertical dune toe position remains related to marine processes. Thus, the dune toe cannot increase to an elevation that is outside of the reach of the total water level.

Future work could include several different aspects that might be able to explain the high DTI. Firstly, the development of the coastal profile could lag behind the changes in SLR conditions, so the equilibrium profile that corresponds to a 1:1 ratio is not reached. Secondly, the influence of other factors besides SLR, like marine and sedimentary processes, should be considered. For instance, temporal variations in the wave climate and tidal range could influence and accelerate an increase in dune toe elevation. Nourishments and vegetation dynamics could change the response of the dune toe on a yearly to decadal-scale by supplying to and trapping sediment at the dune toe. The effect of nourishments might be especially relevant for the Dutch coast considering the

large number of nourishments that are applied along the coast (De Ruig, 1998; Van Der Spek & Lodder, 2015). Specifically, previous research has related nourishments to a reduction of transects with landward dune toe movement (Giardino et al., 2014). Additionally, alongshore transport could also influence the dune toe development, but these influences are minor on the national scale.

For now, the measured deviation between sea level and dune toe elevation change cannot be explained in detail because not all physical processes that influence coastal profile change are fully understood. However, the significant deviation from the 1:1 ratio indicated by the high DTI has large implications for predicting the impact of climate change. Since the dune toe position significantly impacts the dune volume, it will also influence the safety standard of dunes and the basis for spatial planning in the coastal zone. Thus, this finding may change the evaluation, implementation, and planning of future climate change adaptation measures along the coast.

3.7. Consequences of dune toe elevation outpacing SLR

Based on the results, we conclude that along the Holland and Delta coast the increase in dune toe elevation (14-15 mm/yr) outpaces SLR (1.9 mm/yr) by a factor of 7.6, and the dune toe is moving seaward at 1 m/yr. These results show that the decadal-scale behaviour of the coastal profile can strongly deviate from the expected landward horizontal movement and the 1:1 relation with SLR for vertical movement as assumed by some authors (Vousdoukas et al., 2020; Bruun, 1962). We suggest that, based on similar transgressive behaviour in the Holocene, such large ratios might also occur at other locations besides the Dutch coast. If this applies to other coasts, the outpacing of SLR by vertical dune toe translation might significantly alter the predictions of the impact of climate change on coastal dunes. Thus, this finding may change the evaluation, implementation and planning of future climate change adaptation measures along the coast.

3.8. Methods

The dataset with yearly profile measurements (i.e., the Jarkus dataset) used in this research has been collected from 1965 onwards. The transect locations span the entire Dutch coast and are spaced approximately 250-500 m apart. To study the trend in decadal dune toe position the following steps were executed: 1) choosing the dune toe position definition and extraction method, 2) extracting the dune toe positions from the coastal profiles and 3) spatial and temporal filtering of the resulting dune toe positions.

In this research, the dune toe was defined as the boundary between the landward limit of the beach (the top of the backshore) and the dunes. We assumed that the specific location of the dune toe is subordinate to its function as a proxy for coastal profile change. The identification of the dune toe for one individual transect does not have value because there is no 'true' dune toe location that is directly related to the physical processes that shape the coastal profile. However, when applying the extraction method to a long-term and/or spatially extensive dataset, we are no longer studying the specific dune toe position, but the changes in the position. Thus, the analysis of the long-term

change in dune toe position was based on the assumption that the derivation methods can track the development of the dune toe position consistently.

In choosing an automated extraction method for this research, two criteria were used. First, the method should be open-source to allow for public availability of the research results. Second, the method should be compatible with the Jarkus dataset that contains profile measurements of coastal morphology. Therefore, methods based on digital elevation models (DEMs) (Mitasova et al., 2009; Hardin et al., 2012; Wernette et al., 2016) and vegetation (Hesp, 2013; Miot da Silva & Hesp, 2010) were excluded. Applicable methods include those based on profile slope (Stockdon et al., 2007; Elko et al., 2002; Houser, 2013; Pellón et al., 2020; Splinter et al., 2018; Diamantidou et al., 2020), profile volume (Guillén et al., 1999) and profile shape (Itzkin et al., 2020). Among the slope-based methods, which are most commonly used, the second derivative method was selected. In a previous study, this method was applied to the Jarkus dataset and showed robust results compared to in situ visual observations (Diamantidou et al., 2020). Additionally, the recent, innovative and well-documented pybeach method based on machine learning was added to diversify the analysis in an effort to increase the confidence in the observed dune toe development trends.

The second derivative method consists of two main steps. First, the coastal profile is reduced in length with the landward and seaward boundaries depending on the primary dune height and mean high water, respectively. Second, the dune toe is placed at the most seaward location where the first and second derivative of the remaining profile are each larger than their predefined threshold. Thus, some subjectivity is introduced in this method when the boundaries and thresholds are defined (Wernette et al., 2018). A detailed description of the second derivative method and its application to the Jarkus dataset is provided by Diamantidou et al. (2020) together with a dataset consisting of the extracted dune toes (Diamantidou, 2019). The pybeach method extracts the dune toe using machine learning, where the dune toe identifier is based on dune toe identification executed by experts (Beuzen et al., 2019). This method was applied to the same reduced profile as the second derivative method. Given the resolution of the Jarkus dataset (i.e., 5 m) and the extraction technique of both methods, the derived dune toe positions are not sensitive to smaller-scale variations in the coastal profile. The extracted dune toe locations were filtered to remove years and locations with unreliable data or a lack of data availability. The majority of removed transects were deviating coastal profiles that include, for instance, dikes and dams. These transects (± 23% of all transects) were removed from the dataset leaving 77% of the available data points (about 60.000 dune toe positions) for further analysis.

To obtain an indication of the overall profile evolution of the Dutch coast, the average elevation and cross-shore location of the dune toe of all transects per year was calculated. For the period before 1980, the lack of data for a large number of transects resulted in the average values being skewed. The period between 1980 and 2017 has the most reliable data availability and was thus used for the trend analysis shown in Figure 3.2, similar to earlier approaches that used the Jarkus dataset (de Vries et al., 2012).

The results shown in Figure 3.2 and 3.3 are the output of the second derivative method, whilst the results of the pybeach method are shown in Figure A.1 in Appendix

A. Overall, the results of the pybeach method were similar with a DTI of 6.6 for the Delta and Holland coast combined, compared to a DTI of 7-8 for the second derivative method. The comparable results between the second derivative method and the machine learning method of pybeach indicate that the results converge for two different methods when applied to a large dataset. It is expected that other methods based on the profile slope (Stockdon et al., 2007; Elko et al., 2002; Houser, 2013; Pellón et al., 2020; Splinter et al., 2018; Diamantidou et al., 2020) would generate similar results. However, methods that use distinctly different calculation techniques, like those based on volume (Guillén et al., 1999), profile shape (Itzkin et al., 2020) and, especially, based on vegetation (Hesp, 2013; Miot da Silva & Hesp, 2010) might show varying results and would be interesting to explore in future studies.

Data availability

The software used to extract and analyse coastal profile parameters from the Jarkus dataset (i.e., the Jarkus Analysis Toolbox), and the dataset containing the extracted parameters that were generated during this research, are available in the 4TU repository, https://doi.org/10.4121/c.5335433.

Acknowledgements

This work is part of the research programme DuneForce with project number 17064 which is (partly) financed by the Dutch Research Council (NWO). Thanks to the BEADS Lab and Flinders University for support of Patrick Hesp and for sabbatical support to Sierd de Vries in 2019-2020. We would also like to thank Marcel Stive and Ad van der Spek for the input they provided for this article.

4

Measurements of vertical grain size variability due to marine and aeolian processes

The potential impact of sea level rise and sediment supply on coastal dune development was discussed in Chapter 3. To gain a thorough understanding of coastal dune development, it is necessary to investigate these yearly to decadal scale factors, as well as details of coastal aeolian sediment transport. Aeolian sediment transport can be affected by supply-limiting factors such as grain size. The dynamics of grain size variability due to marine and aeolian processes on the beach, and the effect of grain size variability on aeolian sediment transport towards the dunes are not fully understood. The interaction between grain size variability and marine and aeolian processes is addressed in this chapter and Chapter 5. Specifically, this chapter presents a new sand scraper sampling method to determine the extent of the grain size variability on hourly time scales in the intertidal zone.

Chapter highlights:

- We developed a sand scraper sampling method to measure vertical grain size variability in the intertidal zone at a mm-scale.
- The grain size on different beaches showed considerable spatial variations (both vertically and horizontally).
- Marine processes have the biggest impact on short-term grain size variations where considerable morphological change occurs.
- Aeolian transport can result in coarsening of the bed surface, but fining can occur when bedforms are present.

This chapter has been published as:
C.O. van IJzendoorn, C. Hallin, N. Cohn, A.J.H.M. Reniers and S. de Vries (2022). Novel sediment sampling method provides new insights into vertical grain size variability due to marine and aeolian beach processes. *Earth Surface Processes and Landforms*, 1-19.

Abstract

In sandy beach systems, the aeolian sediment transport can be governed by the vertical structure of the sediment layers at the bed surface. Here, data collected with a newly developed sand scraper is presented to determine high-resolution vertical grain size variability and how it is affected by marine and aeolian processes. Sediment samples at up to 2 mm vertical resolution down to 50 mm depth were collected at three beaches: Waldport (OR, USA), Noordwijk (NL) and Duck (NC, USA). The results revealed that the grain size in individual layers can differ considerably from the median grain size of the total sample. The most distinct temporal variability occurred due to marine processes that resulted in significant morphological changes in the intertidal zone. The marine processes during high water resulted both in fining and coarsening of the surface sediment. Especially near the upper limit of wave run-up, the formation of a veneer of coarse sediment was observed. Although the expected coarsening of the near-surface grain size during aeolian transport events was observed at times, the opposite trend also occurred. The latter could be explained by the formation and propagation of aeolian bedforms within the intertidal zone locally resulting in sediment fining at the bed surface. The presented data lays the basis for future sediment sampling strategies and sediment transport models that investigate the feedbacks between marine and aeolian transport, and the vertical variability of the grain size distribution.

4.1. Introduction

Aeolian sediment transport rates and threshold velocities depend on the grain size composition of the bed (Bagnold, 1937b). Meanwhile, aeolian transport alters the composition of the bed surface through grain size-selective pick-up and deposition (Bagnold, 1937a; Bauer, 1991), and underlying sediment layers may be exposed through erosion. When underlying sediment is exposed, aeolian transport rates depend not only on the grain size composition of the uppermost surface layer (< 2 mm) but on the vertical variability in grain size distribution of the bed. In the intertidal zone, the grain size composition is influenced by both aeolian and marine processes (Figure 4.1) as wave and tide induced currents erode and deposit sediment and rework the bed (Reniers et al., 2013; Srisuwan et al., 2015). Since the intertidal zone can be an important sediment source for aeolian transport (de Vries, Arens, et al., 2014), the resulting grain size composition and vertical stratigraphy could impact total transport rates from the beach towards the dunes. This study analyses the temporal and spatial grain size variability of mm-thick vertical layers of the intertidal bed using a new sediment sampling device.

During aeolian sediment transport, the grain size distribution at the sediment surface can change as the wind selectively picks up grains from the surface. Wind-blown sand deposits are generally dominated by sediments with a grain size between 150 and 300 μm, with some grains as fine as 80 μm (Bagnold, 1941). The sediment in the source areas is typically less well-sorted with larger fractions of coarser elements (Bagnold, 1937a; Bauer, 1991). At the bed surface where the wind-blown sediment originates, an increase in the grain size can be expected when the finer grains are removed. This increase in grain size was observed by Field and Pelletier (2018) in an arid dune field.

On a beach in Duck, USA, Cohn, Dickhudt, and Marshall (2022) similarly observed a gradual coarsening within the saltation layer at a sub-hourly timescale despite decreasing wind speeds, which may indicate an increase in grain size at the bed surface. Coarsening of the bed can result in armouring effects that reduce the aeolian transport rates because the coarse particles cannot be moved by the wind. For example, Strypsteen et al. (2021) observed that a coarse armour layer on Texel, the Netherlands, was immobile for wind speeds up to 15 m/s.

The potential for sediment transport by marine processes is expected to be larger, as marine processes are typically a more powerful driver of sediment transport than aeolian processes (e.g., de Vries, Arens, et al., 2014; Hoonhout & de Vries, 2017; van der Wal, 2000a). Marine processes that can affect the grain size layering in the intertidal area are, for instance, sediment overturning and mixing by waves, (tidal) currents, swash and backwash (e.g., Jackson & Nordstrom, 1993; Masselink & Puleo, 2006). Generally, it is thought that the depth of mixing is larger in the lower parts of the intertidal zone, coincident with larger wave dissipation (Anfuso, 2005; Jackson & Nordstrom, 1993; Sherman et al., 1993; Voulgaris & Collins, 2000). Apart from sediment mixing, the removal and supply of sediment through advection can affect spatio-temporal grain size variations (Aagaard & Greenwood, 2008; Jackson et al.,

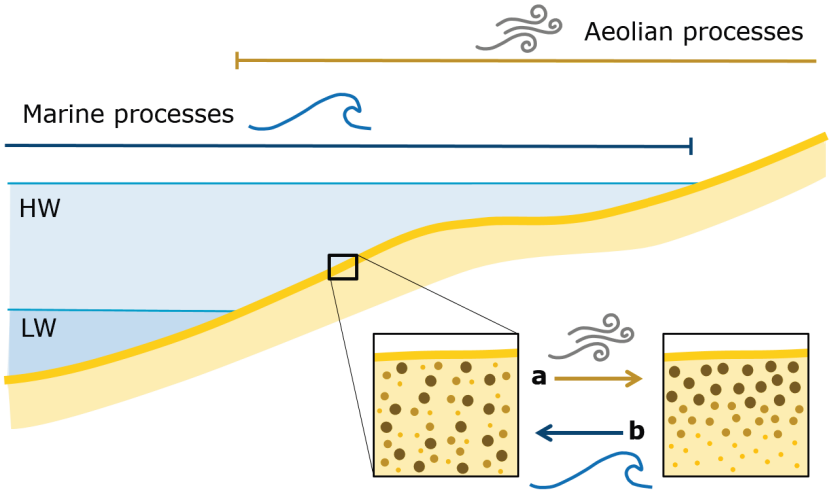

Figure 4.1: Marine and aeolian processes overlap in the intertidal zone between the most seaward location that becomes exposed and the most landward location that becomes inundated. Note that these boundaries vary in time and space depending on beach morphology, tides, waves and run-up. When considering the vertical variability of the grain size distribution, marine and aeolian processes could, e.g., have the following effects: (a) Aeolian transport may cause coarsening of the upper layer of the surface due to selective pick-up by the wind during low tide. (b) Marine processes may cause homogenization of the vertical grain size layering due to mixing occurring during high tide, which results in an increase of fine particles near the surface. It should be noted that the schematized effects of the marine and aeolian processes in this figure are only examples, and that other effects also can occur.

2004; Osborne & Rooker, 1999). Erosion can expose sediment layers with distinctly different grain sizes (Gallagher et al., 2016). Bedform (e.g. bar, berm, rip channels) migration can cause mixing (Sherman et al., 1993). Additionally, cross-shore variations in grain size are caused by these morphological features so they can cause changes in grain size when they migrate (e.g., Sonu, 1972; Gallagher et al., 2011; Medina et al., 1994; Van der Zanden et al., 2017).

The multitude and complexity of marine processes in the intertidal zone make it difficult to predict the resulting grain size distribution and stratigraphy after inundation due to, e.g., high tide, storm surge, wave setup, and swash. Several field studies have shown a cross-shore gradient in grain size across the intertidal zone (Bauer, 1991; Çelikoglu et al., 2006; Sonu, 1972; Edwards, 2001; Stauble & Cialone, 1997). Additionally, several model studies have shown that marine processes may result in a vertical variability in the grain size distribution (Reniers et al., 2013; Srisuwan et al., 2015). Gallagher et al. (2016) observed this type of variability on the decimeter to meter scale in the field. However, from the perspective of aeolian transport, vertical scales of mm up to cm are of interest. Field data on the vertical grain size variability at the sub-centimeter scale within the intertidal zone could provide insight into the influence of the interplay between marine and aeolian processes on the bed composition and sediment supply for aeolian transport.

Several methods and sampling techniques are available for grain size analysis in coastal environments. Surface photographs (Barnard et al., 2007; Buscombe et al., 2010; Rubin, 2004) can be used to study the top of the bed surface. Trenching (Gallagher et al., 2016), sand peels (Yasso & Hartman, 1972; Yokokawa & Masuda, 1991), and sediment coring (Gallagher et al., 2016; Gunaratna et al., 2019) can be used to study larger scale (vertical) patterns in grain size. Another method is surface grab sampling (or bulk sampling), in which typically the top 5-10 cm of the bed surface is collected (Gallagher et al., 2011; Hallin, Almström, et al., 2019; Huisman et al., 2016; Masselink et al., 2007; Medina et al., 1994; Prodger et al., 2017; Reniers et al., 2013; Stauble & Cialone, 1997). Combinations of these methods are possible, for instance, as shown by Gallagher et al. (2016), who used sediment coring, a digital imaging system (similar to surface photographs) and trenching. However, none of these methods have shown to facilitate feasible sub-centimeter detailed sampling of the vertical grain size variability in the intertidal zone.

In this study, a new sand scraper method is introduced that allows for measurements of vertical variability of the grain size distribution with a resolution of 2 mm down to 50 mm depth. The sand scraper is used to collect samples from three different beaches in Waldport (OR, United States), Noordwijk (the Netherlands) and Duck (NC, United States). For these three case studies, it is investigated (1) whether near-surface sediment layers differ in grain size from the median grain size derived from bulk sampling, (2) the effect of aeolian sediment transport on vertical grain size layering, and (3) the effect of marine processes on vertical grain size layering at the intra-tidal time scale.

This chapter presents the methodology and sampling strategy used to obtain the vertical variability of the grain size distribution (Section 4.2). Additionally, the collected data per field site are shown, including samples that were collected to provide insight into the repeatability of the sampling method, the presence of bedforms and the occur-

rence of spatial variability (Section 4.3). Following, the spatio-temporal trends in grain size due to both marine and aeolian processes, the advantages and disadvantages of the sand scraper sampling method, and the implications for sediment availability and future research are discussed (Section 4.4).

4.2. Methodology

4.2.1. Field sites

This study was conducted by collecting sediment samples showing the vertical variability of the grain size distribution in Waldport (Oregon, United States), Noordwijk (the Netherlands) and Duck (North Carolina, United States) (Figure 4.2). The three beaches have different hydrodynamic and morphological characteristics (Table 4.1). Beach widths above mean sea level range from less than 50 m in Duck to 200 m in Waldport. Compared to the other beaches, Waldport has a larger spring tide range and the highest storm waves. The beach in Duck is distinct from the others because it is intermediate (compared to dissipative), micro-tidal, and mixed grained. Additionally, the lower beach morphology in Noordwijk and Waldport are dominated by the presence of intertidal bars, while the beach in Duck has a pronounced berm. The expected median grain size for the different sites ranges from 200–250 μm in Waldport to >300 μm in Duck.

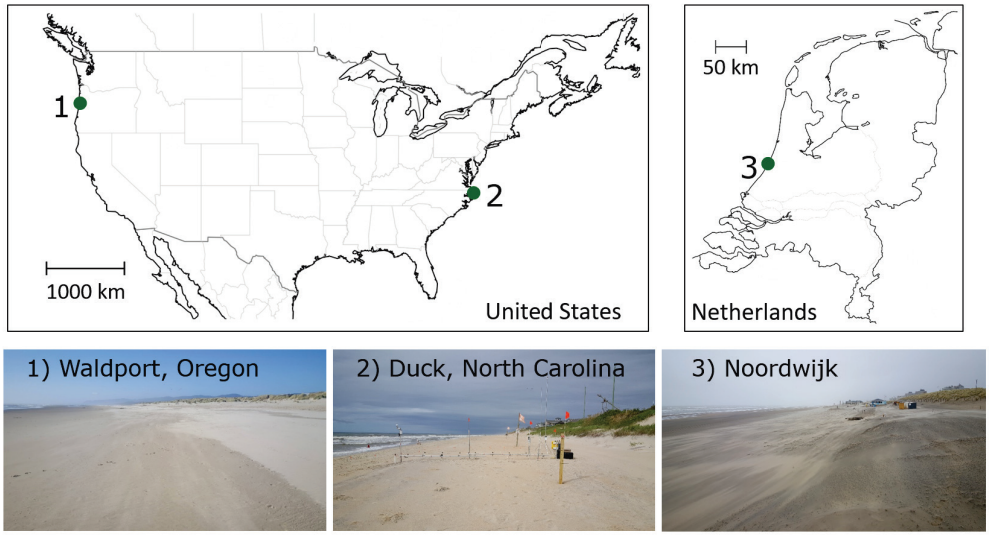

Figure 4.2: Locations where vertical grain size distributions were collected in the United States (Waldport and Duck) and the Netherlands (Noordwijk). The numbers in the maps correspond to those of the photographs. Pictures 1 and 2 were mirrored horizontally to aid comparison between locations. Photos: Christa van IJzendoorn

Table 4.1: Overview of morphological and marine characteristics of field sites in Waldport (Oregon, United States), Noordwijk (the Netherlands) and Duck (North Carolina, United States).

	Waldport	Noordwijk	Duck
Sampling location	N 44°26'13.5", W 124°5'5.1"	N 52°14'31.9", E4°25'29.5"	N 36°11'5.2", W 75°45'6.3"
Beach slope	1:40[a]	1:30	1:15[g]
Beach width	200 m[a]	100–150 m	< 50 m
Tidal range	1.5–2 m[b]	1.4 m[e]	1.0 m
Spring tide range	3–4 m[b]	1.8 m[e]	1.5 m
Mean wave height	1.5 m[c] (summer)	1 m	1 m
Storm wave height	10 m[b]	5 m	6 m[h]
Expected grain size (D_{50})	200–250 μm[d]	250–300 μm[f]	300 μm with coarser present[i]

[a]Based on beach data available through http://nvs.nanoos.org/. [b]Ruggiero et al., 2010. [c]Tillotson & Komar, 1997. [d]Twenhofel, 1946. [e]Ojeda et al., 2008. [f]Bemmelen, 1988. [g]Doran et al., 2015. [h]Larson & Kraus, 1994. [i]Gallagher et al., 2016.

4.2.2. Sediment sample collection and analysis

A new instrument has been developed to measure the vertical grain size variability at the appropriate scales of interest to sediment availability for aeolian sediment transport (Figure 4.3). The custom-made sand scraper was inspired by a surface sediment sampler presented by Wiggs et al. (2004). The sand scraper consists of a base plate (59 x 40 cm) and a sand scraper mechanism (32 x 16 x 28 cm, Figure 4.3a). The base plate can be placed on the beach surface and the sand scraper mechanism is then inserted through the base plate into the sand. A dialing mechanism with depth bars that is attached to the base plate determines how deep the sand scraper mechanism is inserted into the sand (Figure 4.3a). The sediment can be scraped off from the beach surface in precise layers of 2 mm down to 50 mm depth (Figure 4.3b).

The base plate and sand scraper mechanism were constructed out of sheets of stainless steel, and they can fit into a shipping box of 60 x 40 x 40 cm when disassembled. Together, these elements weigh a total of 8.5 kg. Thus, one person can handle the device but for extended walking distances the use of a hand cart for transportation is recommended. The main costs of device construction for this research were labor costs associated with the design and testing of the device. The costs of reproduction will depend on hourly labor costs and the production facilities available. In case of a well-equipped workshop with a water jet cutter and spot welding capabilities at its disposal, production time and cost might be limited to one work week. More information on the design of the sand scraper is available in the 4TU repository (https://doi.org/10.4121/c.5736047).

The scraper was designed for sampling of flat beds within the intertidal area. The device can be used on irregular surfaces but the layered sampling will then be less accurate, especially at the top layer. The maximum sampling depth of 50 mm was chosen to reflect the upper portion of the bed that determines sediment supply for aeolian transport. Thus, it is not expected that the device can fully measure mixing effects that occur due to marine processes as these often have a sediment disturbance that is deeper than 50 mm (Anfuso, 2005; Voulgaris & Collins, 2000). The 2 mm vertical increment was chosen to be only a (few) grain diameter(s) thick to assess micro-scale changes not achievable with conventional grab sampling.

The scraper has a 16 cm radius (0.04 m^2 surface) so that a 2 mm sampling layer results in a big enough sample for sieving, i.e., approximately 150 grams. Depending on the required application needs, multiple 2 mm samples can be combined into one

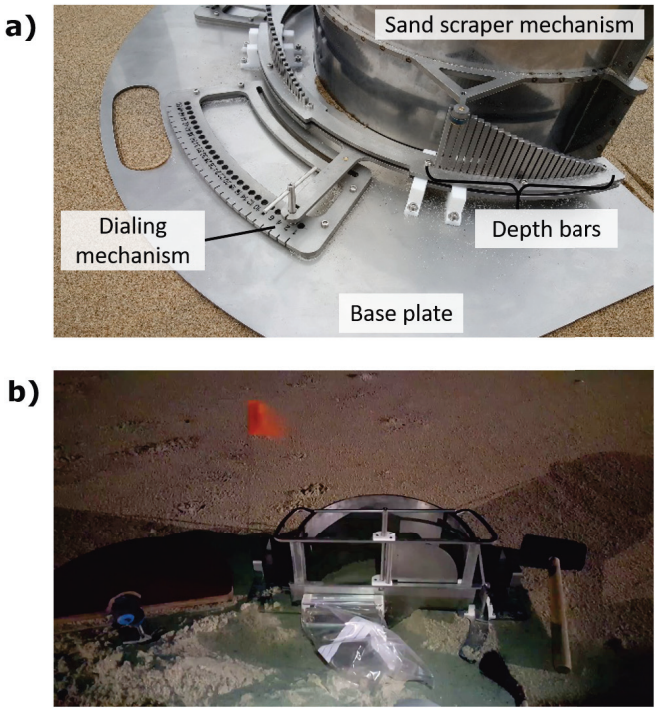

Figure 4.3: Overview of sampling with the sand scraper. (a) The dialing mechanism on the base plate that is used to set the depth at which a sample is collected with the sand scraper mechanism. (b) The sand scraper in use on the beach, surrounded by the top plate, sampling bags, a brush and a small shovel that are used to collect the sand samples. This photo is a still of a video that is published in the 4TU repository as video1.mp4 (https://doi.org/10.4121/c.5736047). The video shows how one layer can be collected in a sample bag. Subsequently, the dialing mechanism can be used to increase the sampling depth, then, the sand scraper mechanism can be pressed deeper into the sand and the layer collection can be repeated with a new sampling bag.

bigger sample to reduce the layering resolution. For this research, a more detailed layering resolution was chosen near the surface (i.e. layers of 2 and 4 mm) compared to deeper in the bed (i.e. layers of 6 mm). In total, ten samples per sampling location were collected when sampling down to 50 mm depth. The sample collection with the sand scraper requires removal of sediment. Therefore, when following the development of the bed through time, consecutive measurements at the same sampling location need to be completed at an adjacent location (< 3 m).

The samples collected with the sand scraper were oven-dried and then analyzed to determine their grain size distribution (Figure 4.4). The grain sizes of the samples from Noordwijk were determined by dry sieving with ten sieve screens ranging from 63 μm to 3350 μm, based on BS1377-2 (1990). The grain sizes of the samples from Waldport and Duck were determined using a Camsizer (Retsch Technology, Germany). The grain size range of the Camsizer was set between 20 and 2000 μm and divided into 200 bins.

From the obtained grain size distributions, various grain size characteristics were determined. First, the median grain size, D_{50} was determined per layer as an indication of the primary grain size characteristics at each site, location and depth. Second, the D_{16}, D_{25}, D_{75}, and D_{84} quantiles were calculated to assess the width of the distribution and the corresponding contributions of the finer and coarser particles within each sample. Third, the weighted average median grain size of all layers in a cross-section, $\emptyset_{50}$, was calculated. This value can be seen as a representation of the D_{50} that would have been found if a bulk sample was collected

The results are presented in colour-coded boxplots. Figure 4.5 illustrates three example results based on synthetic data as a guide to interpreting the results. Figure 4.5a shows an example where the grain size is larger near the surface (2 mm bin) than the grain size sampled at larger depths (e.g., 50 mm depth). When there is a gradual change in grain size between this relatively coarse surface sample and relatively fine deeper sample, this is henceforth referred to as a fining downward gradient. Conversely, the opposite trend in which there is a gradual increase in grain size from the surface to deeper depths, such as shown in Figure 4.5b, is referred to as a coarsening downward gradient. Not all trends shown in the data are gradual. Boundaries, where there are large jumps in grain size, are also noted, as shown in the example in Figure 4.5c at 20 mm depth. The examples provided in Figure 4.5 also show how increased vertical resolution could aid in studying the sediment availability at the bed surface. For instance, Figure 4.5b and 4.5c have a similar $\emptyset_{50}$ but in Figure 4.5b fine sediment is available at the surface, whereas coarse sediment is present at the surface in Figure 4.5c which impedes aeolian sediment transport.

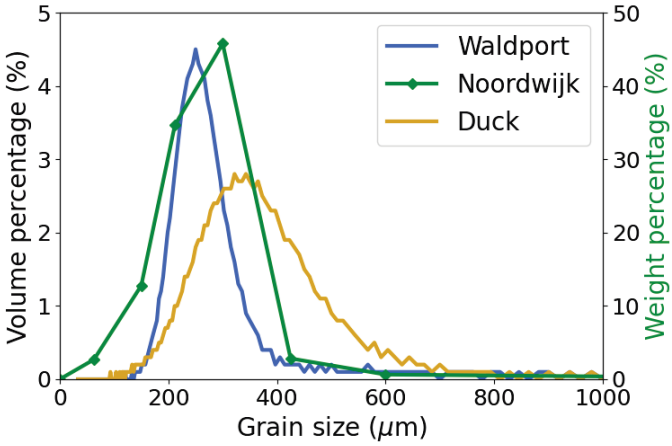

Figure 4.4: Representative grain size distributions for the three different field sites (Waldport, Noordwijk, and Duck). The Waldport and Duck graphs were determined based on 200 grain size bins for which the volume weighted percentage was determined by a Camsizer. The Noordwijk graph was based on sieve analysis, so the weight percentage per sieve size (indicated by the green diamonds) is shown on the right y-axis. When assuming that the particle density is constant, the particle size distribution based on volume and mass are the same, allowing for comparison between the different graphs.

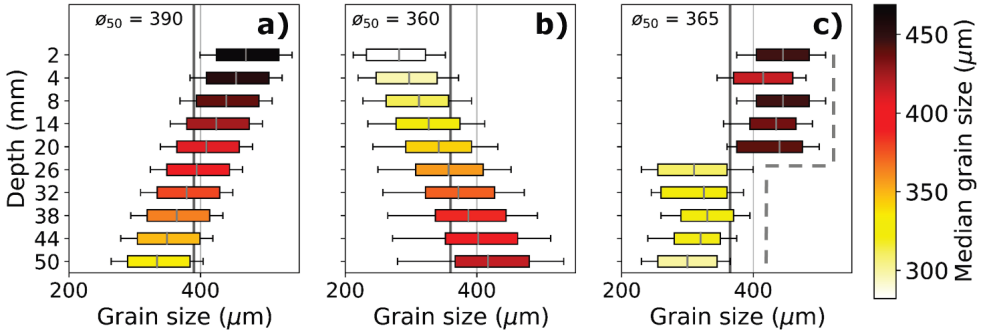

Figure 4.5: Synthetic data used to show examples of vertical variability in the grain size distribution. Colors indicate the median grain size. Box plot dimensions are based on the D_{25} and D_{75}, and the extent of the whiskers on the D_{16} and D_{84}. For each vertical grain size distribution, the $\emptyset_{50}$ is included. a) A fining downward gradient, b) a coarsening downward gradient with widening distribution with depth, c) coarser sediment on top of finer sediment, with a boundary at 20 mm depth, which is emphasized with the grey dashed line.

4.2.3. Sampling Strategy

The influence of marine processes and aeolian transport on the vertical grain size variability was studied by repeating the sand scraper sampling at specific times during the tidal cycle (Figure 4.6). To study the effect of marine processes on the observed grain sizes, samples were collected right before high water (B-HW) and after high water (A-HW), thus, excluding contributions from aeolian transport. To study the bed surface after aeolian transport, samples were collected right after high water and right before high water (A-AT), thereby excluding marine processes. Preferably, measurements were executed during consecutive low and high waters to link the effects of the marine and the aeolian processes. However, in some instances, the environmental conditions

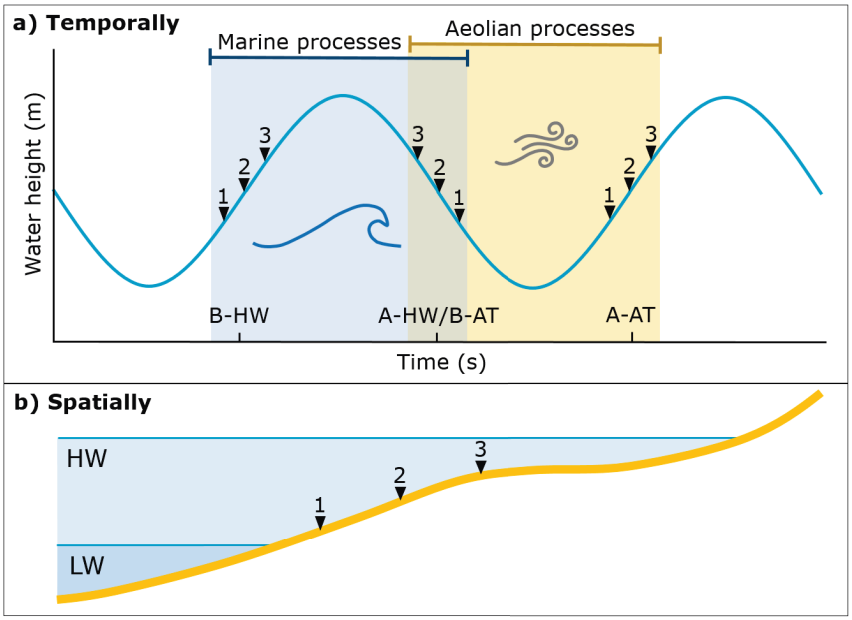

Figure 4.6: Conceptual representation of the spatial and temporal sampling strategy that was used to assess the vertical variability of the grain size distribution in the intertidal zone on the intra-tidal timescale. Black triangles indicate times and locations at which the vertical grain size distribution is sampled. (a) The impact of the marine processes on the vertical grain size variability (blue shaded area) is determined by sampling the bed surface before high water (B-HW) and after high water (A-HW). The inundation during high water could be caused by high tide, storm surge, wave setup, and/or swash. The influence of the aeolian processes (yellow shaded area) is determined by sampling before aeolian transport (B-AT) and after aeolian transport (A-AT), possibly during a low water. (b) Three locations in the intertidal zone, between low water (LW) and high water (HW), are sampled to get an indication of the cross-shore variability in the vertical grain size layering. Each sampling location has a different elevation so they are each exposed and submerged at different times in the tidal cycle. Thus, the sampling time depends on the sampling location, as indicated by the corresponding numbers between subplot a and b.

only allowed sample collection around a single high water or a single aeolian transport event. In most cases, the limiting factor was the occurrence of aeolian transport during low water. Several studies have shown that beaches show a cross-shore gradient in grain size (e.g., Çelikoglu et al., 2006; Stauble & Cialone, 1997), and spatial variations in aeolian transport can occur in the intertidal area related to spatial patterns in moisture content (e.g., Davidson-Arnott et al., 2008) and the fetch effect (e.g., Delgado-Fernandez, 2010). To take these spatial variations into account, three locations throughout the intertidal zone were sampled during each field experiment.

The exact sampling locations in the intertidal zone were determined by the extent of the swash/tide excursion during the high water and extent of the area affected by aeolian transport. The most seaward sampling location should not be too close to the low water line as there is no transport expected due to the high moisture content and, with onshore directed wind, due to the fetch effect. Additionally, the most landward sampling location should be at a low enough elevation to be impacted during high water. Wind predictions, water level predictions, measurements of the maximum runup during the preceeding high tide and visual cues in the field (e.g., the wreck line and berm location) were used to determine the most favorable sampling moment and locations.

Since the sand scraper is an intrusive sampling method, consecutive samples (in time) from the same reference cross-shore location were taken approximately 1–3 m apart in the alongshore direction. Real Time Kinematic (RTK) GPS measurements were collected to determine the exact horizontal and vertical coordinates of each sampling location. Alongshore grain size variability can be expected due to, for instance, aeolian sand strips (Hage et al., 2018; Nield et al., 2011), rips (Gallagher et al., 2011), and lag deposits (Zhenlin Li & Komar, 1992). Thus, the applied alongshore spacing could introduce deviations between consecutive samples that are not related to the temporal signals driven by waves and winds but related to the local alongshore variability. For this study, we initially assume that the signals related to the temporal signals dominate over the local alongshore variability.

Additionally, the sand scraper requires insertion into the bed surface. This invasive process may disturb the near-surface sediments by pushing them upwards, leading to some uncertainty in the precise depth below the surface at which sediment samples are collected. In cases where these disturbances occurred, the maximum vertical deviation is estimated to be around 2 mm. This can translate to vertical deviations between the depth of layers in samples that were collected at the same cross-shore location, but at different times (and thus different alongshore locations). However, these possible vertical deviations are limited, so temporal trends in the vertical variability of the grain size distribution are expected to be visible despite them.

4.2.4. Topographic surveys

At every field site, topographic surveys of the subaerial beach profile were conducted. These profiles were collected to determine the occurrence of erosion and deposition at the bed surface, as this is crucial to interpret the changes in the vertical variability of the grain size distribution. In Noordwijk and Waldport, RTK GPS transects were measured, and in Duck bed elevation data from a co-located continuously scanning terrestrial laser scanner were used (O'Dea et al., 2019). The elevations in the United States were

measured relative to NAVD88 and in the Netherlands relative to NAP. The error margin of the GPS measurements was in the order of 0.01–0.02 m. The largest changes in elevation occurred due to marine processes, so most profiles were measured before and after high water. In Waldport and Noordwijk, the cross-shore location of the maximum swash excursion was measured to indicate the extent of the marine processes during high water. The elevation changes due to the formation of depositional patterns during aeolian sediment transport were often within the error margin of the survey methods. Thus, during experiments where the initiation of these patterns was expected/observed, erosion pins were used to provide a more detailed indication of erosion and deposition.

4.2.5. Experiment specifications

A total of nine experiments were conducted divided over the three field sites (Table 4.2), resulting in 400+ individual samples. During most of the experiments, samples were collected to determine the effect of both marine and aeolian processes on the vertical variability of the grain size distribution (according to the sampling strategy in Figure 4.6). Additional samples were collected to evaluate the sampling method and to determine the effect of spatial variability.

The repeatability of the developed sand scraper sampling method was tested in Duck and Noordwijk by collecting two duplicate samples within 1–2 m distance of each other (repetition sampling, Table 4.2). By comparing these samples an indication of the extent of inherent variations in grain size and vertical deviations can be given.

The effect of marine and aeolian processes on the vertical variability of the grain size distribution were examined at all three field sites. In Waldport, on 23 Aug. 2021 (Table 4.2), samples were collected in the intertidal zone before and after high water (B-HW and A-HW/B-AT, Table 4.3). Subsequently, aeolian transport occurred during low water. However, during this event, aeolian transport was limited (see wind event described in Table 4.4). Thus, sampling after aeolian transport (A-AT) was only carried out at the most landward location where sediment transport had been observed. At this location, bedforms occurred during the event. Samples were collected on the crest and in the trough of the bedform to determine spatial variations in grain size.

In Noordwijk, on 5 Feb. 2020, samples were collected before and after high water (B-HW and A-HW) to determine the effect of marine processes on the vertical variability of the grain size distribution (Table 4.2 and Table 4.3). On 21 Jan. 2021, samples were again collected before and after high water (B-HW and A-HW/B-AT) followed by sampling after aeolian transport (A-AT), which had occurred during low water. The high water event was associated with relatively large waves and a surge that was largest before high tide but reduced to 0.4 m around the high tide peak (Table 4.3). The wind event that caused the aeolian transport was intense with large amounts of transport (Table 4.4).

Table 4.2: Overview of morphological and marine characteristics of field sites in Waldport (Oregon, US), Noordwijk (the Netherlands) and Duck (North Carolina, US).

Field site	Sampling type	Date	Sampling times
Waldport	Marine and aeolian	23 Aug. 2021	11 am (B-HW), 6 pm (A-HW/ B-AT) and 9 pm (A-AT)
	Bedform	23 Aug. 2021	9 pm (A-AT)
Noordwijk	Marine	5 Feb. 2020	8 am (B-HW) and 4 pm (A-HW)
	Marine and aeolian	21 Jan. 2021	4 am (B-HW), 1 pm (A-HW/ B-AT) and 6 pm (A-AT)
	Repetition	21 Nov. 2020	3 pm
Duck	Aeolian	1 Sep. 2021, 2 Sep. 2021	8 am (B-AT), 2 pm (D-AT) and 5 am (A-AT)
	Marine	2 Sep. 2021, 3 Sep. 2021	8 am (B-HW, 2 Sep. 2021), 10 am (A-HW, 3 Sep. 2021)
	Cross-shore	2 Sep. 2021	8 am
	Repetition	1 Sep. 2021	9 am

Table 4.3: Description of the high water events during which samples were collected with the sand scraper.

Event	Wave height	Tidal range	Max water level	Storm surge
Walport 23 Aug. 2021	1.6 m[a]	1.5 m[b]	2.0 m[b]	-[c]
Noordwijk 5 Feb. 2020	1.0 m[d]	1.3 m[e]	0.5 m[e]	-
Noordwijk 21 Jan. 2021	3.4 m[d]	1.3 m[e]	1.3 m[e]	avg. 0.4 m max. 1 m[e]
Duck 2 Sep. 2021 peak from 4 p.m.-1 a.m.	1.3 m[f]	0.8 m[g]	1.4 m[g]	0.3 m[g]

[a]Wave height from NOAA station 46098 offshore of Newport. [b]Predicted value from NOAA station 9434939 in Waldport. [c]No storm surge expected based on measurements at nearby stations. [d]Euro platform offshore of Noordwijk. [e]Scheveningen water level station. [f]NOAA station 44056 offshore of Duck. [g]NOAA station 8651370 on FRF pier.

Table 4.4: Description of the three wind events that resulted in aeolian transport during which sample samples were collected with the sand scraper.

Event	Wind direction	Average wind speed	Wind gusts
Walport[a] 23 Aug. 2021	Alongshore winds slightly onshore	7 m/s	up to 12.5 m/s
Noordwijk[b] 5 Feb. 2020	Alongshore winds slightly offshore	14 m/s	up to 23 m/s
Duck[c] 1 Sep. 2021 peak from 12 a.m.-6 p.m.	Alongshore winds slightly onshore	7 m/s	around 12 m/s, up to 15 m/s

[a]NOAA station 9435380 in Newport. [b]KNMI station in Hoek van Holland. [c]Measured at 5.5 m above the dune.

In Duck, sampling took place during a wind event and storm surge event related to remnants of Hurricane Ida as it passed along the east coast of the United States (Beven et al., 2022). Samples were collected to determine the effect of both marine and aeolian processes on the vertical variability of the grain size distribution. The samples were collected before, during, and after aeolian transport (B-AT, D-AT, and A-AT) that occurred during the peak of the wind event on 1 Sep. 2021 (Table 4.4). The vertical variability of the grain size distribution measured after the aeolian transport event was supplemented with beach surface samples down to 8 mm depth along an array with a cross-shore spacing of 1–2 m. The purpose of this experiment was to get a more detailed indication of the cross-shore gradients in grain size that were present in Duck, which were not fully captured by the three cross-shore sample locations.

The winds continued after 1 Sep. 2021 but they were not strong enough to cause aeolian transport. However, during the daytime of 2 Sep. 2021, the wind got a more onshore directed component, which resulted in a surge of approximately 0.3 m along the coast (Table 4.3). Samples were collected before and after the storm surge (B-HW and A-HW) to determine the effects of this high water event on the grain size distribution.

4.3. Results

In this section, the observed spatio-temporal patterns and vertical grain size variability in Waldport, Duck, and Noordwijk are presented. First, the repeatability of the new sampling method is shown. Then, each sampling occasion that provides insight into the marine and aeolian processes on the vertical variability of the grain size distribution is shown per field site. For most of the sampling locations, a comparison is made between the grain size distribution in each layer and the $\emptyset_{50}$ (weighted average median grain size of all layers in a cross-section) to provide insight into the comparison between bulk sampling and sampling with the sand scraper. Additionally, locations are pointed out

where the vertical grain size variability could have an effect on the sediment availability for aeolian sediment transport. To provide insight into the spatial variations in the vertical grain size layering, the spatial variability due to bedforms in Waldport, and the spatial variability due to cross-shore gradients in Duck are discussed.

4.3.1. Repetition samples

Repetition samples were collected in Noordwijk and Duck to determine local grain size variability at the beach surface, and assess the repeatability of the new sampling method (Figure 4.7). Here, we qualitatively compare the two adjacent samples that were taken at each field site. The samples from Noordwijk showed a comparable gradient with finer sand on top of coarser sand. However, there was a vertical shift in the boundary between the finer and coarser sand (dashed line in Figure 4.7). Possibly, the layer at 14 mm depth for Noordwijk 2 consisted of a mixture of the layers at 8 and 14 mm in Noordwijk 1, which would explain the intermediate grain size. In that case, the vertical deviation is smaller than 6 mm. Correcting for this vertical shift, corresponding layers from the two sample locations displayed minor deviations in median grain size, ranging from 5–15 μm. The repetition samples from Duck, show similar variations in vertical grain size as those from Noordwijk. Perhaps, the gradient from the surface down to 38 mm in Duck 1, where there is first fining and then coarsening, corresponds to the gradient down to 26 mm depth in Duck 2 (dashed line in Figure 4.7). The averaged median grain size, $\emptyset_{50}$, varied in the order of 5 μm and the vertical deviation is in the order of 6 mm.

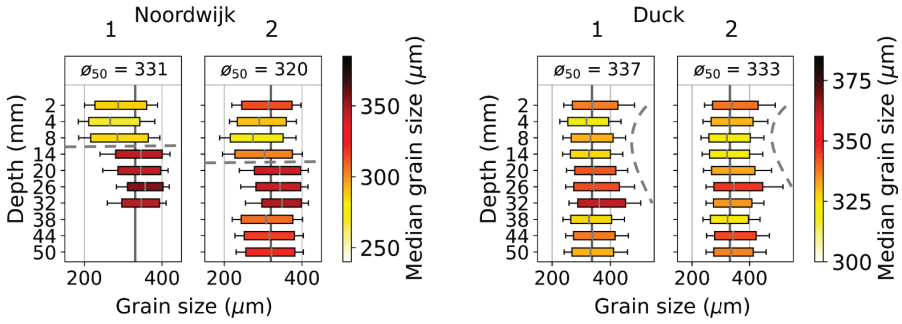

Figure 4.7: Vertical variability of the grain size distributions measured on 21 Nov. 2020 in Noordwijk, and 2 Sep. 2021 in Duck. Colors indicate the median grain size. Box plot dimensions are based on the D_{25} and D_{75}, and the extent of the whiskers on the D_{16} and D_{84}. $\emptyset_{50}$ indicates the averaged D_{50} in μm. At each field site, two samples were collected within 2 m of each other. The dashed grey lines indicate comparable trends that are present in the samples of each field site. For Noordwijk, the dashed grey lines emphasize a boundary between fine and coarse sediment which occurs in both samples, and for Duck they emphasize a vertical gradient that occurs in both samples.

4.3.2. Measured spatial and temporal variations in Waldport

The influence of marine and aeolian processes on the vertical grain size variability in Waldport was investigated through repeated sampling before (B-HW) and after high water (A-HW/B-AT), and after aeolian transport (A-AT) (Figure 4.8). After aeolian transport, sampling was only repeated at Location 3, since this was the only location with observed transport. Data were collected down to 50 mm at all sample locations in Waldport except at Location 1, where layers were only collected down to 32 mm due to rising tides during the B-HW collection.

Distinct spatial variations were visible in the vertical variability of the grain size distributions sampled from Location 1 (lower intertidal zone) to Location 3 (upper intertidal zone). The averaged median grain size, $\emptyset_{50}$, decreased in the landward direction (Figure 4.8). Additionally, the grain size distribution was most narrow and the D_{50} per layer resembled most closely the $\emptyset_{50}$ for Location 3. In contrast to for Location 1, where the vertical variability in the grain size distribution was the most heterogeneous, with the D14 and D86 covering a range from 210–460 μm.

The total water level covered all three sample locations between the B-HW and A-HW collections, and all locations showed a change in the vertical variability of the grain size distribution A-HW compared to B-HW. At Location 1, the D_{84} showed less peaks above 400 μm, and finer sand was available at the surface after high water, indicating that the sediment availability for aeolian transport might have increased. Before high water (B-HW), Location 2 showed fining downwards down to 32 mm depth, and coarsening in the deeper layers. This gradient was not as distinct after high water and larger variations in grain size occurred. This change in the vertical grain size variability is probably related to the morphological change (approximately 0.05 m of erosion) that occurred at this location (Figure 4.8a). Location 3 was influenced by only several swash excursions. In the 2 mm thick surface layer, the median grain size increased from 242 to 267 μm after the high water. Below the upper layer, there were small changes (order of 10 μm) in the vertical variability of the grain size distribution A-HW compared to B-HW. Given the lack of marine influence at the upper limit of the intertidal zone, these variations are more likely to be related to natural spatial variations in grain size than the effect of marine processes.

At Location 3, a 2 mm layer of finer sand was present on top of coarser material (2–8 mm depth) after the aeolian transport event (A-AT). The coarser material is probably related to the coarse deposit seen in the upper 2 mm A-HW. Potentially, there was a different distribution of the coarse layer between the sampling layers of the sand scraper resulting in the inclusion of more fine sediment in the samples and thus more moderate grain sizes. Four erosion pins were used in the field within 2 m of Location 3 during the aeolian transport event, which showed accretion in the order of 3 to 9 mm. Thus, it seems that the coarse bed surface was buried with a thin layer of fine sediment. This deposition might have been related to a meter-scale bedform that formed during the aeolian transport. Samples from the crest and in the trough of the bedform (Figure 4.9) show that the vertical grain size layering of the crest consisted of a 2 mm thick, fine sand layer on top of downward fining sediment. This downward fining gradient is also visible in the cross-section from the trough; however, the fine sediment layer on top is not present.

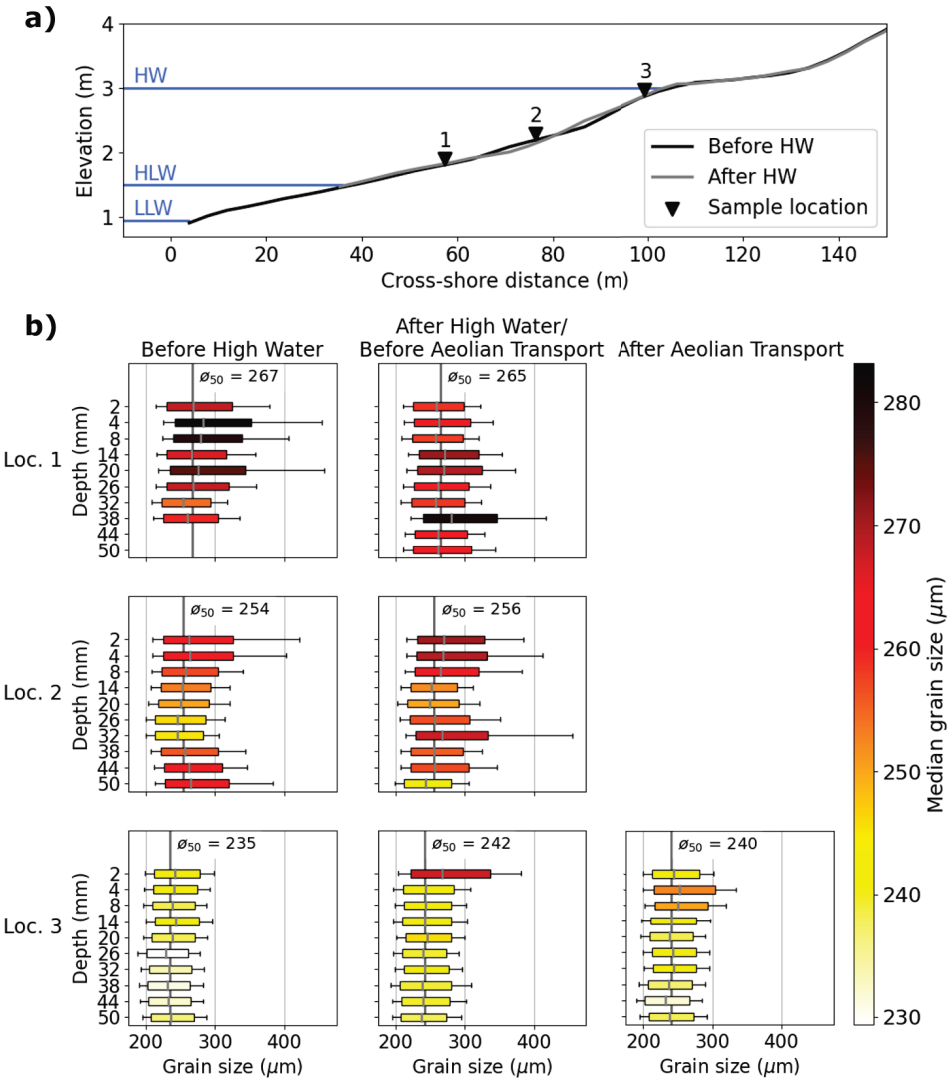

Figure 4.8: Overview of transects and the vertical variability of the grain size distributions measured on 23 Aug. 2021 in Waldport. a) Cross-shore profiles measured before (black) and after (grey) high water (HW). The upper blue line indicates the maximum swash excursion during high tide. The two lower blue lines indicate the low low water (LLW) that occurred before the HW and the high low water (HLW) that occurred after the HW. Sample locations are indicated by black triangles. b) Vertical grain size distributions sampled before high water (B-HW), after high water (A-HW/B-AT) and after aeolian transport (A-AT) which occurred during the subsequent low water. Colors indicate the median grain size. Box plot dimensions are based on the D_{25} and D_{75}, and the extent of the whiskers on the D_{16} and D_{84}. The $\emptyset_{50}$ indicated by the dark grey vertical line represents the averaged D_{50} in μm. Location numbers correspond to the locations in a).

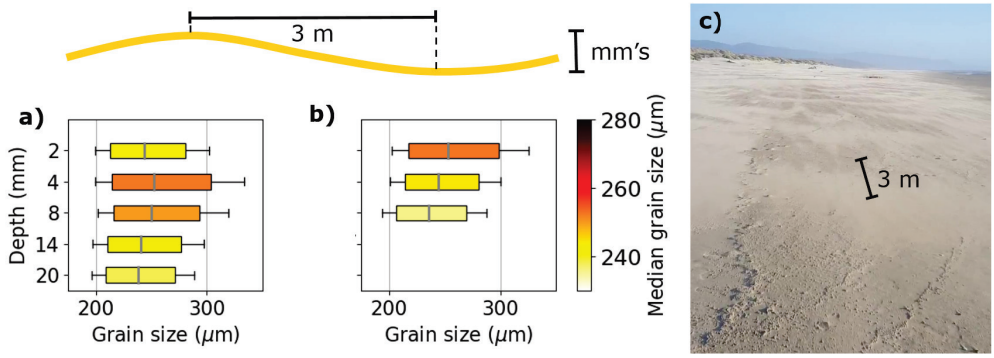

Figure 4.9: Schematic representation of a meter-scale bedform with a height in the order of millimeters and the vertical variability of the grain size distributions in its crest (a) and trough (b) as measured on 23 Aug. 2021 in Waldport. The bedform occurred on the landward end of the intertidal zone after a period of aeolian transport, as shown in panel c. Colors in panel a and b indicate the median grain size. Box plot dimensions are based on the D_{25} and D_{75}, and the extent of the whiskers on the D_{16} and D_{84}.

4.3.3. Measured spatial and temporal variations in Noordwijk

In Noordwijk, the vertical grain size variability due to the influence of marine processes was studied by sampling before (B-HW) and after high water (A-HW) on 5 Feb. 2020 (Figure 4.10). In both the B-HW and A-HW samples, the coarsest grain sizes were found on the landward side of the coastal profile (Location 3), but the $\emptyset_{50}$ of Locations 1 and 2 did not show a distinct cross-shore trend.

For Location 1, the vertical grain size layering was reversed after high water, with fine sand on top instead of in the deeper layers as before the high water. Despite this clear change in the vertical layering, the $\emptyset_{50}$ remained approximately the same. Thus, a bulk sample would have shown a relatively small change in grain size, whereas the vertical layering shows an increase in the availability of fine sand near the surface. The coastal profiles (Figure 4.10a) show that the bar moved landward (cross-shore distance = 20 m), corresponding to elevation changes up to 0.1 m and, thus, indicating mobilisation of a considerable amount of sediment around Location 1. This is in contrast to Location 3, where the calculated elevation change for Locations 2 and 3 was around 0.005 m, which was within the error margin of the GPS measurements. At this Location, only the upper limit of the gradient (dashed grey line in Figure 4.10) showed an upward 6 mm shift and the layers beneath that a shift of up to 18 mm.

On 21 Jan. 2021, a second field experiment was completed in the intertidal zone of Noordwijk. Samples were collected before and after high water (B-HW and A-HW/B-AT) and after the occurrence of aeolian transport (A-AT) during low water when a wind event occurred (Figure 4.11). Large amounts of transport were observed during the field data collection period (see conditions in Table 4.4). Thus, even when the A-HW/B-AT sampling was executed within an hour of the water receding, aeolian transport was already occurring. For Location 2, the exposure to aeolian transport was approximately

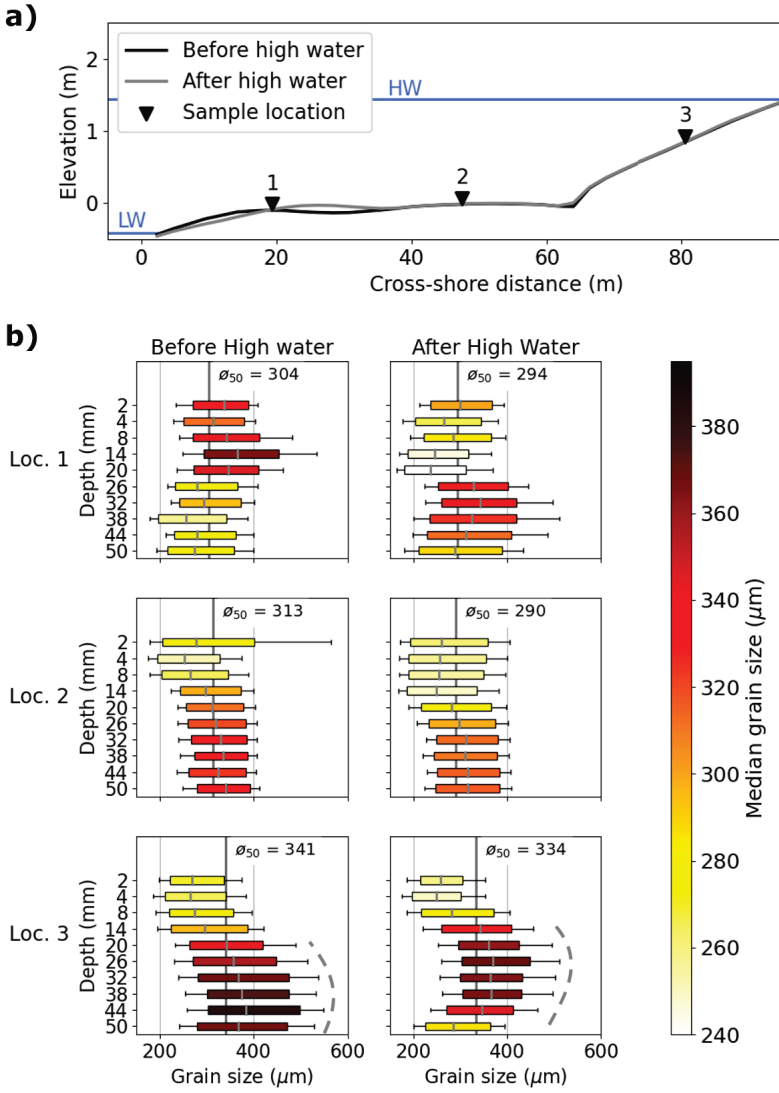

Figure 4.10: Overview of transects and vertical variability of the grain size distributions measured on 5 Feb. 2020 in Noordwijk. a) Cross-shore profiles measured before (black) and after (grey) high water. The upper blue line indicates the maximum swash excursion during high tide. The lower blue line indicates the low water (LW) elevation. Sample locations are indicated by black triangles. b) Vertical grain size distributions sampled before high water (B-HW) and after high water (A-HW). Colors indicate the median grain size (D_{50}). Box plot dimensions are based on the D_{25} and D_{75}, and the extent of the whiskers on the D_{16} and D_{84}. The $\emptyset_{50}$ indicated by the dark grey vertical line represents the averaged D_{50} in μm. Location numbers correspond to the locations in a). The dashed grey lines emphasize a comparable vertical gradient that was present in the samples from B-HW and A-HW at Location 3.

half an hour, and for Location 3, one hour. Similarly, the GPS transect measured after high water (Figure 4.11a, grey line) can also include some elevation changes due to aeolian transport that occurred. It was collected around low water when the profile had already been affected by aeolian sediment transport.

The largest change in the vertical variability of the grain size distribution after the high water event can be seen at Locations 1 and 3 (Figure 4.11b). Before high water, the vertical grain size variability at Location 3 was relatively uniform, with an averaged median grain size of 281 μm. However, after high water, a 14 mm thick layer of finer sand (255 μm) covered a layer of coarser sand (298 μm). This vertical layering, indicated by a dashed grey line in Figure 4.11b, is not shown by the change in $\emptyset_{50}$ (from 281 μm B-HW to 285 μm A-HW). This change in the vertical variability of the grain size distribution at Location 3 corresponded to a considerable change in morphology (Figure 4.11a). At Location 1, comparable downward coarsening gradients were present in the sediment B-HW and A-HW (dashed grey lines in Figure 4.11b). However, the lower limit of this gradient, defined here as the coarsest grain size present, became 12 mm deeper. Changes at Location 2 were relatively small, although the difference in grain size between the upper and lower layers became more pronounced (dashed grey line in Figure 4.11b). This resulted in a 7 μm increase of the $\emptyset_{50}$, although the grain size in the upper layers decreased.

The vertical variability of the grain size distribution changed considerably after the aeolian transport in Locations 2 and 3. During the aeolian transport, meter-scale bedforms were migrating past Locations 2 and 3. On the contrary, Location 1 did not show any major changes, and no clear bedforms were present. At Location 2, the vertical grain size variability became more uniform, with relatively fine sand compared to the other sampling locations and times. This might be related to the presence of aeolian deposits related to the bedforms that had an elevation in the order mm's to cm's (based on measurements with erosion pins). At Location 3, finer sand (256 μm) was present in the upper 14 mm before aeolian transport (dashed grey line in Figure 4.11b). After aeolian transport, Location 3 was located outside of a depositional patch. The layer of finer sand was no longer present, and the grain size of the upper 14 mm increased to 289 μm. This could indicate that erosion of the fine sediment occurred during aeolian transport.

4.3.4. Measured spatial and temporal variations in Duck

On 1 Sep. 2021, three locations on the dry beach in Duck were sampled (Figure 4.12). They were located above mean high water on a flat berm susceptible to inundation during storms (Figure 4.12a). The sampling on 1 Sep. 2021 was repeated before, during, and after the aeolian transport event (B-AT, D-AT, and A-AT), during a period where none of the three locations were inundated. The measured vertical variability of the grain size distributions showed vertical gradients but no clear spatial or temporal coherence (Figure 4.12b).

Overall in Duck, no clear temporal trend was visible in the vertical grain size variability of each location between the B-AT, D-AT, and A-AT sampling times. Still, there are large variations visible between the different times of each location, as indicated by variability in the $\emptyset_{50}$ and changes in the apparent vertical distributions of grain size (Figure 4.12b).

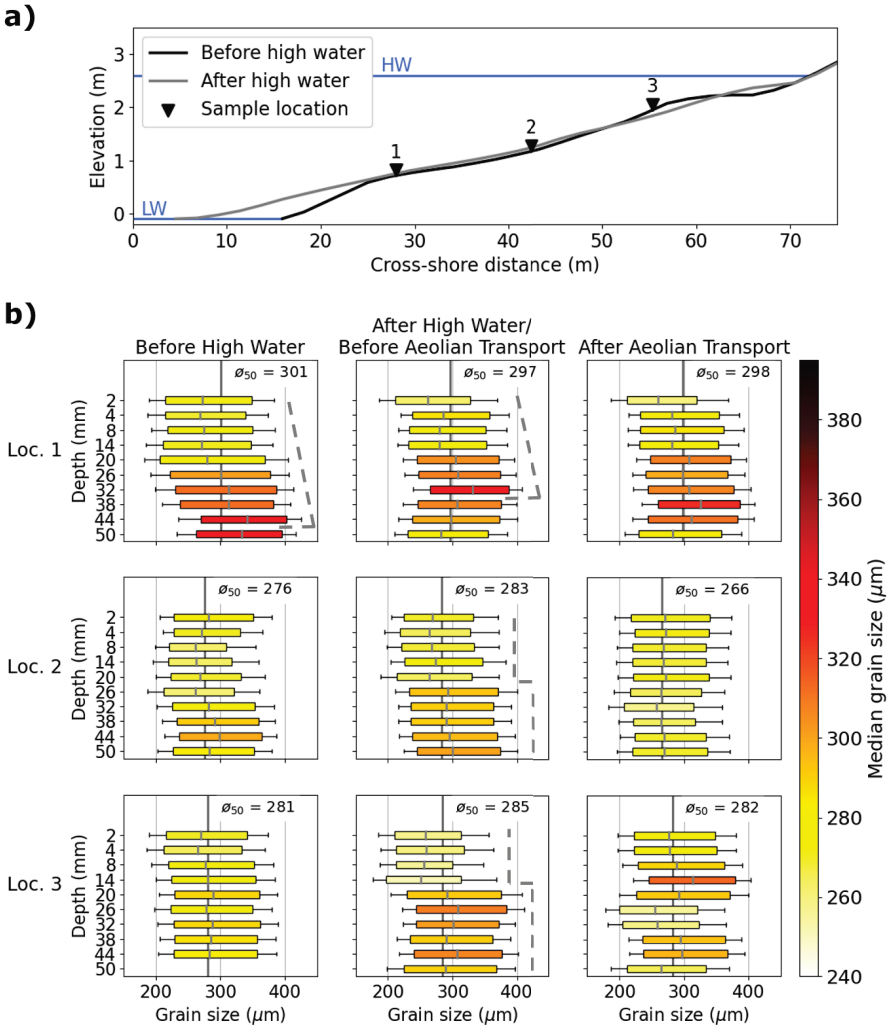

Figure 4.11: Overview of transects and vertical variability of the grain size distributions measured on 21 Jan. 2021 in Noordwijk. a) Cross-shore profiles measured before (black) and after (grey) high water. The upper blue line indicates the maximum swash excursion during high tide. The lower blue line indicates the low water (LW) elevation. Sample locations are indicated by black triangles. b) Vertical grain size distributions sampled before high water (B-HW), after high water (A-HW/BAT) and after aeolian transport (AAT) which occurred during the subsequent low water. Colors indicate the median grain size. Box plot dimensions are based on the D_{25} and D_{75}, and the extent of the whiskers on the D_{16} and D_{84}. The $\emptyset_{50}$ indicated by the dark grey vertical line represents the averaged D_{50} in μm. Location numbers correspond to the locations in a). The dashed grey lines in the vertical distributions of Location 1 emphasize a coarsening downward gradient that was present both B-HW and A-HW. The dashed grey lines in the vertical distributions of Locations 2 and 3 emphasize a boundary between finer sediment and coarser sediment that is present A-HW/B-AT at both of these locations.

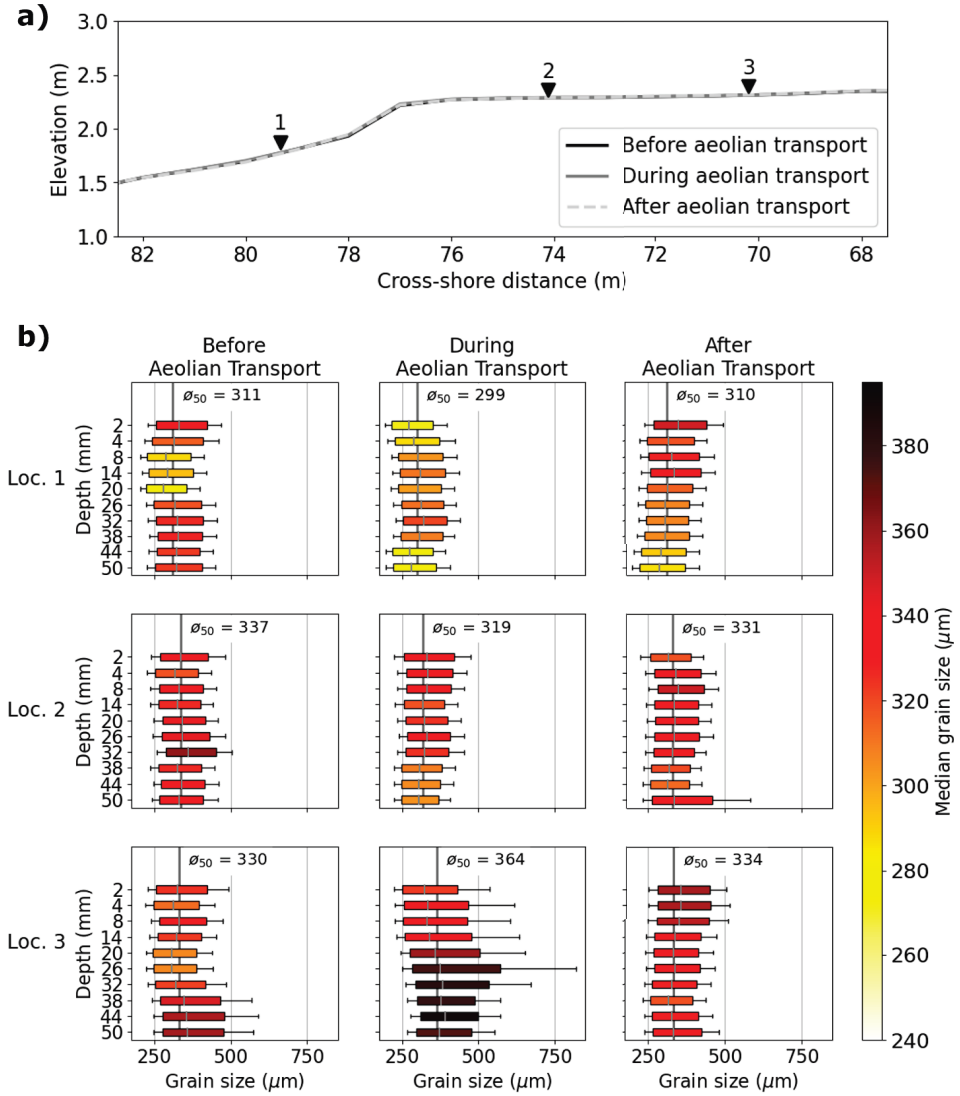

Figure 4.12: Overview of transects and vertical variability of the grain size distributions measured on 1 Sep. 2021 and 2 Sep. 2021 in Duck. a) Cross-shore profiles measured before (black), during (grey), and after (grey, dashed) aeolian transport. b) Vertical variability of the grain size distributions sampled before (B-AT), during (D-AT) and after aeolian transport (A-AT). Colors indicate the median grain size. Box plot dimensions are based on the D_{25} and D_{75}, and the extent of the whiskers on the D_{16} and D_{84}. The $\emptyset_{50}$ indicated by the dark grey vertical line represents the averaged D_{50} in μm. Location numbers correspond to the locations in a).

The lidar-derived topography data (Figure 4.12a) indicates that there was < 0.01 m of vertical change at all sampling sites over this period. Given these small net variations, limited observations of aeolian bedforms, and the absence of marine processes at the sampling locations, the observed temporal variability is presumed to reflect alongshore spatial variations more so than changes due to the occurrence of aeolian transport.

In the cross-shore, the averaged median grain size, $\emptyset_{50}$, for Location 1 (most seaward) was finer than those at Locations 2 and 3 (most landward). However, due to the large grain size variability, no clear cross-shore trend was present (Figure 4.12). Cross-shore sampling with decreased horizontal spacing (1–2 m compared to 4–6 m) was executed after the aeolian transport event (A-AT) (Figure 4.13). At this resolution, there was still significant vertical variability in the grain size distribution but an increase in grain size in the landward direction was visible.

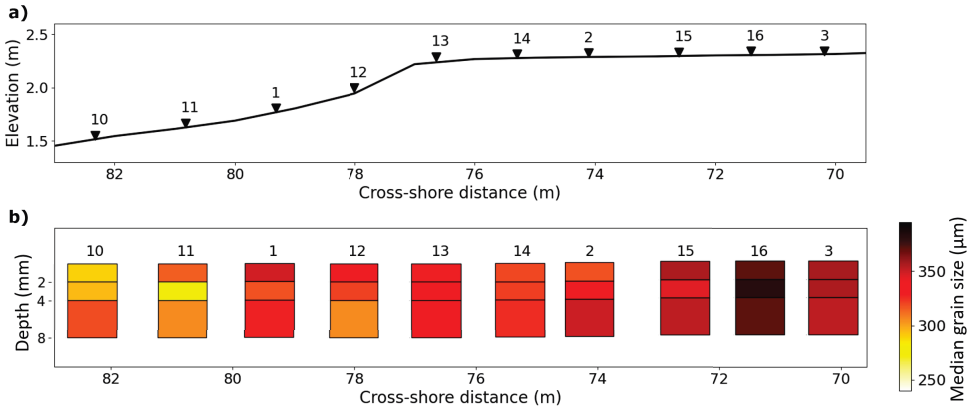

Figure 4.13: Overview of transect and vertical variability of the grain size distributions measured on 2 Sep. 2021 in Duck. a) Cross-shore profile based on laser scan with sampling locations indicated by black triangles. b) Vertical grain size variability sampled after aeolian transport. Colors indicate the median grain size. Location numbers correspond to the locations in a).

After the aeolian transport event, the wind became more onshore directed, which contributed to a storm surge of approximately 0.3 m along the coast (Table 4.3). Several locations were sampled before inundation (B-HW) and after inundation (A-HW) to determine the effect of marine processes (Figure 4.14). During the high water event, considerable erosion occurred, which resulted in the formation and landward movement of a beach scarp (± 0.2 m high, Figure 4.14a). Before inundation, Location 1 was on the dry beach near the most landward edge of the intertidal zone. After inundation, the scarp had formed and retreated landward of Location 1, resulting in bed lowering at Location 1 and marine inundation during high tide. At this point, Location 12 became the most seaward point landward of the scarp. During the high tide of the high water event, this location was influenced by some wave runup.

The vertical grain size variability in the intertidal zone changed considerably where erosion occurred during the high water event (Figure 4.14b). The most seaward location (Location 10), showed downward coarsening in grain size before inundation, which

changed into a downward fining gradient. Although, these additional samples had a maximum depth of 8 mm, which is far smaller than the total net erosion (up to 0.2 m) in this zone.

The vertical gradient in the grain size distribution at Location 12 kept fining downwards, although the range between the D_{16} and D_{84} became larger A-HW compared to B-HW. Especially, the surface layer became coarser which may be related to swash-related sediment transport that occurred at this location. In contrast, Locations 11 and 1, where the scarp moved landward, showed more substantial changes. Both locations changed from a vertical layering with the coarsest grain sizes on top to coarse sediment overlain with a 4–8 mm thick layer of fine sand. Based on visual inspection, the coarse material measured after inundation at 8 mm depth for Location 11, and 14 mm depth for Location 1 continued for at least several centimetres into the bed.

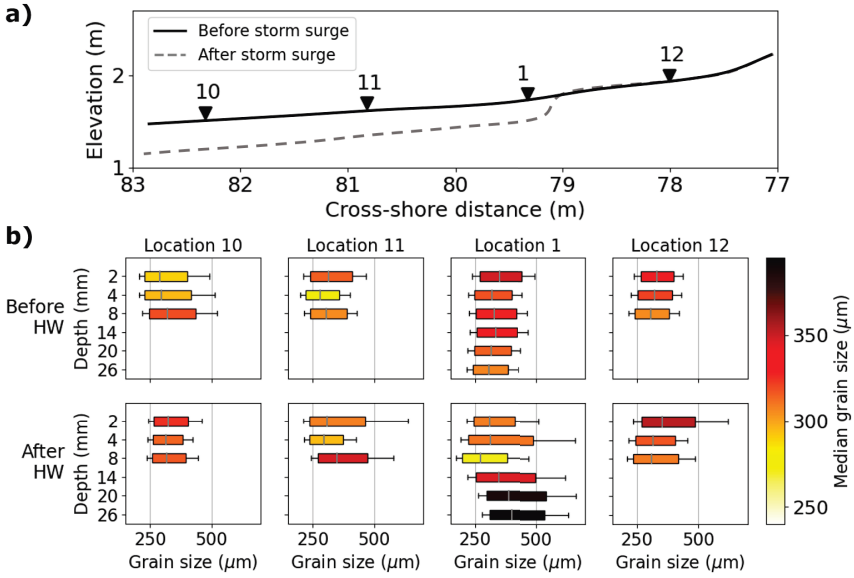

Figure 4.14: Overview of transects and vertical variability of the grain size distributions measured on 2 Sep. 2021 and 3 Sep. 2021 in Duck. a) Cross-shore profile based on laser scans and sketches from before (black) and after (grey, dashed) a storm surge occurred. b) Vertical variability of the grain size distributions sampled before marine (B-HW) processes and after marine (A-HW) processes occurred due to the storm surge. Colors indicate the median grain size. Box plot dimensions are based on the D_{25} and D_{75}, and the extent of the whiskers on the D_{16} and D_{84}. Location numbers correspond to the locations in a). Location 1 corresponds to Location 1 in Figure 4.9. The sampling before marine processes occurred after after aeolian transport, which corresponds to Figure 4.9, A-AT.

4.4. Discussion

A newly developed sand scraper was used to measure vertical grain size variability in the intertidal area at Waldport, Noordwijk, and Duck. Based on these case studies, we discuss to what extent marine and aeolian processes influenced the observed grain size variability and sediment availability for aeolian transport at the three field sites. Additionally, we discuss the applicability of the new sand scraper sampling method, and how the findings collected with the sand scraper can inform future research and modeling.

4.4.1. Observed spatial grain size variability

In agreement with previous studies (e.g., Çelikoglu et al., 2006; Stauble & Cialone, 1997), cross-shore gradients in grain size were observed at all three field sites (Figure 4.15). The maximum range in the $\emptyset_{50}$ measured horizontally between sampling locations was 32 μm for Waldport, 51 μm for Noordwijk and 65 μm for Duck. The data collected in Duck indicates that there can be alongshore variations in grain size that have a similar magnitude as the cross-shore variations, even at alongshore distances < 10 m. The longshore variability of grain size at Duck might be related to alongshore morphological features, such as beach cusps, or bioturbation due to ghost crab burrowing (Chakrabarti, 1981; Schlacher et al., 2016). Additionally, the considerable spatial grain size variation at Duck could be related to the wide grain size distribution that is present at this field site.

Despite this large heterogeneity in sediments alongshore at Duck, there was a clear cross-shore gradient in grain size when additional locations were added to increase

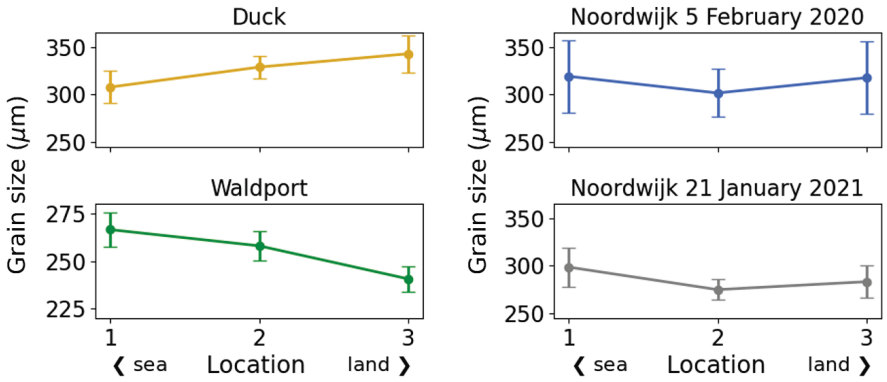

Figure 4.15: Overview of the cross-shore gradients in grain size and the associated standard deviation (shown as errorbars), calculated as the temporally averaged $\emptyset_{50}$ and standard deviation per field site, respectively. The cross-shore and marine sampling from Duck were excluded due to the limited sampling depths. Note that the sampling locations (1, 2, and 3) belonging to each panel (i.e., each sampling occasion) are not necessarily in similar locations along the coastal profile. However, Location 1 is always on the seaward side (sea) and Location 3 is always on the landward side (land), indicated by the arrows.

spatial resolution. This indicates that more spatially frequent sampling may be required to characterize the full heterogeneity of the spatio-temporal grain size dynamics of the bed. Combining the sand scraper with other grain size measurement methods could provide a viable solution. We especially recommend this approach for intermediate, mixed grain beaches where considerable spatial grain size variations could be expected.

4.4.2. Observed temporal grain size variability

By using the sand scraper, this study could show the detailed grain size layering at the bed surface and how it changed through time due to marine and aeolian processes. The most distinct temporal variations occurred where there was a significant morphological change after a high water event. This is consistent with studies from other field sites, which have attributed changes in grain size of the bed surface within the intertidal zone to sediment advection and sediment mixing due to, for instance, sandbar, bedform and berm migration (e.g., Sonu, 1972; Gallagher et al., 2011; Jackson & Nordstrom, 1993; Medina et al., 1994; Sherman et al., 1993).

The measurements show that marine processes resulted in fining of the surface sediments in several cases. At the Noordwijk site Location 1 in Figure 4.10, a bed of fine sand overlain with coarser sand before the high tide changed into coarse sand overlain with finer sand after the high tide. Similar trends were noted at both Location 3 in Figure 4.11 (Noordwijk) and Location 1 in Figure 4.14 (Duck), where temporal fining occurred. In these cases, the contrast between the upper finer and the lower coarser layers increased after the high water event. The measured morphological change at these sampling locations was typically small, < 0.1 m, except in the case at Duck. Still, the changes in the intertidal profile indicated that a combination of both sediment advection and mixing likely had occurred. Based on the available data, the exact hydrodynamic mechanisms that affected sediment redistribution within the intertidal zone cannot be determined. However, the results indicate that marine processes can be an important means of introducing fine sediments to the bed surface.

Meanwhile, other observations indicate that the marine processes can also result in coarsening of surface sediments. There were two cases where the surface layer changed and became coarser after the high water at the upper portion of the intertidal zone, in Waldport Location 3 in Figure 4.8 and Duck Location 12 in Figure 4.14. In the Waldport case, it appears that a thin veneer of coarser grains was deposited directly on top of the fines. Bauer (1991) observed a similar veneer and related it to a large wave's swash excursion that occurred during high tide. According to Bauer (1991), the coarse sand was transported by the uprush, followed by rapid deposition as considerable infiltration reduced the flow during the downrush. A different formation mechanism was given by Clifton (1969) and Sallenger (1979), who described how vertical segregation of grains during wave backwash can result in lamination with coarse grains near the surface. In this research, the specific explaining mechanism is unclear. However, both occasions of near-surface coarsening that were recorded were located near the upper limit of wave run-up during high tide, indicating that formation of the coarse layer could indeed be related to the backwash that occurred during receding tide. In summary, the results show that marine processes alter grain size variability and that these processes, depending on which small-scale processes are occurring and which antecedent bed

composition is present, may lead to either coarsening or fining of the surface sediment.

When considering aeolian sediment transport, the surface layer was expected to become coarser due to grain size-selective pickup by the wind. However, the observations following aeolian transport events saw both coarsening and fining of the bed surface. At Noordwijk Location 3 in Figure 4.11, the grain size in the surface layer coarsened after an aeolian transport event, possibly due to the removal of fine sand. In contrast, there were two occasions, Waldport Location 3 in Figure 4.8 and Noordwijk Location 2 in Figure 4.11, where the grain size in the surface layer decreased. The decrease in grain size was associated with an increase in the bed elevation, indicating deposition of aeolian transported sediment. The deposition in Waldport occurred during conditions with alongshore winds that caused meter-scale bedform formation (Figure 4.9). On the crest of the bedform, fining of the bed surface occurred, while coarser sediment was present in the surface layers of the trough. The observations show that fine sediment, which increases the sediment availability, could be supplied to the intertidal zone from upwind areas during aeolian transport events.

4.4.3. Implications for sediment availability for aeolian transport

Aeolian transport rates are influenced by grain size in many ways. In the commonly used aeolian transport equations by Bagnold (1937b), the transport rate, threshold velocity, and parameterization of the bed roughness all depend on the grain size. de Vries, Arens, et al. (2014) proposed that the intertidal zone is an important source area for aeolian transport towards the dunes. A following study demonstrated wind-induced erosion of about 20 mm/h in the intertidal area during low tide using a terrestrial laser scanner (e.g., de Vries et al., 2017). Thus, the grain size of the upper layers in the intertidal zone is assumed to be important for the sediment supply of aeolian transport towards the dunes.

The observations in this study showed that individual layers could significantly deviate from the vertically averaged median grain size, $\emptyset_{50}$, in the upper 50 mm of the bed surface. If vertical grain size variability were determined based on the $\emptyset_{50}$, it would be assumed that the sediment availability for aeolian sediment transport is uniform in the vertical. Such assumptions could lead to errors because of the strong relationships between grain size and aeolian transport processes. For example, in the case of the Duck measurement campaign the measured D_{50} for Location 1 (A-AT) was 349 μm at 2 mm and 286 μm at 50 mm below the bed surface (Figure 4.12b), with a $\emptyset_{50}$ of 310 μm. These measurements result in threshold velocities for aeolian transport of 10.1 m/s, 9.1 m/s, and 9.5 m/s, respectively, as calculated according to Bagnold (1937b) for wind speeds at 2 meter above the bed. Since sediment transport rates are commonly expressed as a cubic relation with the threshold velocity (Bagnold, 1937b; Kawamura, 1951; Lettau & Lettau, 1978; Sherman & Li, 2012), differing sediment fluxes may be expected for each of those D_{50} values for the exact same wind speed.

4.4.4. Sand scraper methodology advantages and limitations

The sand scraper was developed with the aim to provide a method to determine the vertical variability in grain size at the beach surface, which can impact the sediment

availability for aeolian sediment transport. In agreement with previous studies (e.g., Emery, 1978; Masselink et al., 2007), the measurements with the sand scraper showed considerable vertical variability in grain size in the layers that make up the upper 50 mm of the bed surface. The maximum range in D_{50} measured vertically within the top 50 mm was 29 μm for Waldport, 119 μm for Noordwijk and 67 μm for Duck. Specifically, Waldport Location 2 in Figure 4.8, Noordwijk Location 3 in Figure 4.10, and Duck Location 1 in Figure 4.11 all show places where the D_{50} of the individual layers show relatively large deviations from the $\emptyset_{50}$, the average D_{50} of the vertical profile. In these cases, the sand scraper provides detailed information about the bed composition that could not be attained using grab sampling or surface imagery observations.

The sand scraper has some limitations regarding labour intensity, the intrusive nature of the method, and the specific dimensions of the device. Labour intensity limits the applicability of the sand scraper due to the time required to collect (15–30 minutes per location) and subsequently analyse (multiple hours per location) the grain size of each sample. This makes it difficult to sample over large spatial scales with a high temporal resolution compared to, e.g., conventional grab sampling. It is recommended to combine the sand scraper with bulk sampling or photo-based analysis to, for instance, more clearly distinguish cross-shore grain size trends and sub-hourly temporal developments of the surface grain size. To limit the analysis time of the samples collected with the sand scraper, only their grain size was determined. However, shell content, and mineralogical and density properties can be expected to affect aeolian sediment transport rates. Further analysis that is needed to study these factors would not be possible with, e.g., camera imagery, but can be executed on samples collected with the sand scraper due to the direct sampling approach.

However, the intrusive nature of the sampling method limits the application of the sand scraper since sediment is removed from the beach during sampling. Thus, temporal changes in the bed cannot be studied at the exact same location; the sampling needs to be repeated some distance away. Repeatability tests within 1–2 m distance showed that the grain size of corresponding layers between adjacent samples could vary by about 5–15 μm (Figure 4.7). Part of the variability was associated with vertical offsets in bed layering (relative to the bed surface). However, the observed differences were small enough to compare vertical variability in grain size between repeated samples. Due to the labour intensity of collecting measurements, the repeatability was addressed mostly qualitatively. By executing a focused field effort, more extensive sampling could allow for a more quantitative, statistical analysis of the repeatability in the future.

Lastly, the sand scraper has specific dimensions that limit its application. For example, the scraper takes a discrete set of slices with a minimum resolution of 2 mm. This is suitable for a flat bed of sand-sized sediment ($<$ 2 mm), but these slices might not fully represent larger structures such as wind-driven ripples and shells. Specifically, variations in grain size that occur in wind-driven ripples with coarser grains at the crests and finer grains in the troughs (observed by, e.g., Uphues et al., 2022), would likely not be recorded with the sand scraper sampling methodology. Ripples were not present in the areas sampled in this research. The sampling surface can also be disturbed by shells and coarser grains, causing vertical offsets in the 2 mm thick vertical slices. Thus, a larger layer thickness is recommended when shells or coarse sand are present. Another

limiting dimension is the sampling depth limit of 50 mm, which was selected based on the intended purpose of measuring grain size variability at the beach surface to analyse sediment availability for aeolian transport. For applications where sampling to larger depths is needed, the scraper would require a redesign.

While the sand scraper limitations should be taken into account when applying the methodology, the main advantage of the device is that it provides the ability to study the spatial and temporal variations in grain size at a consistent vertical resolution at the sub-centimeter scale that was previously not attainable with, e.g., grab sampling and sediment coring.

4.4.5. Future measurements and modelling

Most previous studies have inferred changes in sediment availability in the bed from measured changes in sediment fluxes (e.g., de Vries, Arens, et al., 2014). In contrast, this study focused on resolving changes in bed properties directly by observing changes in grain size distributions in the bed surface. Future studies are expected to focus on additional measurements and modelling of grain size variability.

This study demonstrated significant spatio-temporal variability in grain size in the intertidal zone, both in the vertical and horizontal, which is expected to influence aeolian transport rates. However, the extent to which the changes in vertical grain size variability affect the aeolian transport is still unknown. A combination of both in-situ measurement techniques for measuring sediment transport rates and patterns, in addition to coincident tracking of bed composition changes, could provide further insight. Future research questions concern how spatial gradients in sediment transport that cause local erosion or deposition result in changes in bed characteristics, and how those bed characteristics directly alter the transport field through altering the threshold velocity and sediment supply.

Contrary to the spatio-temporal variations in grain size found in the sand scraper measurements, most simulations of coastal sediment transport processes are based on sparse grain size data and commonly assume a homogeneous bed composition within the model domain (M. A. Davidson & Turner, 2009; Hallin, Almström, et al., 2019; Hoonhout & de Vries, 2019; Vousdoukas et al., 2011). Numerical models for coastal applications are typically based on reduced complexity approaches to achieve numerical stability and reasonable simulation times. For most applications, it will not be feasible to incorporate the level of detail on grain size information that was presented in this study. However, exploratory process-based modelling with variable bed composition could give insights into the errors associated with generalizations of bed composition. Furthermore, a combination of field and model data could be used to explore possible parameterizations of the grain size variability related to marine and aeolian processes.

In the measurements presented in this study, variations in grain size caused by marine processes were often related to morphological change due to bar or berm movement and scarp erosion, matching previous research that showed abundant morphological change in the intertidal zone at the tidal time scale (e.g., Brand et al., 2019; Masselink et al., 2007; Phillips et al., 2019). When erosion occurs, the new vertical variability in grain size is likely partially determined by the exposure of lower-lying sediment layers (Gallagher et al., 2016). Thereby, antecedent sediment deposition can be important

for the prediction of sediment availability for aeolian sediment transport. In accretive conditions, synchronization between the transfer of sediment by marine processes and the sediment supply for aeolian sediment transport can occur (Houser, 2009). Coupled numerical models of marine and aeolian processes (e.g., Cohn, Hoonhout, et al., 2019; Roelvink & Costas, 2019) could be used to quantify the potential influences of horizontal and vertical redistribution of sediments by marine processes on aeolian transport rates.

The effect of marine processes on the grain size distribution can be studied further by collecting additional samples with the sand scraper. These samples can provide the grain size composition that marine processes act upon and consequently the grain composition they leave behind. In this research, measurements were collected at three field sites on only one or several (separate) occasions. However, sampling efforts could be extended in time to investigate the effect of different conditions (varying wave heights, surge heights, etc.) on grain size. For example, Yokokawa and Masuda (1991) showed that variations in deposit thickness were related to the tidal range of a tidal cycle. Thus, samples could be collected throughout a neap-spring cycle to assess the effect of varying tides on changes in grain size distribution. Consequently, these measurements could act as verification for marine process models that show vertical variability in grain size (Reniers et al., 2013; Srisuwan et al., 2015).

4.5. Conclusions

In this research, a newly developed sand scraper was used to measure the near-surface vertical grain size variability and analyse the effect of marine and aeolian processes on grain size dynamics in the intertidal zone of three different field sites. The sand scraper provides the ability to study the spatial and temporal variations in grain size at a consistent mm-scale vertical resolution that was previously not attainable.

The data collectively indicate that there is a cross-shore gradient in grain size across all the measured beaches, reinforcing the concept that beach grain size characteristics are far from homogeneous. Further, alongshore variability, which was prevalent on the mixed-grain, intermediate beach studied here, can dominate over the cross-shore and temporal variability. These insights highlight the limitations of sparse sediment sampling and assumptions that those data are representative for the bed composition over large spatial domains.

The most distinct cases of change in the vertical variability of the grain size distribution by marine processes occurred in cases with significant morphological change during high water. The marine processes resulted both in fining and coarsening of the surface layer. The coarsening was assumed to be related to the formation of a veneer of coarse sediment near the upper limit of wave run-up.

During aeolian transport, the expected coarsening of the near-surface grain size was observed in some measurements, however, fining also occurred. The observed sediment fining at the bed surface may be explained by deposition that occurred due to the formation and development of aeolian bedforms within the intertidal zone. The measurements collected with the sand scraper showed that individual layers can considerately deviate from the vertically averaged median grain size in the upper 50 mm

of the bed surface. In addition, the device and data presented in this research can be used to inform future sediment sampling strategies and sediment transport models that investigate the feedbacks between marine and aeolian transport, and the vertical variability of the grain size distribution.

Data availability

The sand scraper design, the grain size and elevation data, and the software used to analyze the data and create the figures in this chapter are available in the 4TU repository, https://doi.org/10.4121/c.5736047.

Acknowledgements

This work is part of the research programme DuneForce with project number 17064, which is (partly) financed by the Dutch Research Council (NWO). This research could not have been possible without the help of Pieter van der Gaag who designed the Sand Scraper in collaboration with Christa van IJzendoorn and constructed the device together with DEMO (TU Delft). Thanks to DEMO for their close collaboration during the construction and development of the Sand Scraper. We would like to thank the many people that came out to help Christa van IJzendoorn during fieldwork, especially Sander Vos (TU Delft) and Hailey Bond. Thanks to Meagan Wengrove, John Dickey, Peter Ruggiero, and Jeff Wood from Oregon State University for providing support for the field experiment in Waldport, Oregon. Field efforts in Duck, North Carolina, at the U.S. Army Engineer Research and Development Center's (ERDC's) Field Research Facility were executed as part of the During Nearshore Event Experiment (DUNEX), which was facilitated by the U.S. Coastal Research Program (USCRP), and with aeolian transport R&D funding for Nick Cohn through the ERDC Basic Research Program, Program Element 601102/Project AB2/Task 01.

5

Modeling the impact of grain size variations on aeolian sediment transport

Chapter 4 showed that considerable variations in grain size can be present on the beach. These variations occur in the alongshore, cross-shore and vertical dimensions. It is unknown to what extent these spatial grain size variations result in relevant effects on aeolian sediment transport. Therefore, this chapter uses scenarios that are inspired by the results presented in Chapter 4 to implement simplified grain size variations into an aeolian transport model. Simulations with this model are used to determine the effects of different grain size distributions and spatial grain size variations on aeolian sediment transport and coastal dune development.

Chapter highlights:

- We created scenarios to test the effect of varying grain size distributions and spatial grain size variations on aeolian transport with the AeoLiS model.
- The median grain size can be used as a representative grain size in aeolian sediment transport modeling on a time scale of days to years.
- Vertical layering influences aeolian transport on minute time scales but its effect is limited on time scales longer than days.
- The grain size at the bed surface in the upwind, source area might be the most relevant to include in aeolian sediment transport models.

This chapter was submitted for publication in *Journal of Geophysical Research: Earth Surface* as:
C.O. van IJzendoorn, C. Hallin, A.H.J.M. Reniers and S. de Vries (2023). Modeling multi-fraction coastal aeolian sediment transport with horizontal and vertical grain size variability.

Abstract

Grain size affects the rates of aeolian sediment transport on beaches. Sediment in coastal environments typically consists of multiple grain size fractions and exhibits spatiotemporal variations. Still, conceptual and numerical aeolian transport models are simplified and often only include a single fraction that is constant over the model domain. It is unclear to what extent this simplification is valid and if the inclusion of multi-fraction transport and spatial grain size variations affects aeolian sediment transport simulations and predictions of coastal dune development. This study applies the numerical aeolian sediment transport model AeoLiS to compare single-fraction to multi-fraction approaches for a range of grain size distributions and spatial grain size scenarios. The results show that on timescales of days to years, single-fraction simulations with the median grain size, D_{50}, often give similar results to multi-fraction simulations provided the wind is able to mobilize all fractions within that time frame. On these timescales, vertical variability in grain size has a limited effect on total transport rates, but it does influence the simulation results on minute timescales. Horizontal grain size variability influences both the total transport rates and the downwind bed grain size composition. The results provide new insights into the influence of beach sediment composition and spatial variability on total transport rates towards the dunes. The findings of this study can guide the implementation of grain size variability in numerical aeolian sediment transport models.

5.1. Introduction

Sediment available for aeolian transport in coastal settings is characterized by a grain size distribution that is typically described with a range of grain size fractions (Krumbein, 1934). Grain size affects aeolian sediment transport due to the larger drag and lift force that is necessary to displace coarser grains (Durán et al., 2011; Sarre, 1987). Grain size also alters the creep and saltation trajectory of sediment (e.g., Cheng et al., 2015; P. Zhang et al., 2021). Therefore, different grain size fractions lead to different rates of sediment transport.

Field measurements on beaches have shown considerable spatial variations in grain size in the alongshore (Hallin, Almström, et al., 2019), cross-shore (Bauer, 1991; Çelikoglu et al., 2006; Edwards, 2001; Sonu, 1972; Stauble & Cialone, 1997; van der Wal, 2000a; van IJzendoorn et al., 2022). These horizontal and vertical grain size variations are expected to have a complex, combined effect on aeolian sediment transport, especially since grain size and sediment transport continuously interact. However, it is unknown how the spatial grain size variability influences the rate of aeolian transport towards the dunes.

Despite the variable transport rates for the different grain size fractions available in beach sediment, aeolian models (e.g., Hoonhout & de Vries, 2016; Van Dijk et al., 1999; Roelvink & Costas, 2019; Hallin, Larson, & Hanson, 2019) are typically simplified by using a single fraction throughout the model domain (e.g., Hallin, Huisman, et al., 2019; Hoonhout & de Vries, 2016; van der Wal, 2000b). However, some models can simulate multi-fraction transport, including the effect of sorting and the associated changes to the grain size distribution in the bed. An example of such a model is

AeoLis, a process-based aeolian sediment transport model. The model has been used for multi-fraction simulations (e.g. Hoonhout & de Vries, 2016, 2019) but the difference in transport rates compared to single-fraction simulations has not yet been fully quantified.

We hypothesize that the inclusion of multi-fraction transport and spatial grain size variations in aeolian transport simulations has a considerable effect on the calculated sediment transport. Investigating these effects in an aeolian sediment transport model can provide new insights into the functioning of the aeolian sediment transport chain. Additionally, quantifying the effects of grain size is expected to provide important recommendations for grain size as an input parameter in future aeolian transport modeling that is used for coastal dune development predictions. This quantification can also impact the use of grain size as a design parameter in the implementation of interventions in the coastal dune system (e.g., Kroon et al., 2022).

This research investigates to what extent sorting in multi-fraction sediment transport modeling and spatial grain size variations impact aeolian sediment transport. The important processes in the aeolian sediment transport chain are discussed in Section 5.2.1. The choice for a numerical model as study tool is explained in Section 5.2.2. The numerical implementation of different grain size scenarios that were simulated are presented in Section 5.3. In Section 5.4, the aeolian transport rates that resulted from the different grain size scenarios are presented. These results are discussed in Section 5.5 and the conclusions are drawn in Section 5.6.

5.2. Background

5.2.1. Modeling the aeolian sediment transport chain

Model concepts of the impact of multi-fraction transport and spatial grain size variations require that all relevant aeolian sediment transport processes are represented in the model (Figure 5.1). The bed stratigraphy consists of vertical layering with varying grain size distributions (van IJzendoorn et al., 2022). The wind forcing, the horizontal influx (upwind) and outflux (downwind) of sediment, and the sediment available at the bed surface determine the rate of deposition/erosion that occurs (de Vries, Arens, et al., 2014; Houser, 2009). High wind scenarios increase the probability of erosion, however, coarse sediment at the surface can impede pickup of sediment when armoring occurs (Gao et al., 2016; McKenna Neuman & Bédard, 2017).

Additionally, bed roughness and the fetch effect may impact whether erosion or deposition takes place. A larger bed roughness increases the transport capacity (Bagnold, 1937b). Bed roughness can vary greatly on the beach as the bed characteristics are variable and dynamic (Bristow et al., 2022; Field & Pelletier, 2018; Owen, 1964; van Rijn & Strypsteen, 2020; Sherman, 1992). The fetch effect describes how the sediment concentration in the air column increases downwind from the start of the domain until fully developed transport is reached (Bauer & Davidson-Arnott, 2002; Delgado-Fernandez, 2010; Gillette et al., 1996). Fully developed transport occurs when there is no additional pickup of sediment anymore and the influx and outflux at a certain location are equal. Erosion and deposition of sediment results from the difference between actual and equilibrium transport.

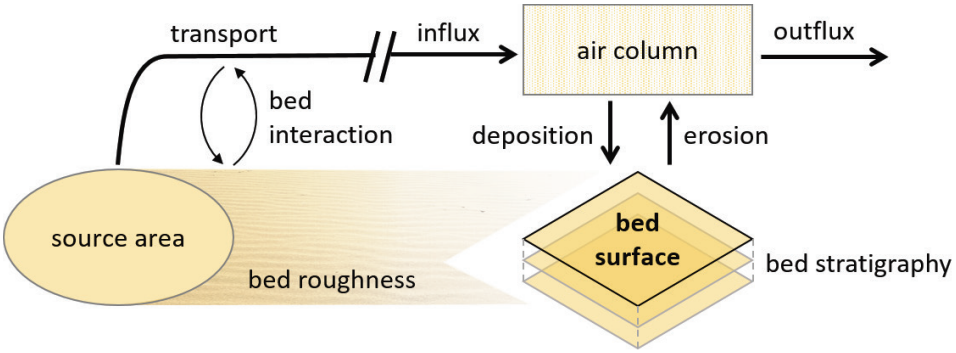

Figure 5.1: Conceptual representation of the interaction between grain size on the bed surface and in the air column during aeolian sediment transport on the beach.

In case of erosion, the change in bed surface grain size will be dominated by the bed stratigraphy, especially as underlying sediment layers can be exposed and armor layers can form (Hoonhout & de Vries, 2016). In the case of deposition, the change in bed surface grain size will be dominated by the grain size of the sediment in the air column. The sediment composition in the air column is determined by processes that occur upwind of the bed surface location. The sediment in the air column was picked up from the source area during antecedent wind conditions and was transported towards the bed surface location (i.e. advection). During this transport, bed interaction (i.e. the splash process) might have resulted in an exchange of sediment between the air and the bed (Anderson & Haff, 1988). This exchange can alter the grain size distribution of the sediment in the air column depending on the sediment composition of the beach between the source area and the bed surface location (Dong et al., 2004).

5.2.2. Studying the role of grain size in the sediment transport chain

In the field, it is difficult to distinguish the effect of grain size variability from other varying environmental conditions, such as the wind field, bedforms, and surface moisture. Field measurements are often limited to a single location, which means they can show temporal patterns in grain size composition that are related to transport processes occurring upwind (Cohn, Dickhudt, & Marshall, 2022; Field & Pelletier, 2018). Furthermore, it is difficult to observe the vertical bed composition at a relevant scale with non-invasive observation techniques (van IJzendoorn et al., 2022). Here, modeling has a major advantage as it allows the recording and investigation of the transport chain, including the source area, advective transport through the air, and bed surface grain size throughout the domain.

The numerical aeolian sediment transport model AeoLiS was selected as a tool to simulate the effect of grain size on aeolian transport in this research. AeoLiS provides a systematic approach to studying spatiotemporal grain size variations. Distinguishing the impact of grain size from the many other factors that affect aeolian sediment transport on the beach is challenging. Therefore, wind tunnel experiments, in which the environmental conditions can be controlled, have been used to isolate individual

aspects of aeolian sediment transport (e.g., grain size by Bagnold, 1937a, and shells by McKenna Neuman et al., 2012). However, it would be difficult if not impossible to set up experiments with complex bed composition variations at reasonable monetary, time, and labor costs. Numerical modeling provides an opportunity to gain useful insights into this type of variations at relatively low cost.

5.3. Methods

5.3.1. Model description

The multi-fraction approach of the AeoLiS model makes it suitable to study the effect of grain size variations on aeolian transport. The sediment bed in the model consists of a user-defined number of vertical layers and horizontal grid cells. The definition of vertical layers is crucial for describing the process of coarsening and fining and its associated vertical grain size gradients in the model. The bed composition, which is the initial spatial grain size variation of the bed throughout the domain, can be prescribed in the latest version of the model (AeoLiS v2.1.0 by AeoLiS Development Team, 2023). Transport, erosion and deposition are calculated for each grain size fraction individually (Figure 5.2), allowing for surface armoring to occur as finer grains are removed, and coarse grains stay behind (Hoonhout & de Vries, 2016).

In AeoLiS, the equilibrium transport rate for each grain size fraction is calculated based on an adapted version of the Bagnold equation (Bagnold, 1937b), formulated as

$$Q = C\frac{\rho_a}{g}(u_* - u_{t,*})^3 \tag{5.1}$$

in which Q (kg/m/s) is the aeolian sediment transport rate in the case of saturated transport, where C (-) is a constant equal to 1.5 that accounts for sediment gradation, ρ_a (kg/m^3) is the density of air, and g (m/s^2) is the gravitational constant. The u_* is the surface shear velocity which represents the force exerted on the surface by the wind. The $u_{t,*}$ is the threshold shear velocity which represents the shear velocity at which grains at the surface start to move (initiation of motion).

The threshold shear velocity is expressed as

$$u_{t,*} = A\sqrt{\frac{\rho_s - \rho_a}{\rho_a} g d} \tag{5.2}$$

in which ρ_s (kg/m^3) is the density of the sediment, d is the grain size diameter, and A is a constant coefficient equal to 0.085. The shear velocity is expressed as

$$u_* = u_w \frac{\kappa}{\ln \frac{z}{z_0}} \tag{5.3}$$

in which u_w (m/s) is the wind velocity at height z (m) and z_0 (m) is the aerodynamic roughness. The κ (-) represents the Von Karman constant. The z_0 depends on the surface characteristics of the bed (i.e., the bed roughness). It should be noted that, in

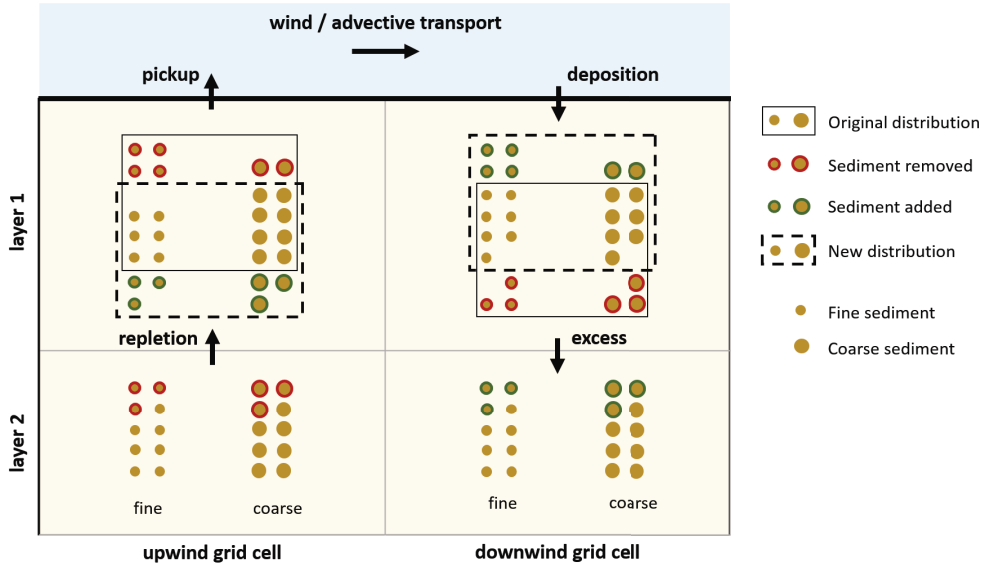

Figure 5.2: Schematization of the implementation of discrete layering in AeoLiS and the effects of erosion and deposition on the grain size distribution. The total mass in each grid cell of each layer is normalized. This normalization is represented by the fact that the grain size distribution in each grid cell (indicated by solid and dashed, black rectangles) should contain exactly 20 sediment grains. In the upwind grid cell, the bed surface layer shows coarsening due to differential erosion of the sediment fractions. In the downwind grid cell, the bed surface layer shows fining because the deposited sediment is a reflection of the predominantly fine sediment available in the air column. The movement of repletion sediment in the upwind grid cell is dependent on the grain size distribution in layer 2, whereas the movement of excess sediment in the downwind grain cell is dependent on the original distribution in layer 1. Adapted from Hoonhout and de Vries (2016)

this research, the Nikuradse roughness method was used to calculate the aerodynamic roughness ($z_0 = d/30$), as it allows for spatially varying grain sizes to impact the bed roughness through the median grain size, D_{50}, of the bed surface in each individual grid cell.

The equilibrium transport rate resulting from Equation 5.1 is used in a 1-D advection scheme (de Vries, van Thiel de Vries, et al., 2014),

$$\frac{\delta c}{\delta t} + u_z \frac{\delta c}{\delta x} = \frac{c_{sat} - c}{T} \tag{5.4}$$

This equation is applied to calculate the sediment mass per unit area c (kg/m^2) throughout time, indicated as t (s), and space, indicated as x (m). The u_z (m/s) represents the wind velocity at height z (m). The bed exchange, which consists of erosion and deposition, is determined as the difference between the saturated sediment concentration c_{sat} (kg/m^2) and the instantaneous sediment concentration c (i.e., the sediment concentration already present in the air) divided by an adaptation time scale T (usually 1 s). The adaptation time scale results in a simulation of the fetch effect (e.g., Bauer

& Davidson-Arnott, 2002; Gillette et al., 1996), where the sediment concentration increases downwind from the start of the domain. The increase to the maximum sediment concentration (i.e., where the normalized sediment concentration equals 1) requires a longer fetch with larger wind speeds and finer grain sizes as the saturated sediment concentration increases. Additionally, the bed exchange is maximized by the sediment that is available at the bed.

For this study, the AeoLiS model was extended with the capability to input spatially varying bed grain size properties both in the horizontal (cross-shore and longshore) and vertical domains. The source code and documentation are open-source and are hosted at `https://github.com/openearth/aeolis-python`. More details on the model concepts in AeoLiS and their numerical implementation can be found in de Vries, van Thiel de Vries, et al. (2014) and Hoonhout and de Vries (2016).

The set-up of the model used in this study was based on an idealized beach environment. The 1D domain was 200 m long with a grid size of 1 m. The seaward boundary (x=0 m) had zero influx of aeolian sediment, and the landward boundary was open (x=200 m), so sediment can leave the domain. In the idealized beach environment, the effect of waves and tides was excluded, and only the wind that blows over a flatbed was taken into account. The wind direction was constant, and blowing in the direction of the grid from 0 to 200 m. In all simulations, nearly all default parameters of AeoLiS (v2.1.0) were used (AeoLiS Development Team, 2023). Only the parameters related to different grain size scenarios and time scales (discussed in Section 5.3.2 and 5.3.3), and the bed interaction (set to 0.05, following Hoonhout & de Vries, 2016) deviated from the default settings.

The idealized beach environment was used to create scenarios with different temporal scales and different spatial grain size variations. To enable the execution of the different scenarios two main input parameters were varied: the wind forcing and the bed composition. The impact of these variations were studied by recording the sediment flux that leaves the domain. The model setup used for all scenarios, and the python code used for the analysis and generation of the figures in this chapter are freely available (van IJzendoorn, 2023).

5.3.2. Grain size scenarios

Several grain size scenarios were tested to investigate the effect of grain size variability: single-fraction, multi-fraction, horizontal variation, and vertical layering. The different grain size scenarios were simulated over different timescales with both static and variable winds to investigate the impact of sorting and wind climate. For all scenarios, a corresponding single-fraction reference grain size was used to quantify the effect of the scenario on the sediment transport. An overview of the scenarios and the 25 different cases that were formulated is presented in Table 5.1.

Table 5.1: Overview of the different grain size scenarios and their associated cases, including the time scales at which the cases were executed. The underlined time scales are not shown in the Results section because they exhibit behavior comparable to the other time scales.

Scenario	# of cases	Case description		Time scale
Single-fraction	6	125, 250, 300, 375, 500, 1000 and 2000 μm		10 min, 1 day, 1 year
Multi-fraction	1	Two fractions	50%-50%	1 day, 1 year
	3		20%-80%	1 day, 1 year
	4		varied percentage	1 day, 1 year
	6	Full particle size distribution		1 day, 1 year
Spatial variations	3	Horizontal		10 min, 1 day, 1 year
	2	Vertical		10 min, 1 day, 1 year

A single fraction scenario and a multi-fraction scenario, which included cases with two-fraction mixes and full particle size distributions (PSDs), were executed to investigate the effect of including multi-fraction transport in aeolian sediment transport simulations (Figure 5.3). For the single-fraction scenario, cases were created with one grain size class between 125 and 2000 μm that was the same in the entire bed (Figure 5.3a). In the two-fraction mix cases, grain size classes between 125 and 2000 μm were used. Two grain size classes were chosen with different weights assigned to both classes for each case (Figure 5.3b, c and d). The percentages used in the context of grain size distributions indicate weight percentages. The single-fraction reference for the 50-50% and 80-20% mixes was defined as the average grain size. The single-fraction 125 μm case was used as a reference for the varied percentage mix.

For the particle size distribution cases, 6 PSDs were created with Qgrain (Liu et al., 2021). The shape parameters (i.e., mean, standard deviation, weight and skewness) of the average grain size distribution of all samples collected in Noordwijk as presented in van IJzendoorn et al. (2022) were determined by fitting a skewed normal distribution.

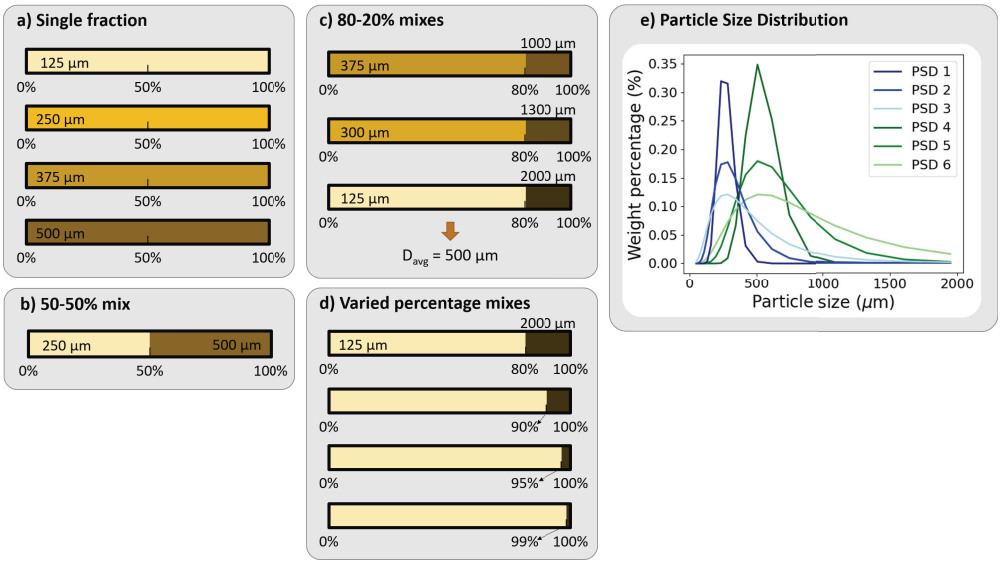

Figure 5.3: Overview of the different grain size scenarios that were used in simulations with a spatially invariant grain size. For (c) the 80-20% mixes all had the same average grain size (D_{avg} = 500 μm). In (d) the varied percentage mixes, two fixed grain size classes were used (i.e. 125 and 2000 μm), but the median grain size varied as the mass distribution over two fixed grain size classes was varied. The (e) particle size distribution scenario consisted of 6 different PSDs with a median grain size of approximately 250 (blue) or 500 μm (green) and varying distribution widths.

Subsequently, the median grain size (250 and 500 μm) and standard deviation (σ = 0.32, 0.62 and 0.92) were varied to create 6 PSDs (Figure 5.3e). The median grain size of each PSD was used as the reference case. The full particle size distribution was expressed as the mass weight of each grain size class with 20 classes ranging from 50 to 1950 μm.

The effect of spatial grain size variations on aeolian sediment transport simulations was investigated with horizontal variation and vertical layering scenarios (Figure 5.4). Horizontal variations were implemented with a coarse-fine, fine-coarse and fine-coarse-fine gradient (Figure 5.4a). To create these gradients, the weight of a fine fraction (250 μm) and a coarse fraction (500 μm) were varied between 0 and 100% along the domain. In all cases, the average distribution of the two fractions was 50-50%, thus, the average grain size of 375 μm was used as a reference case. The different spatial distributions represent fining and coarsening gradients found in the field. Specifically, the gradient with coarse material in the middle represents field situations where the coarsest sediments have been found on the berm. The horizontal spatial gradients were applied to all vertical layers in the domain, including the lowest one. This results in the initial grain size gradient being continuously supplied from below. This assumes that the initial bed stratigraphy is uniform with depth.

The effect of grain size variations in the vertical dimension was investigated with a

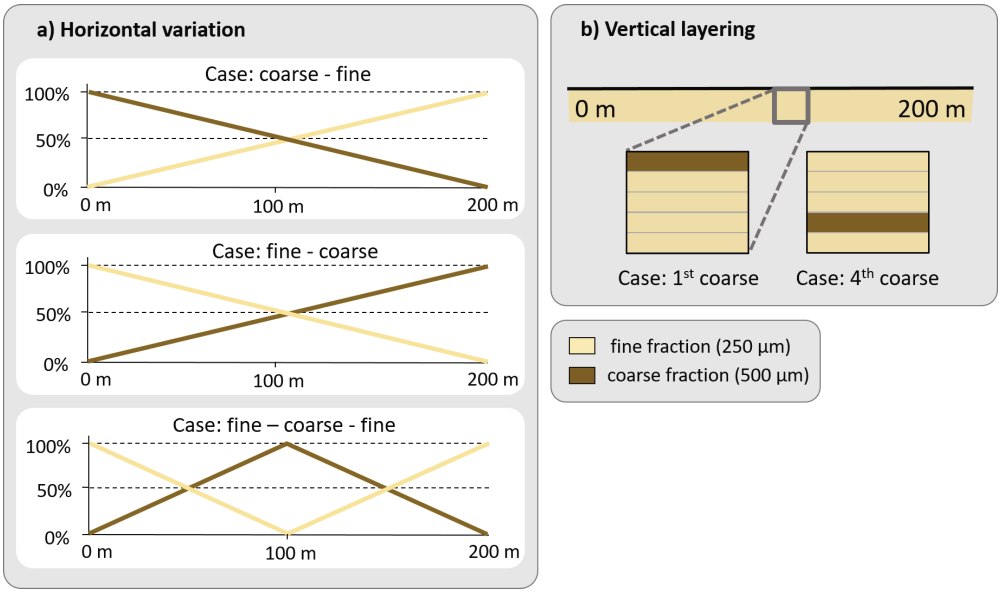

Figure 5.4: Overview of the different grain size scenarios that were used in simulations with a spatially varying grain size gradients. (a) The horizontal variation scenario consisted of three different gradients where a fine (250 μm) and coarse (500 μm) grain size class were spatially mixed. (b) In the vertical layering scenario, all layers consisted of the fine grain size class (250 μm) apart from one coarse layer (500 μm).

vertical layering scenario. In this scenario, the grain size layering at the beach surface was represented by 5 layers, consisting of either fine (250 μm) or coarse (500 μm) sediment (Figure 5.4b). In the first case, the upper layer consisted of coarse sediment, whereas in the second case, the fourth layer consisted of coarse sediment. Both cases have an average grain size of 300 μm, so a single-fraction case was executed for comparison with the vertical layering scenario. In both cases, the fifth layer consisted of the same grain size class (250 μm). This lowest layer determines the supply from below. Thus, by assigning the same grain size, large deviations between the cases were prevented that would have occurred if all superimposed sediment was eroded.

5.3.3. Simulation time and wind forcing

Runs of 10 minutes, 1 day, and 1 year were executed to assess the effect of grain size variations across time scales. The 10-minute runs involved constant wind speeds between 0 and 30 m/s. The 1 day and 1 year academic cases were simulated with varying winds that were created with the wind generator in AeoLiS. The wind generator creates a random wind velocity time series with a given mean and maximum wind speed using a Markov Chain Monte Carlo approach based on a Weibull distribution. A mean wind speed of 10 m/s with a maximum wind speed of 30 m/s was used as input for the wind generator. Generated wind speeds fluctuate on the scale of the model timestep, dt, which was varied based on the simulation time (Table 5.2).

Table 5.2: AeoLiS model settings and wind input for scenarios with different temporal scales.

Simulation time	dt	Output _times	Wind regime	# of layers	Layer_ thickness
10 minutes	1	10	Constant, range from 0 to 30 m/s	5	0.00005
1 day	60	600	Variable, mean 10 m/s, max 30 m/s	5	0.0001
1 year	3600	86400	Variable, mean 10 m/s, max 30 m/s	5	0.01

The layer thickness used in the simulations (Table 5.2) was scaled to the time step. This was done to avoid sediment depletion in the surface layer during time steps with peak transport, which would influence calculated transport rates. Increasing the resolution for the longer time scales is possible with a reduced time step. However, this would greatly increase the computation time needed for each simulation. We tested whether increasing the vertical resolution from 5 to 50 layers would have an effect on the 10-minute time scale of the vertical layering scenario with a constant 10 m/s wind. The test showed that the sediment flux remained similar (i.e., a difference $< 3\%$). However, there were some minor differences in the temporal trends of the pickup of the coarse and fine sediment, which were related to (numerical) diffusion of the vertical grain size gradient in the 5 layer test. These effects might be exacerbated at longer time scales and with the inclusion of varying wind speeds in a simulation. Therefore, the quantitative aeolian sediment transport results that were obtained at different time scales for each case, were not directly compared in this chapter.

5.4. Results

5.4.1. The transport of single-fraction sediment

Distinct variations in the way different grain sizes reacted to varying wind speeds on the 10 minute time scale were observed in the model results (Figure 5.5a). Below 10 m/s, the threshold for transport was barely exceeded, and little to no sediment flux occurred for grain sizes between 250 and 500 μm. Between 10 and 15 m/s, the differentiation between the grain size cases was the largest. For these wind speeds, the behavior of the shear velocity and threshold shear velocity following Equation 5.2 and 5.3 is shown in Figure 5.5b. As finer grain sizes have a lower threshold velocity (red line in Figure 5.5a), transport was initiated at lower wind speeds. For wind speeds above 15 m/s, sediment transport occurred in all grain size cases. Because the shear velocity increased with the wind velocity (Equation 5.2) and the sediment flux is cubically related to the difference between the shear velocity and the threshold shear velocity (Equation 5.1), the transport that occurred at a 30 m/s wind speed was more than an order of magnitude higher than that at a 15 m/s wind speed.

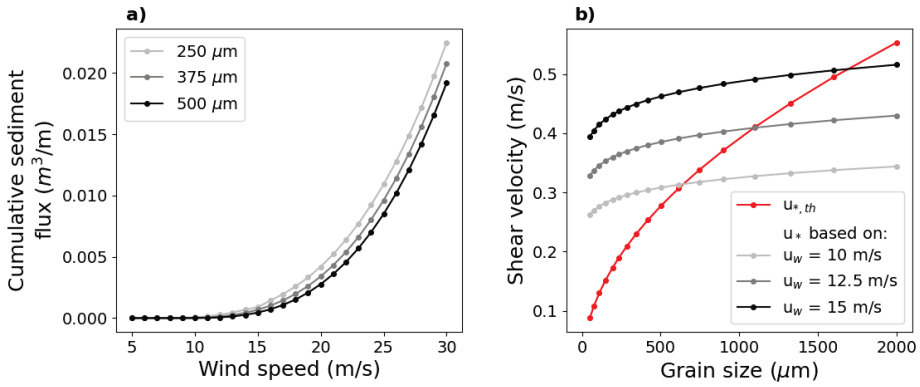

Figure 5.5: (a) The cumulative sediment flux after 10 minutes for wind speeds of 0 to 30 m/s for grain sizes of 250, 375 and 500 μm. (b) The relation between grain size and the threshold shear velocity $u_{*,th}$ as follows from Equation 5.2 in red, and the relation between grain size and the shear velocity u_* for three different wind speeds as follows from Equation 5.3 (greyscale lines). The shear velocity u_* varies with grain size due to the dependence of the aerodynamic roughness z_0 on the grain size in Equation 5.3.

On the 1-day time scale, a larger transport magnitude occurred for the 250 and 375 μm cases than the 500 μm case (Figure 5.6b). The difference in transport between the three cases was largest in the moments with high wind speeds. Throughout time, the difference in the cumulative sediment flux between the grain size cases increased (Figure 5.6c), which is the result of both the difference in threshold velocity and the transport magnitude. For finer grain sizes, the lower threshold velocity resulted in a longer time period in which transport could occur, and in that time period, the transport was higher than that for the coarser grain sizes (Figure 5.6a).

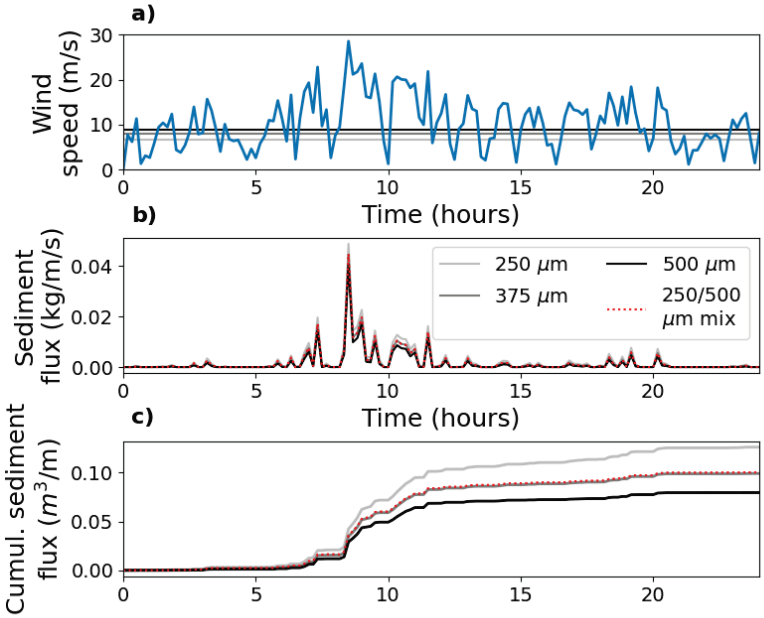

Figure 5.6: (a) One-day variable wind scenario which results in the (b) sediment flux and (c) cumulative sediment flux of the single-fraction cases of 250, 375, and 500 μm and of a two-fraction 250/500 μm mix (50-50% mix, Figure 5.3b). The horizontal lines in the wind plot indicate the threshold velocity for the single-fraction case with the corresponding color in (b) and (c).

5.4.2. Comparison between single-fraction and two-fraction mixes

The 50-50% mix with the 250 and 500 μm sediment fractions resulted in similar transport rates as the single-fraction simulation with the average grain size of 375 μm (Figure 5.6c). For the simulated wind climate, there was little effect of the coarsening of the top layer. There was some differentiation between the mix and the 375 μm case in periods where the wind speed was around the threshold velocity of the different fractions. However, the highest wind speeds resulted in the largest contribution to the sediment flux. Thus, the differentiation at lower wind speeds was negligible on the scale of the total cumulative sediment flux during the one-day simulation. For the higher wind speeds, the larger and smaller transport that occurred for the 250 μm and 500 μm fractions in the mix balanced each other, making the resulting cumulative transport comparable to the 375 μm case. This equalization may occur because the shear velocity and threshold shear velocity in Figure 5.5b show approximately linear trends for this relatively limited grain size range. At the yearly time scale, the behavior of the two-fraction mix was also closely replicated with a single fraction equal to the average grain size of the mix.

The effect of armoring was further investigated with 80-20% mixes of varying grain sizes (125/2000 μm, 300/1300 μm, and 375/1000 μm) with a constant average grain

size equal to 500 μm. At a yearly timescale, the cumulative sediment flux varied for the different mixes (Figure 5.7). The 375/1000 μm case aligned with the result of the average grain size, the 300/1300 μm mix was slightly larger, and the 125/2000 μm mix showed larger deviations. At the start of the year, the cumulative sediment flux of the 125/2000 μm mix exceeded that of the average grain size. Within the first 50 days, it even exceeded the cumulative sediment flux of the single-fraction 125 μm case. The explaining mechanism is the increase of the aerodynamic roughness in the mix that was caused by the coarse fraction. A larger aerodynamic roughness increases the shear velocity (greyscale lines in Figure 5.5b) and, thus, the transport capacity which is dependent on the difference between the shear velocity and the threshold shear velocity

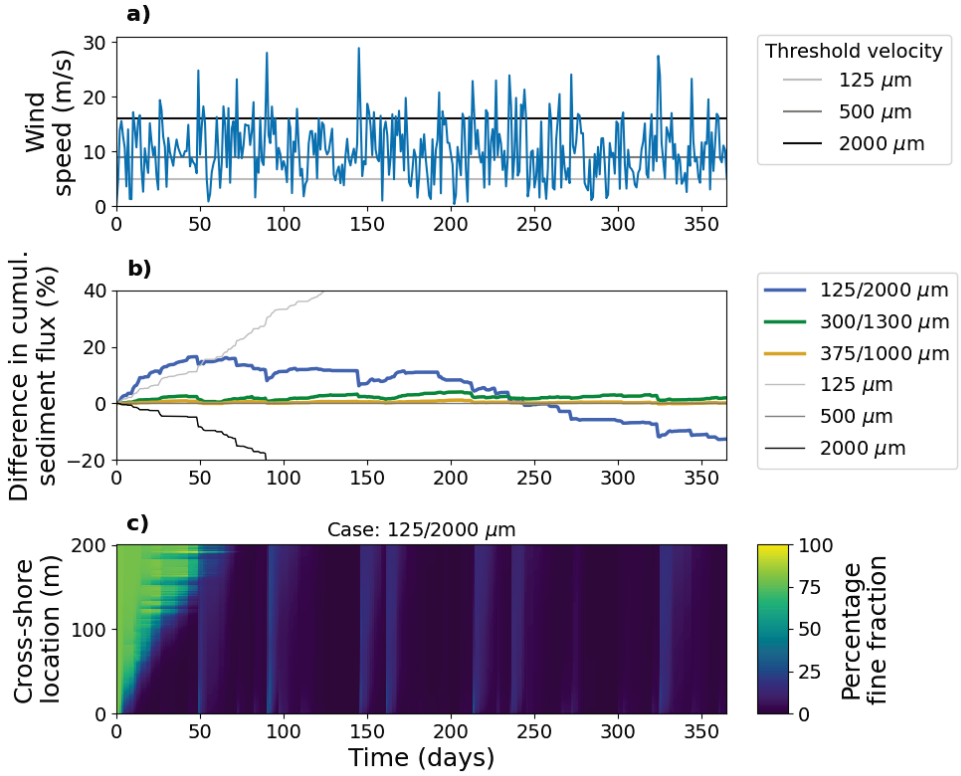

Figure 5.7: (a) 1-year variable wind scenario. The horizontal lines in the wind plot indicate the threshold velocity for single-fraction cases with colors corresponding to the sediment fluxes in (b). (b) Cumulative sediment flux of the single-fraction cases of 125 μm (light grey), 500 μm (grey), and 2000 μm (black), compared to the cumulative sediment flux that occurs for the 80-20% mixes (Figure 5.3c) in blue, green, and yellow that all have an average grain size of 500 μm. Note that the single-fraction case of 500 μm is used as the reference case. (c) Time-stack of the development of the percentage of fine fraction that is present in the top layer of the bed surface for the 125/2000 μm mix through time (x-axis) and space (y-axis).

(Equation 5.1). After the 50-day period, this increased transport capacity was counteracted by the coarsening of the bed surface (Figure 5.7), and the cumulative sediment flux progressively got closer to the reference case. After 240 days, the cumulative transport of the 125/2000 μm case became even lower than the reference case, eventually resulting in approximately 15% less cumulative transport at the end of the year. Similar fluctuations in the difference in cumulative sediment flux occurred for the 300/1300 μm mix, although, the cumulative sediment flux was never less than the reference case.

5.4.3. The effect of coarse fraction percentage on sediment transport

Not only the size but also the relative percentage of the coarse fraction affects the cumulative sediment flux (Figure 5.8). The effect of the percentage of coarse fraction was investigated by varying the coarse sediment percentage between 1 and 20% in a 125/2000 μm mix (Figure 5.3d). The 80-20% case showed a strong deviation in the cumulative sediment flux compared to the reference case (100% 125 μm) resulting in a decrease in the yearly cumulative transport rate of more than 50% (Figure 5.8b). The decrease in transport due to armoring occurred from 70 days and onwards. For the 90-10% case, it took 150 days for this deviation to occur, and the deviation after a year was smaller, at approximately 30% less transport than the reference case. The cases where only 1 or 5% of coarse fraction was present did not show a considerable deviation from the sediment flux of the fine fraction within the 1-year time frame. All cases showed how wind speed peaks affect the cumulative sediment flux. The wind speed peaks cause mobilization of the coarse fraction at the bed surface, which exposes finer fractions that are more easily transported (Figure 5.8c).

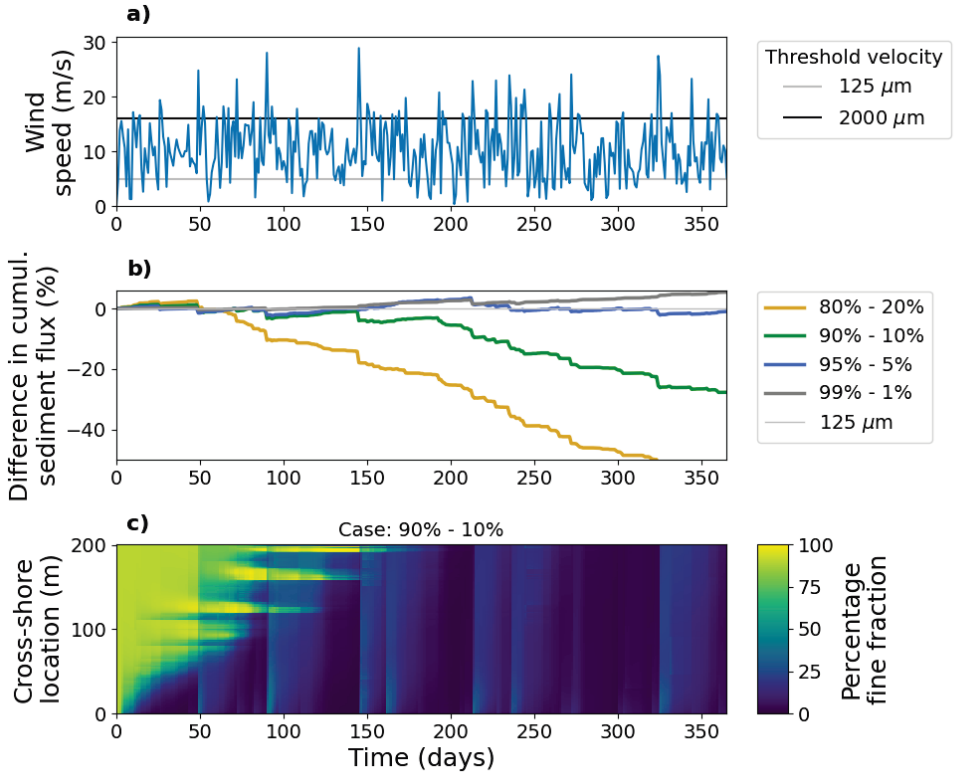

Figure 5.8: (a) 1-year variable wind scenario. The horizontal lines in the wind plot indicate the threshold velocity for the single-fraction case of 125 μm (light grey) and 2000 μm (black). (b) Cumulative sediment flux of the reference single-fraction case of 125 μm (light grey), compared to the cumulative sediment flux that occurs for two-fraction mixes in yellow, green, blue, and grey that consist of varying percentages of the 125 and 2000 μm fractions (Figure 5.3d). (c) Time-stack of the development of the percentage of fine fraction that is present in the top layer of the bed surface through time (x-axis) and space (y-axis), visualized for the 125/2000 μm mix that starts with 90% fine and 10% coarse fraction.

5.4.4. The effect of different particle size distributions on sediment transport

Compared to the two fraction mixes, the simulations with full particle size distributions resulted in less deviation from the reference case (median grain size of the PSD). The maximum difference in cumulative sediment flux was 15% and 7.5% less transport after the 1-day (Figure 5.9) and 1-year period (Figure 5.10), respectively. Overall, all PSDs showed comparable trajectories, except for PSD 6, which has the widest distribution. In the 1-day period, PSD 6 showed several hours with a larger cumulative sediment flux than the reference grain size. This might have been related to a relatively large aerodynamics roughness and fine fraction abundance, caused by the shape of PSD 6 (Figure 5.3e). In the 1-year period, PSD 6 remained relatively close to the reference grain size up until day 200, whereas the other PSDs already showed significant deviations near the start of the simulation. Again, this behavior might be caused by the balance between the presence of coarse and fine fractions in the grain size distribution.

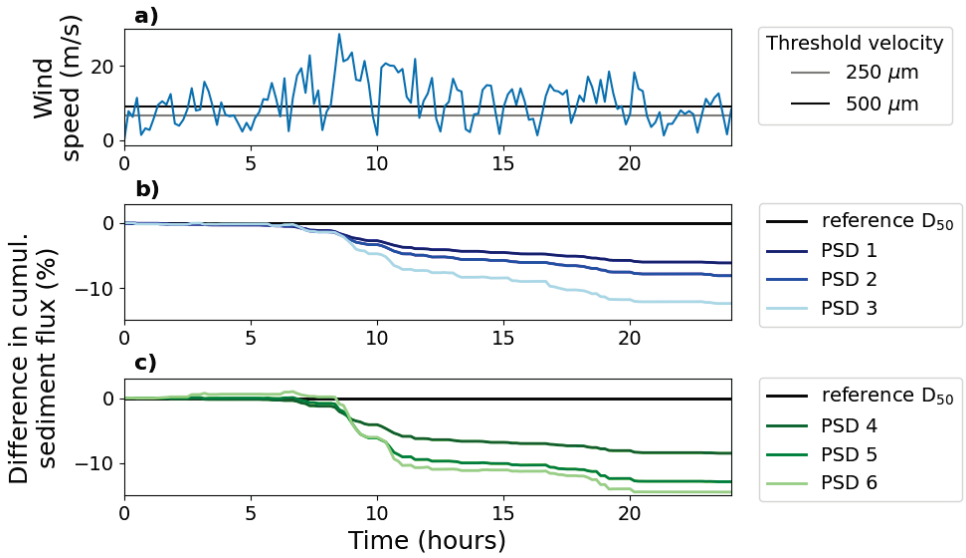

Figure 5.9: (a) 1-day variable wind scenario. The horizontal lines in the wind plot indicate the threshold velocity for the single-fraction case of 250 μm (grey) and 500 μm (black). (b) and (c) Cumulative sediment flux of each tested particle size distribution (PSD) as shown in Figure 5.3e, compared to the reference case (black). For each PSD, the reference case corresponds to the median grain size of the PSD. The blue colors in (b) have a median grain size of around 250 μm, the green colors in (c) have a median grain size around 500 μm.

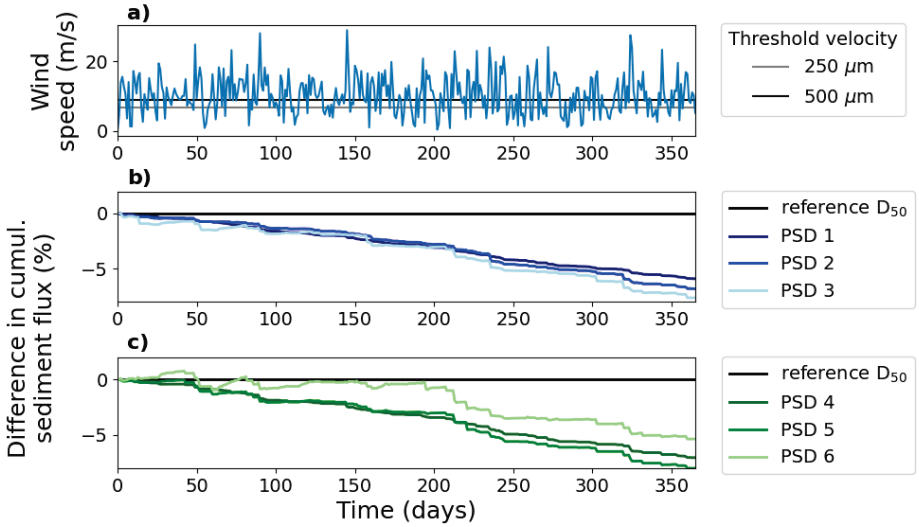

Figure 5.10: (a) 1-year variable wind scenario. The horizontal lines in the wind plot indicate the threshold velocity for the single-fraction case of 250 μm (grey) and 500 μm (black). (b) and (c) Cumulative sediment flux of each tested particle size distribution (PSD) as shown in Figure 5.3e, compared to the reference case (black). For each PSD, the reference case corresponds to the median grain size of the PSD. The blue colors in (b) have a median grain size of around 250 μm, the green colors in (c) have a median grain size around 500 μm.

5.4.5. The impact of grain size variability in the horizontal dimension

The horizontal variation cases with different spatial gradients showed distinctly different cumulative sediment fluxes when simulated for a 10-minute period with a constant 10 m/s speed. The finer the sediment at the start of the domain, the higher the cumulative sediment flux (Figure 5.11). In Figure 5.11b, c, and d, the erosion area in the domain is indicated with white hatching, where leftward leaning hatching indicates pickup of the fine fraction and rightward leaning hatching indicates pickup of the coarse fraction. The variation in the cross-shore expanse of the erosion area between the different scenarios indicates a variation in the fetch length, which could have been caused by a difference in the magnitude of the equilibrium transport. Coarse sediment resulted in a lower equilibrium transport magnitude (Equation 5.1), so based on the implementation of the adaptation timescale, the distance needed to reach the equilibrium transport was smaller than with fine sediment at the start of the domain which is related to a larger equilibrium transport. The larger bed roughness that occurred for the coarse sediment counteracted this effect slightly. In conclusion, the fetch length is shorter when coarser sediment is present at the start of the domain, and as fully developed transport was reached at the end of the erosion area, there was no significant impact of the bed surface gain size composition further along the domain.

The 1-day and 1-year simulations of the horizontal grain size variations resulted in

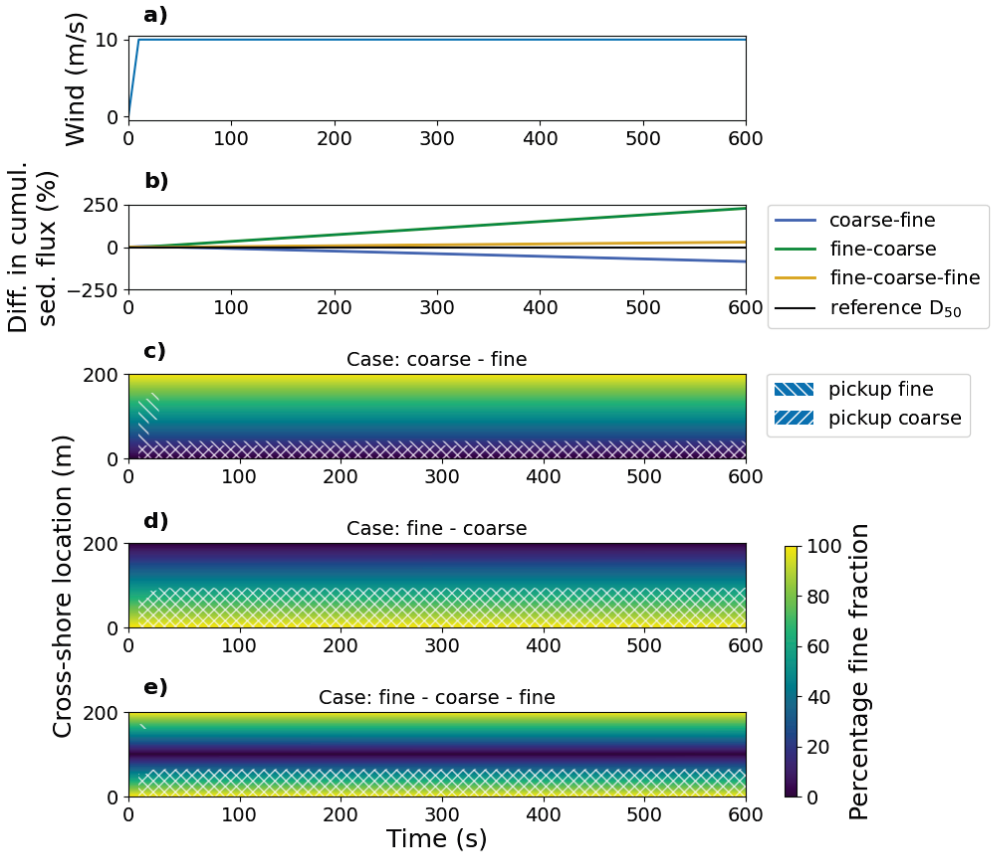

Figure 5.11: (a) Cumulative sediment fluxes under a 10-minute, constant 10 m/s wind speed for the horizontal variation scenario (Figure 5.4a), which includes a coarse to fine (blue), fine to coarse (green) and fine to coarse to fine (yellow) gradient, compared to the reference grain size of 375 μm (black). Time-stack of the development of the percentage of fine fraction that is present in the top layer of the bed surface for the (b) coarse to fine, (c) fine to coarse and (d) fine to coarse to fine case.

similar sediment flux behavior. The coarse-fine case resulted in less transport than the reference D_{50} and the fine-coarse and fine-coarse-fine cases resulted in more transport (Figure 5.12). The bed surface layer development of the coarse-fine case showed coarsening of the surface (Figure 5.12c), whereas the fine-coarse case showed fining (Figure 5.12d). For each case, a unique cross-shore equilibrium bed composition developed at the bed surface. The occurrence of pickup throughout the domain seemed most strongly related to the wind speed. However, after the formation of the equilibrium grain size gradient, the region with pickup became much larger for both periods and all cases.

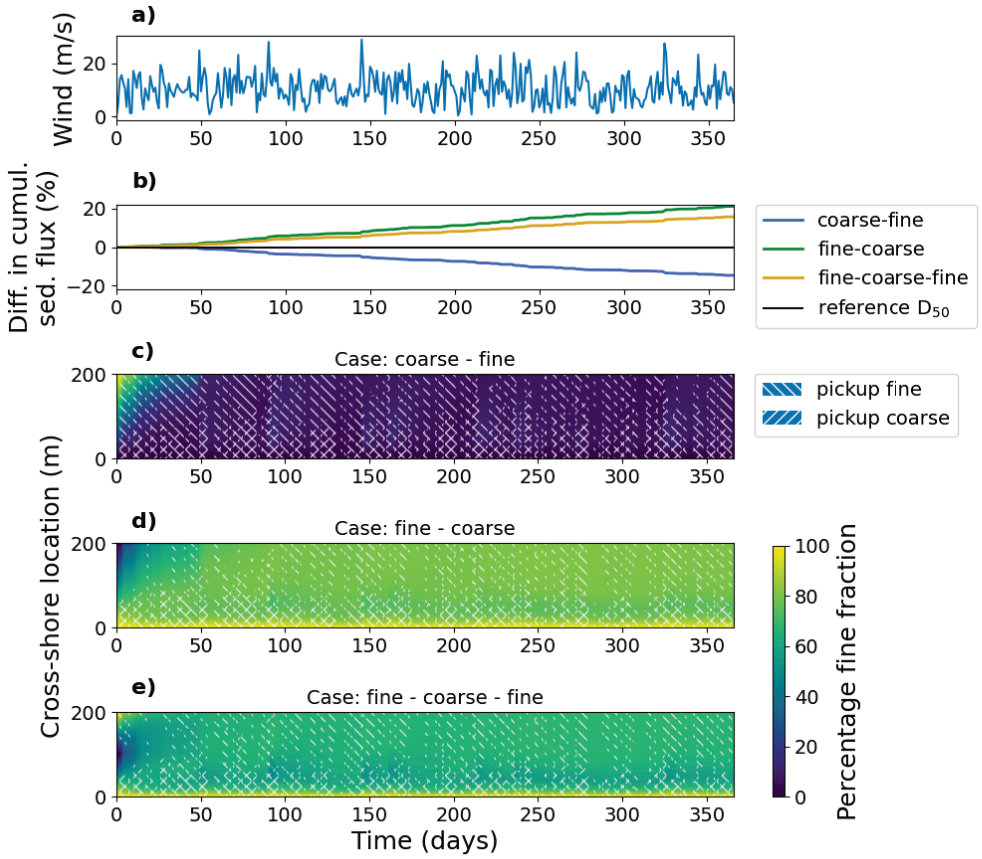

Figure 5.12: (a) 1-year variable wind scenario. (b) Cumulative sediment fluxes of the horizontal variation scenario (Figure 5.4a), which includes a coarse to fine (blue), fine to coarse (green) and fine to coarse to fine (yellow) gradient, compared to the reference grain size of 375 μm (black). Time-stack of the development of the percentage of fine fractions that is present in the top layer of the bed surface for the (b) coarse to fine, (c) fine to coarse and (d) fine to coarse to fine case.

5.4.6. Sediment transport variations due to vertical grain size variability

The vertical grain size layering directly affected the amount and timing of aeolian transport during the different time scales. For the 10-minute simulations, varying behavior was observed depending on the wind speed and the vertical location of the coarse layer (Figure 5.13). At a wind speed of 10 m/s, little transport occurred due to the relatively low wind speeds, and the grain size fraction in the upper layer of both cases dominated the cumulative sediment flux (Figure 5.13a). At 20 m/s, the removal of the coarse and fine fraction for the 1st layer coarse and 4th layer coarse case, respectively, resulted in a reduction of the difference in the cumulative sediment flux compared to the reference grain size (Figure 5.13b). At 30 m/s, both the fine and coarse sediment were

easily mobilized by the wind, resulting in a considerably lower difference in cumulative sediment flux compared to the reference grain size (Figure 5.13c).

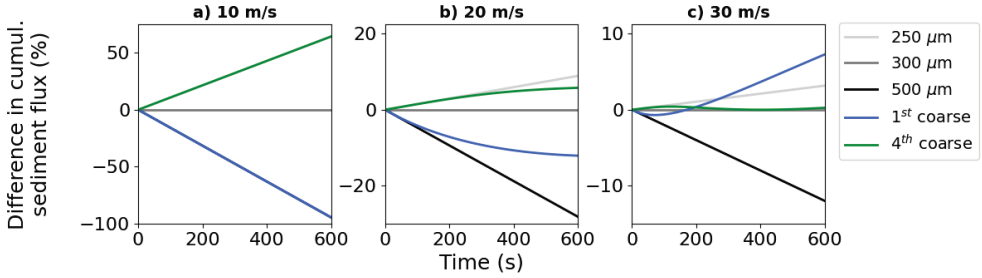

Figure 5.13: Cumulative sediment fluxes of the vertical layering scenario (Figure 5.4b) compared to the reference grain size 300 μm (grey) for 10-minute simulations with a constant wind speed of (a) 10 m/s, (b) 20 m/s, and (c) 30 m/s. The scenario includes the case where the top layer (blue) and the fourth layer (green) consisted of a coarse fraction (500 μm). The other layers consisted of a fine fraction (250 μm). For comparison, the cumulative sediment flux of the single-fraction case of 250 (light grey) and 500 μm (black) are shown.

On the scale of a 1-day simulation, the main differentiation in the cumulative sediment flux between the vertical layering cases and the reference grain size (Figure 5.14b) occurred during the wind peak between hours 5 and 10 (Figure 5.14a). This wind peak caused the coarse and fine sediment of, respectively, the 1st coarse case and 4th coarse case to be removed from the surface layer (Figure 5.14 c and d). Subsequently, a relatively stable spatial grain size gradient formed, and the difference in cumulative sediment flux showed limited change for both cases. As the spatial grain size gradient of the bed surface layer changed, the extent of the pickup area, especially for the coarse fraction, increased. Overall, the 1-year simulation, showed comparable trends to the 1-day simulation, although the difference in cumulative sediment flux compared to the reference was lower (around 1% vs. 5%).

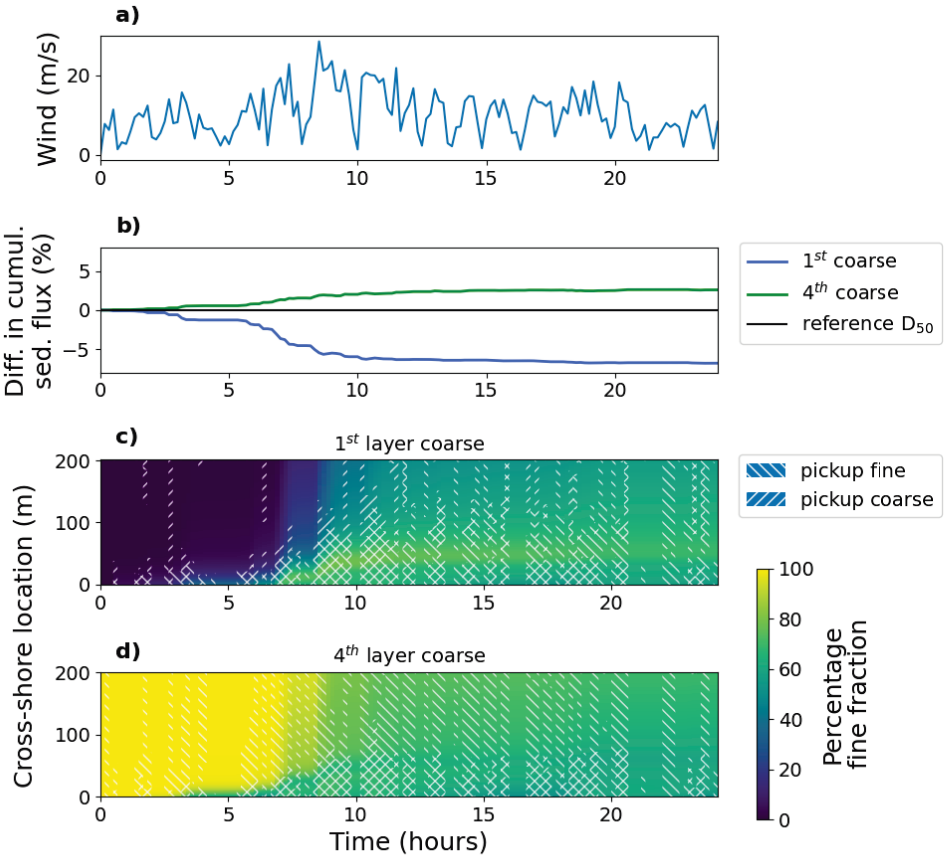

Figure 5.14: (a) 1-day variable wind scenario. (b) Cumulative sediment fluxes of the vertical layering scenario (Figure 5.4b) compared to the reference grain size 300 μm (black). The scenario includes case 1 (blue), where the top layer consisted of a coarse fraction, and case 2 (green), where the fourth layer consisted of a coarse fraction (500 μm). The other layers consisted of a fine fraction (250 μm). Time-stack of the development of the percentage of fine fractions that is present in the top layer of the bed surface for (b) case 1 and (c) case 2.

5.5. Discussion

5.5.1. Using a single-fraction representative grain size in aeolian sediment transport modeling

The cumulative sediment flux calculated with multi-fraction transport and its approximation with a single-fraction reference grain size were similar on time scales of days to years. There only was a considerable impact on the yearly cumulative transport when a relatively large content of coarse grains, > 10% of 2000 μm sediment, was present. The full PSD scenarios, which are similar to the grain size distribution of beach

sand, resulted in a maximum transport reduction of 15% over one day and 7.5% over one year compared to the median grain size. These values are in a similar order of magnitude as those found by Hoonhout and de Vries (2016), although the presence of shells further exacerbated the resulting reduction in their study. The results indicate that for most scenarios, the median grain size can be used as a pragmatic metric for natural grain size distributions in aeolian sediment transport models at daily to yearly time scales.

However, there are some limitations to simplifying grain size distributions with the median grain size. In some of the single-fraction simulations, larger transport rates were recorded than in the corresponding multi-fraction simulation. Wide PSDs might include a relatively large contribution of both coarse and fine fractions. The fine fraction abundance may result in a relative increase of total transport compared to narrower PSDs (e.g., PSD 6 compared to PSD 4 and 5 in Figure 5.10). Additionally, several multi-fraction cases showed that increased transport can occur despite an increase in the reference grain size (e.g., the 125/2000 μm mix in Figure 5.7). This sediment transport increase is related to an increase in the bed roughness and the shear velocity (Equation 5.3). In all cases, the effect was temporary, as coarsening due to the removal of fines counteracted the increase in transport caused by the roughness.

The suitability of the D_{50} as a representative grain size can also be affected by armoring that limits the aeolian sediment transport. These armoring effects occur when a considerable amount of coarse grains is present. Whether specific grain sizes will result in armoring depends on the local wind climate. During energetic wind events, wind peaks can cause an increase in sediment transport and mobilization of coarse grains from the bed surface, which can expose underlying sediment (e.g., the 125/2000 μm mix in Figure 5.7). For the synthetic wind climate that was generated and used in this study, about 2000 μm was a critical grain size. Future work could further quantify for which wind climates and grain size distributions the use of the D_{50} as a representative grain size is valid. For now, a representative wind forcing could be created based on the wind climate and used in an aeolian sediment transport model to determine to what extent specific coarse fractions are expected to be mobilized.

Besides wind speed peaks, hydrodynamic processes and trampling can also break up and alter armor layers. Hydrodynamic processes can cause erosion, deposition and mixing that directly affect the top layers of the bed surface on a time scale of seasons (e.g., Abuodha, 2003; Prodger et al., 2017), events (e.g., Gallagher et al., 2016) and tides (e.g., van IJzendoorn et al., 2022). Future work could investigate the effect of temporally varying grain sizes due to hydrodynamic processes on the sediment flux by including temporal grain size variations in modeling simulations by making simplified assumptions (e.g. based on findings by van IJzendoorn et al., 2022) or coupling with a numerical model (Reniers et al., 2013; Srisuwan et al., 2015). Trampling is also expected to affect the grain size at the bed surface (Moayeri et al., 2023; Reyes-Martínez et al., 2015). Its effects could be included in aeolian sediment transport models with mixing of surface layers in locations where human activity is expected.

5.5.2. The implementation of spatial grain size variations in aeolian sediment transport modeling

Significant vertical grain size variations at the bed surface have been measured (e.g., van IJzendoorn et al., 2022) and over larger soil depths (e.g., Gallagher et al., 2016; Gunaratna et al., 2019). The measurements of van IJzendoorn et al. (2022) showed a maximum range of 119 μm in the D_{50} of different layers in the top 5 cm of the bed surface. Based on our results, we expect that these variations could be simulated relatively accurately on the daily and yearly timescales with the D_{50}. On the minute-scale, we expect that the sediment flux could significantly be altered, especially when layers with a significant contribution of coarse fraction are present near the bed surface. We recommend the inclusion of vertical grain size layering in aeolian sediment transport models where short-term time scales are considered. On time scales longer than days, they can be omitted.

The source area at the beginning of the domain has a significant impact on the cumulative sediment flux across all time scales. As a result, there can be a disconnect between the grain size that is at the bed surface and the transport that occurs at that location. Consider a point measurement at the end of the domain of the coarse - fine and fine - coarse - fine cases for the 10-minute time scale (Figure 5.13). The grain size at these locations was comparable but the cumulative sediment flux deviated considerably. This difference was mostly related to the grain size of the material present in the source area where pickup of fine and coarse sediment occurred. This shows it is important to consider the grain size that is present in the source area when explaining minute-scale sediment transport measurements, as previously indicated by Cohn, Dickhudt, and Marshall (2022), Field and Pelletier (2018) and Uphues et al. (2022). These grain size measurements should be recent because wind speed peaks can cause temporal variations in the bed surface grain size and the related aeolian sediment transport.

The intertidal area was found to be an important source for aeolian sediment transport towards the dunes by de Vries, Arens, et al. (2014). Our findings show that this upwind source of sediment is important for the bed surface grain size development across the domain and the sediment transport magnitude. Thus, the results suggest that the grain size in the intertidal area (e.g., Bascom, 1951) might be the most important to include in aeolian sediment transport models that are used for coastal dune development predictions. These findings align with measurements of aeolian sediment transport in the intertidal area by Swann et al. (2021), who found similar grain sizes in the air column as on the bed. Future work could further validate or falsify these findings by combining minute-scale quantitative sediment transport measurements with bed surface grain size measurements that can show a temporal variation through time. Furthermore, the importance of the grain size in the intertidal area emphasizes the need to study sediment supply by hydrodynamic processes and, specifically, its effect on grain size composition.

5.6. Conclusions

The sorting of multi-fraction sediment, spatial variations in grain size, and their impact on aeolian sediment transport were studied using a numerical aeolian sediment transport model. Results show that, in general, the D_{50} can be used as a representative grain size in aeolian sediment transport modeling on a time scale of days to years. For wide grain size distributions, the multi-fraction sediment flux may differ from the single-fraction flux of the reference grain size. In these cases, simplified model runs that include the full particle size distribution and a wind forcing representative for the wind climate to test the impact on the sediment flux could be considered.

On a time scale of 10-minutes, the bed surface grain size has a direct effect on the aeolian sediment transport flux. Due to this strong relation between grain size and sediment transport, vertical grain size layering may be required in models that predict aeolian sediment transport at this time scale. On time scales from days to years, modeling the effect of vertical layering may not be needed if a representative grain size is used.

The effect of horizontal grain size variations is relevant across all time scales. The grain size in the upwind part of the domain can directly affect the transport magnitude across the domain. The intertidal area can be the dominant source of aeolian sediment transport that affects coastal dune development. In these cases, we recommend to include the grain size present in this region in aeolian sediment transport models and consider its impact on point measurements of sediment transport recorded on the beach. Additionally, we recommend to further investigate the supply of sediment to the intertidal zone by marine processes, specifically focusing on grain size.

Data availability

Version 2.1.0 of the AeoLiS software used for the aeolian sediment transport simulations in this research is preserved at https://doi.org/10.4121/22215562, available via GPL-3.0 and developed openly on Github (https://github.com/openearth/aeolis-python). The Python code used for the analysis and figure generation is hosted at Github and is preserved at https://doi.org/10.4121/22220134, version 1.1.0, under GPL-3.0.

Acknowledgements

This work is part of the research programme DuneForce with project number 17064, which is (partly) financed by the Dutch Research Council (NWO).

6

Synthesis

The processes discussed in Chapters 3 - 5 span from minute-scale aeolian sediment transport processes on the scale of grains to long-term dune development on the scale of coastal dunes (Figure 1.3). This corresponds to a wide range of research methods that were applied, including data-analysis of long-term coastal profiles, development of a new device to collect sediment samples, and the use of a numerical model (Chapter 2). To connect insights gained from these methodologies and to identify next steps, the work presented in this dissertation is placed within the framework of the Adapted Burland Triangle (ABT) (Figure 6.1).

The work presented in Chapter 3 fits into an extensive line of research into long-term coastal dune development based on topographical transects (e.g., Wijnberg & Terwindt, 1995 and Hinton & Nicholls, 1998) that relates to the observed behavior component of the ABT. Previous research in the Netherlands has investigated, amongst others, the dune toe (Ruessink & Jeuken, 2002) and the dune volume (de Vries et al., 2012). Additionally, many other studies into long-term dune development are available across the world (e.g., Walker et al., 2017, Strypsteen et al., 2019 and Doyle et al., 2019). As Walker et al. (2017) stated, it is key to correlate coastal dune development to its forcing variables. Thus, in many cases, attempts are made to relate long-term dune development to drivers that can be characterized as physical properties within the ABT. For example, wind and wave climate have been used to represent aeolian, recovery processes and marine, erosive processes, respectively (Ruessink & Jeuken, 2002; de Vries et al., 2012; Strypsteen et al., 2019).

It should be noted that this type of research is usually executed for a single location, and caution is needed when when extracting generic process information from local comparisons between dune development and drivers. In Chapter 3, it was determined by analyzing the behavior of the coastal profiles along the Dutch coast, that other processes dominate over sea level rise on a decadal scale. This shows that building experience on other physical processes than sea level rise should be prioritized, and that models that exclude sea level rise might be able to simulate coastal profile behavior. However, these conclusions are only valid in locations with characteristics similar to the Dutch coast. The Dutch coast is urbanized and heavily affected by human interference. Especially the nourishments that take place along the Dutch coast might have a large

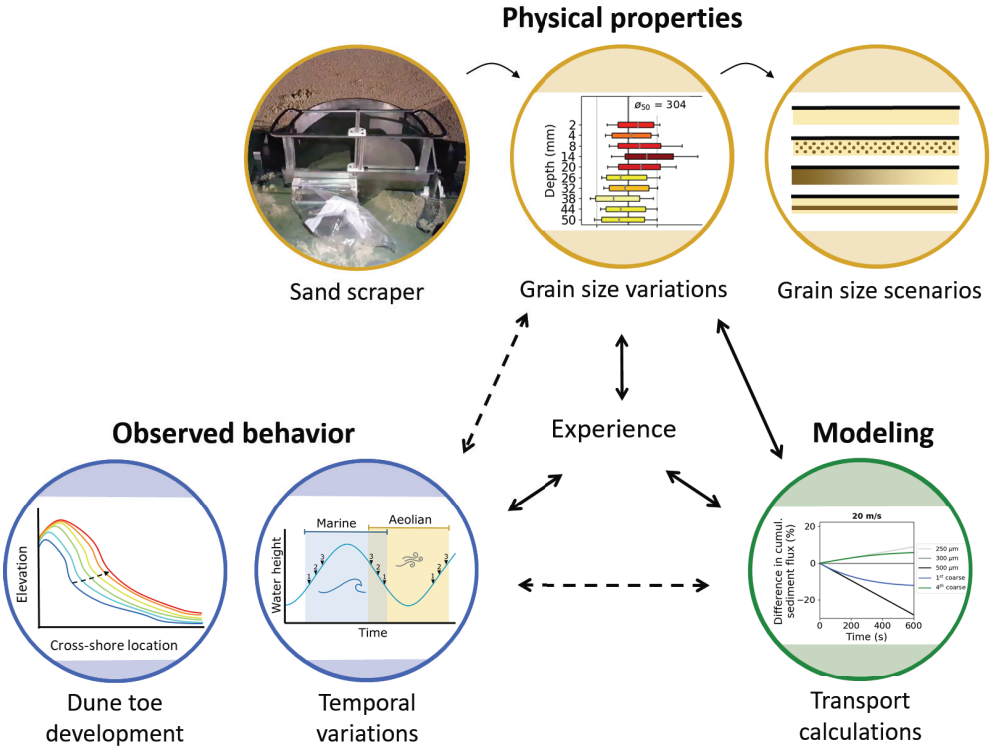

Figure 6.1: The configuration of the content of this dissertation within the Adapted Burland Triangle. Colors correspond to the components in 2.1. Dashed arrows indicate where connections between the components have not yet been made.

impact on the dune toe development. Other urbanized coastal regions with similar coastal management might show similar behavior. Investigating the dune toe behavior in regions that are distinctly different could give additional information, as they might expose which drivers cause different behavioral trends. In Chapter 3, the Dune Translation Index (DTI, the ratio between sea level rise and vertical dune translation) was introduced to promote comparison between different regions. For example, Mehrtens et al. (2023) studied dune toe behavior along the German coast and used the DTI to compare their results to the DTI that was found along the Dutch coast.

The sand scraper measurements in Chapter 4 were executed at three field sites to characterize grain size as a physical property at a range of different beach systems. The sand scraper can be used on other beaches to extend this characterization. For example, the sand scraper was used on the beach of the Prins Hendrik Zanddijk (Strypsteen et al., 2021) by researchers from Utrecht University. The grain size variability measurements that were presented in this dissertation are similar to measurements of detailed variations in other supply-limiting factors like shells (Carter & Rihan, 1978) and moisture (Smit et al., 2018). Often, descriptions of supply-limiting factors are combined

with aeolian sediment transport measurements (e.g. Davidson-Arnott et al., 2008; de Vries, Arens, et al., 2014). However, we focused on measuring the variability of the supply-limiter that was present in the field, as the characterization of this variability could be used for modeling purposes.

Chapter 4 demonstrated that there is a large variability in grain size on the beach, as is true for many other physical properties (e.g., Smit et al., 2018; Masselink et al., 2007). Taking into account the widespread variability that is present in coastal systems seems an impossible task. Especially as generic conclusions cannot be drawn based on a limited amount of locations and sample occasions. However, by connecting the measurements of physical properties to modeling, more purposeful experience can be built. The experience gained on the presence of spatial grain size variation in the field in Chapter 4 was used to formulate modeling scenarios that were used in Chapter 5. These scenarios were based on the most important grain size trends that were present in the field data. Thus, the variation in the bed composition in the field was reduced and abstracted. This allowed for the model simulations to be more generic and for (quantified) recommendations for future modeling and field efforts to be given.

The research presented in Chapter 4 and Chapter 5 covered all three components of the ABT. The measurements of the spatial variations in grain size with the sand scraper provided a characterization of the bed composition (i.e., a physical property). These measurements were repeated through time to investigate the effect of marine and aeolian processes on grain size (i.e., observed behavior). The effect of grain size on aeolian sediment transport was simulated with AeoLiS (i.e., modeling). However, the application of the ABT shows that the connections of the observed behavior component with the physical properties and modeling components were not yet explored (dashed lines in Figure 6.1). These missing links may be addressed in future research. For example, the insights into the temporal grain size variation and its relation to the occurrence of marine and aeolian processes could be used in modeling. A conceptual model could be developed that relates temporal grain size variations to the occurrence of marine and aeolian processes based on an idealization of the results. Additionally, the bed surface grain size variations simulated with the AeoLiS model could be verified with field measurements.

The range of methods, temporal and spatial scales that were presented in this dissertation, all relate to determining the relevance of specific processes for the development of coastal dunes. Through the ABT, an integrated framework was presented that provides a pathway to combine the investigation of fundamental physical processes and properties, with quantification. This first application of the ABT in a coastal context demonstrated how the ABT may be used to connect field measurements and modeling, and to identify research needs. Applying the ABT in future coastal research projects, may contribute to clarifying project goals and streamlining the integration of modeling with other research approaches.

7

Conclusions and outlook

7.1. Conclusions

Coastal dunes provide a variety of functions, such as flood safety, recreation and ecology. Thus, understanding the processes that determine coastal dune development is key. The development of coastal dunes is driven by interactions between aeolian and marine processes across different temporal and spatial scales. The processes that impact the aeolian sediment supply to the dunes can occur on both the short and long term. In this research, the effect of sea level rise was addressed on a decadal scale, and aeolian processes related to grain size were addressed on time scales of minutes to years. Their effect on aeolian sediment transport and dune development were studied and quantified using long-term coastal profile development data (Chapter 3), field measurements (Chapter 4), and exploratory modeling (Chapter 5). New insights into the effect of sea level rise and grain size-related aeolian sediment transport processes have been gained, which can guide their quantitative implementation in modeling,

The conclusions relating to the research objectives (Section 1.3) are formulated below:

1. Investigate the link between sea level rise and coastal dune development at a decadal scale

The potential impact of sea level rise was investigated by analyzing long-term coastal profile measurements along the Dutch coast. The coastal profile measurements show a linear increase of the dune toe elevation on the order of 13–15 mm/year during recent decades. The increase in dune toe elevation coincides with a seaward movement of the dune toe, which shows similarities to prograding coasts in the Holocene both along the Dutch coast and elsewhere. It was shown that the dune toe elevation increases 7-8 times faster than the rate of sea level rise along the Dutch coast. This may indicate that the dune development along these coastal stretches is dominated by other factors than sea level rise on the yearly to decadal time scale.

2. Measure the extent of grain size variability due to marine and aeolian processes in the intertidal zone

Field measurements of spatial and temporal grain size variability in the intertidal area were collected at three different field sites to investigate grain size variations on the beach. A new device, the sand scraper, was developed that provides the ability to study and quantify the spatial and temporal variations in grain size that occur at a millimeter scale in the bed surface. The measurements collected with the sand scraper showed that cross-shore gradients in grain size were present at all beaches, and that individual sediment layers can deviate considerably from the vertically averaged median grain size in the upper 50 mm of the bed surface. These findings reinforce that beach grain size characteristics are far from homogeneous, and that sparse sediment sampling is not necessarily representative for the bed composition of large spatial domains. Both fining and coarsening of the bed surface due to marine and aeolian processes were observed. Marine processes caused the most distinct changes in the vertical variability of the grain size where significant morphological change occurred during high water. During aeolian transport, coarsening of the bed surface was observed in some measurements. However, the bed surface grain size fined where deposition occurred due to the formation and development of meter-scale aeolian bedforms within the intertidal zone. The spatial grain size variations that were found, informed grain size scenarios used in the aeolian sediment transport modeling related to research objective 3.

3. Determine the extent to which the grain size distribution and spatial grain size variability impact the aeolian sediment transport magnitude

Most simulations of coastal sediment transport processes assume a single fraction and spatially uniform bed composition within the model domain. A numerical aeolian sediment transport model was used to investigate to what extent sorting in multi-fraction sediment transport modeling and spatial variations in grain size may impact aeolian sediment transport. By applying multi-fraction, and vertical and cross-shore ranges in grain size in the aeolian transport model, their relevance for aeolian sediment transport was investigated. The simulations show that using the median grain size, D_{50}, as a representative grain size in aeolian sediment transport modeling causes limited deviations from simulations using a full particle size distribution. To test the magnitude of these deviations for wide grain size distributions, simplified model runs with the full particle size distribution and a climate-representative wind forcing may be used. On a 10 minute time scale, the bed surface grain size directly impacts aeolian sediment transport, so model predictions of sediment fluxes may require the implementation of vertical grain size layering. On longer time scales, vertical layering may not be required if a representative grain size is used. Across all time scales, the effects of horizontal grain size variations are relevant as they can affect both the total transport rates and the downwind bed grain size composition. Because the intertidal zone is often the sediment source of aeolian sediment transport, it is advised to include the grain size in this zone in modeling and point measurement analysis.

Besides addressing these research objectives, the Adapted Burland Triangle (ABT) was presented, which can be used to guide the development and application of modeling in the coastal research and engineering field. It was shown that the wide range of research approaches that were presented in this dissertation can be connected within the ABT. It was also demonstrated that the ABT can be used for the identification and prioritization of missing links and knowledge gaps. For example, the relation between grain size variations in the intertidal zone and marine processes may need further attention, and bed surface grain size variations simulated with aeolian sediment transport models may need to be verified with field data. In the future, the ABT can contribute to clarifying the purpose of research and engineering projects, which will advance the coastal research and engineering field as a whole.

7.2. Outlook

Several pathways for future research and development were identified throughout this dissertation. Here, five of these pathways are discussed in detail. It is described how making the analysis of long-term coastal data more accessible can allow more knowledge to be derived from these data (Section 7.2.1). It is also explained how getting a more complete view on the aeolian sediment transport chain can be achieved by combining state-of-the-art measurement techniques (Section 7.2.2). Additionally, further investigation of the relation between marine processes and grain size variations in the intertidal zone is discussed (Section 7.2.3). Recommendations are made for the investigation of the contribution of aeolian bedforms to total aeolian sediment transport (Section 7.2.4), and for further development and application of aeolian sediment transport models like AeoLiS (Section 7.2.5).

7.2.1. Analysis of long-term local coastal data world-wide

The long-term coastal data that is available worldwide provides an abundance of information. However, finding out which data is available and where can be hard. Thus, we see the opportunity for a worldwide overview of available coastal topography datasets. This collection of coastal datasets around the world would make it possible to quickly familiarize new people in the field with the data that is being collected and it would be an efficient way to retain experience. For now, a preliminary collection of coastal datasets around the world, which was gathered during the creation of this dissertation, is available online.

The analysis of long-term coastal data can require considerable effort. The work presented in Chapter 3 was accompanied by the Jarkus Analysis Toolbox which is a resource for research and education as it aims to make analysis of the long-term coastal morphology dataset in the Netherlands more accessible. For example, our experience has shown that the toolbox lowers the threshold for BSc and MSc students to use the database in (thesis) projects. In the future, we anticipate more generic tools that can handle not just one, but many coastal datasets. For example, the analysis tool *pybeach* (Beuzen et al., 2019) was set up more generically which allowed its implementation into the Jarkus Analysis Toolbox. These publicly available analysis methods will provide a

transparent way of analyzing coastal datasets, which prevents miscommunication about coastal parameters (Smith et al., 2020) between researchers from different fields.

There is still a treasure of information available within the available long-term coastal data. Analysis of these data could allow us to gain additional knowledge on physical properties and observed behavior. In Chapter 3 long-term data was used to estimate the importance of sea level rise along the Dutch coast. Similar approaches could be adopted to study the contribution of, for example, alongshore sediment transport. Alongshore transport impacts the sediment budget and Hallin, Huisman, et al. (2019) showed it can be related to dune development. Additionally, many characteristic parameters, like the beach width and dune face slope, were included in the Jarkus Analysis Toolbox, but only the dune toe was used in Chapter 3. Thus, there are still many coastal profile parameters that could be used to analyze coastal profile behavior and expose relations that are not yet known.

7.2.2. Relating sediment properties to measured aeolian transport

Aeolian sediment transport processes were a crucial part of this dissertation, but not a single, direct measurement of aeolian transport was collected. In Chapter 5 it was discussed that the spatial context is important when investigating and explaining aeolian sediment transport on a beach. Thus, point measurements of aeolian sediment transport might show trends that cannot be explained without assumptions about this spatial context (Cohn, Dickhudt, & Marshall, 2022; Field & Pelletier, 2018; Jackson et al., 2006). We propose building a more complete image of aeolian sediment transport by combining state-of-the-art measurement techniques.

In the past decade, innovative techniques have been introduced that can aid in measuring aeolian sediment transport and supply-limiting factors, such as grain size variations, in a broader spatial context. A 3D-printed Instagrain camera is being developed that takes a snapshot of the sand surface and determines the grain size (Goldstein et al., 2022). This device is faster in use than the sand scraper presented in Chapter 4, so it could increase the temporal and spatial resolution at which measurements are collected. To ensure quality control, the sand scraper could provide detailed surface samples that could be used for the validation of the surface photographs. Additionally, the use of a holographic camera to study grain size variations in the air column was recently introduced by Cohn, Dickhudt, and Marshall (2022). Combining this device with bed surface grain size measurements could provide insights into the relation between the grain size of transported sediment and the bed surface grain size. A remote way to study aeolian sediment transport was developed by Nield and Wiggs (2011) and Cohn, Dickhudt, and Brodie (2022), who showed that a lidar scanner is able to detect the saltation cloud on a beach. Further development and application of this technique and its combination with in-situ sediment flux measurements could result in further quantification of aeolian sediment transport.

These new measurement methods all give insights into parts of the spatial chain of physical processes that affect aeolian sediment transport (see Figure 5.1). Bringing these techniques together in different configurations will result in a new and more complete view of aeolian sediment transport. This would contribute to the quantification of the relation between sediment properties and measured aeolian sediment transport on

the beach, which could act as validation for aeolian sediment transport models.

7.2.3. Investigating grain size variations due to marine processes in the intertidal zone

The bed composition in the intertidal zone can show considerable variations in grain size (Chapter 4). Simultaneously, the grain size in the intertidal area affects aeolian sediment transport on the beach and into the dunes (Chapter 5). To better understand the effect of grain size in the intertidal zone on aeolian sediment transport and coastal dune development, future studies could execute additional field measurements, develop empirical formulations, and apply more complex models.

The sand scraper and other grain size sampling methods (e.g., Goldstein et al., 2022) can be used to sample at an increased spatial and temporal resolution compared to the measurements in Chapter 4. These measurements could give a more detailed image of the grain size variations that occur due to marine processes and their relation to environmental conditions. Insights from these measurements could be combined with model simulations to explore parameterizations of the effects of marine processes on grain size variations in the intertidal zone. These insights might especially be valuable in coastal settings where the D_{50} is not a suitable approximation of the grain size distribution for aeolian sediment transport modeling, as identified in Chapter 5.

Model simulations of grain size variations due to marine processes can be executed with numerical models that include multi-fraction sediment transport (Reniers et al., 2013; Srisuwan et al., 2015). Field measurements can enable validation of the spatial and temporal grain size variabilities that are simulated by these marine process models. Exploratory analyses with the multi-fraction XBeach model (Reniers et al., 2013) were executed by Breedveld (2022). These simulations showed the formation of a cross-shore grain size pattern in the intertidal area, which was similar to the pattern observed in the field. The variations in the cross-shore grain size pattern were governed by the spring-neap cycle and the storm time scale. It is expected that the fine sediment supply for aeolian transport is also controlled on these time scales, which indicates that they are the most relevant time scales to focus on in future research.

Numerical models of marine and aeolian processes that allow multi-fraction sediment transport could be coupled to simulate the interaction of marine and aeolian processes that determine grain size variations in the intertidal zone. Such a coupled model can record how aeolian and marine processes affect the bed composition (Gallagher et al., 2016). Also, a coupled model can quantify the potential impact of horizontal and vertical sediment redistribution by marine processes on aeolian transport rates. This would allow identification of marine conditions that inhibit and stimulate aeolian sediment transport through alteration of the bed composition. Additionally, the coupled model could be used to investigate to what extent the grain size variations in the intertidal area on time scales of hours to days are relevant for dune development on the time scale of years to decades.

7.2.4. Quantifying sediment transport by aeolian bedforms

Aeolian bedforms with a horizontal scale of meters and a vertical scale of centimeters, also called aeolian sand strips, occurred during the fieldwork of which the data was presented in Chapter 4. The sand strips had a considerable impact on the sand scraper measurements that were collected at a vertical scale of millimeters. This impact highlighted the dimensions and volume of these bedforms. Previous research has analyzed the behavior of aeolian sand strips based on video imagery (Hage et al., 2018) and with a terrestrial laser scanner (Nield et al., 2011). However, the contribution of aeolian sand strips to coastal dune development has never been quantified. Measurements with a permanent laser scanner (Vos et al., 2022) could provide the elevation data that is needed to estimate transport volumes by aeolian sand strips. For this purpose, a sand strip detection and analysis method is currently being developed at Delft University of Technology using data from a permanent laser scanner in Noordwijk, the Netherlands.

From lidar data alone, the relative contribution of aeolian sand strips to total aeolian sediment transport cannot be determined. However, determining the ratio between sediment fluxes due to aeolian sand strips and other forms of transport (e.g., creep and saltation) can clarify which transport type is most relevant for coastal dune development. Fieldwork could be executed that combines the measurements of sand strip behavior with measurements of aeolian saltation. Alternatively, beach and dune volume changes could be extracted from coastal morphology measurements and compared to the observed behavior of the aeolian sand strips. Depending on the outcome of these investigations, it could be decided to include the contribution of aeolian sand strips in aeolian sediment transport models.

7.2.5. Applying and validating aeolian sediment transport models

In this dissertation, I focused on aeolian processes and the potential impact of sea level rise, however, other marine dynamics, and soil moisture, vegetation, and wind field dynamics (Figure 7.1) can also impact coastal dune development. Important aspects of these dynamics have recently been included in the aeolian sediment transport model AeoLiS, which was used in Chapter 5. A soil moisture module that simulates soil moisture dynamics was introduced and implemented by Hallin et al. (2023). The soil moisture module calculates the moisture content of the upper 2 mm of the surface based on wave runup, precipitation, evaporation, infiltration, and capillary rise from the groundwater table. The empirical formulation of Palmsten and Holman (2012) was introduced in AeoLiS to include the effect of dune erosion during storm conditions. Vegetation dynamics have been implemented in the model based on approaches proposed by Durán and Herrmann (2006), Durán and Moore (2013) and Keijsers et al. (2015). Wind field perturbation dynamics have been introduced based on methods by Kroy et al. (2002), Weng et al. (1991) and Sauermann et al. (2001). Additionally, Dickey et al. (2023) implemented an adapted version of the Okin shear coupler (Okin, 2008), which takes into account the effect of vegetation on the shear velocity.

Several future advances in the dynamics that are implemented in AeoLiS are expected. The relevance of the effect of flow dynamics on dune accretion was recently shown by (Bauer & Wakes, 2022). Efforts are being made at the Technical University Twente

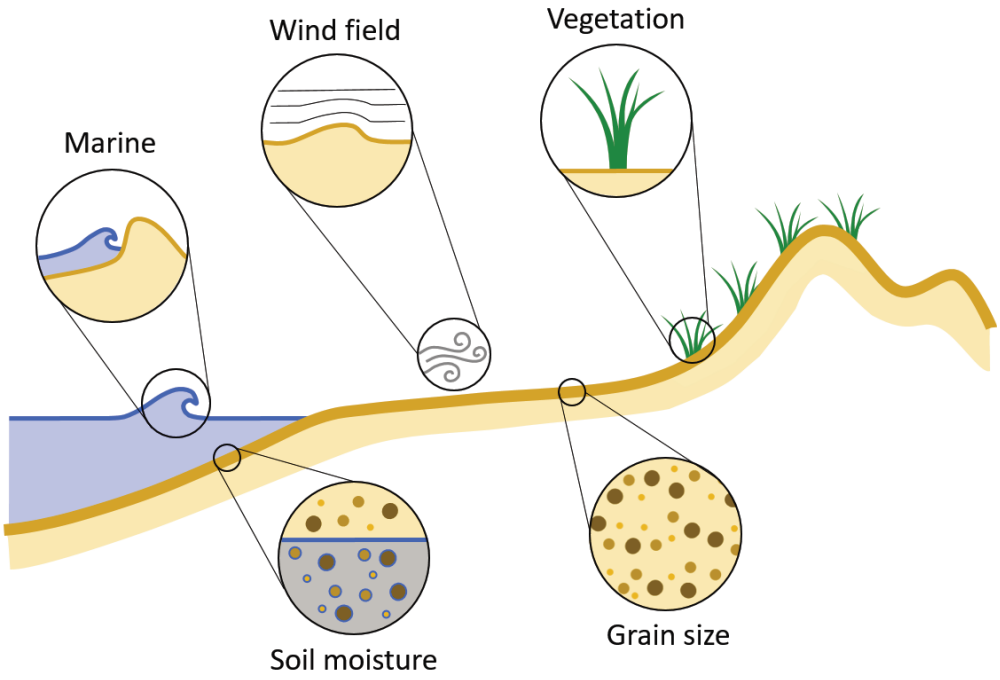

Figure 7.1: Different dynamics that affect coastal dune development and have been implemented in the aeolian sediment transport model AeoLiS.

to include flow dynamics caused by dune faces and beach buildings by implementing the output of the Computational Flow Dynamics (CFD) model OpenFOAM into AeoLiS. Additionally, progress in the integration of the vegetation dynamics is expected based on work at Oregon State University that focuses on the implementation of different vegetation types. At Wageningen University & Research, investigations are ongoing that quantify the processes of germination, establishment and survival of dune vegetation. The recent and upcoming implementations are expected to greatly improve the representation of physical processes in AeoLiS. However, there remain many important factors that are not well-represented. For example, the impact of alongshore transport (Hallin, Huisman, et al., 2019) and anthropogenic impacts like bulldozing (Barbero-García et al., 2023) and nourishments (Hallin, Huisman, et al., 2019) have not yet been included.

There remains an endless amount of physical processes that could be taken into account in process-based numerical models. However, it remains a question which marine, aeolian, ecological, anthropogenic and hydrological processes should be included and in what detail across different spatial and temporal scales. In Chapter 5, it was determined that the effect of the grain size distribution is limited if certain exceptions are taken into account. Thus, analysis of the impact of grain size through a transparent and generic sensitivity analysis was used to reduce the degrees of freedom in numerical models. As the functionalities in AeoLiS develop, I expect that more of these types

of studies are executed. For example, the effects of soil moisture content and vegetation dynamics can be further examined as the processes are better represented in the model. In this way, the most important dynamics can be identified, which provides focus for their further development and application. Additionally, the combined effect of different physical processes can be studied. For instance, the combined effect of grain size and surface moisture variability on velocity thresholds is largely unknown. As both of these factors are included in the AeoLiS model, this will provide the opportunity to investigate their interaction and the resulting effect on aeolian sediment transport.

Ultimately, AeoLiS is being developed to achieve quantitative predictions that are suitable for engineering purposes. In this dissertation AeoLiS was mostly used as an academic tool to test the relevance of grain size on coastal aeolian sediment transport. The academic and applied uses of the model can exist in parallel. However, the connection between modeling and observed behavior as prescribed by the Adapted Burland Triangle is still underexposed in the development of AeoLiS. Thus, increased efforts to apply the model to real-world cases are key for validation and calibration. These real-world cases do require sufficient high-quality data on environmental conditions, ecological properties, and morphological change. To apply AeoLiS to existing dunes, the collection of long-term local coastal data that is available world-wide may be a good starting point. Often local hydrodynamic data is available in these locations and satellite imagery could be used to retrieve ecological properties (Laporte-Fauret et al., 2020). Additionally, there are many dune restoration and creation projects around the world (e.g. Rozé & Lemauviel, 2004 and Darke et al., 2016) that provide cases where monitoring data of newly formed dunes are available. As the model is applied to different types of settings and locations, there will be variations in the relative importance of different physical processes. This will push the applicability of the model and provide opportunities to further improve it. Moreover, application of the model will provide valuable knowledge and recommendations for coastal communities as they try to balance the different functions of the coastal dune system.


CAL POLY
SPACE INVA

Acknowledgements

I don't know if it was the PhD, the covid, or if this is just what happens in your mid-twenties, but the past 4 years were hectic to say the least. Thankfully, there were many amazing people that made this roller coaster a smoother ride.

I want to deeply thank my parents. I can always rely on them and I am very lucky to have their support. Mam, although my pubescent self was stubborn, I am now very happy to give you credits, in black-and-white, for suggesting that having a look at the Earth Sciences BSc in Utrecht might be a good option for me. You put me onto an academic path that we still haven't seen the end of... Pap, your sincere way of engaging with people is a great inspiration to me. When I lose myself in a task or project, I sometimes realize that I am turning into my father, but that really is not a bad deal. Losing ourselves in DIY projects was just what I needed before I moved to Zoetermeer, thank you for that.

Many thanks to my brother, Gerben. Much of the good music you introduced me to has been part of dragging me through writing this dissertation. Please keep it coming! And that also accounts for the open and introspective conversations we have been having more of in the past years. Marjolein, thank you for showing interest in my work and all my adventures. It is always a joy to be at your place and your amazing desserts will keep me coming back for more.

Lieve Hilde en Rosan, jullie tante doet onderzoek naar zand en water, maar dat kan jullie gelukkig helemaal niks schelen! Samen spelen, rennen, springen, vliegen en fietsen waren heerlijke momenten waarop ik me niet meer alleen onderzoeker maar ook mens voelde. Wat jullie ook gaan doen in de toekomst laten we zo samen blijven genieten!

Christien, many thanks for listening to my wishes and designing the beautiful cover of this dissertation. Aside from the name, I feel like our similarities have been increasing in recent years. Thank you for being an inspiring role model in my life.

Anne, having an office buddy that was going through the same process at the same time was such a blessing. Writing a dissertation, being a woman in academics and having covid together are surprisingly similar: it is just much easier when you can share all the ups and downs. I am very grateful that we can finish this crazy ride as each other's paranymphs. Traveling together in Australia was an absolute highlight - your Wombat Waddle is etched into my memory.

Elise, thank you for showing up for me when I needed you. In the past years, I have been lucky to go on amazing vacations with you. From nerding in Pompeii, cycling up some crazy mountains with you as my safety driver, to accidentally looking like a couple in Portugal. Playing games with you always breaks my brain, but it's a great way to snap me out of work mode.

One thing I have learned throughout the years is that Earth Scientists are amazing friends. Dear Quintet (Dennis, Jip, Pascal & Vera), our Skype meeting name is a testament to you all being there when I most needed it. Thank you for keeping the online meetings going throughout the pandemic and after. I really enjoy playing silly games together, watching WIDM and doing pub-quizzes so Vera can win them. I promise that I will be joining from the US as well! Pascal, I feel like any task we tackle together goes smoothly, whether it is moving, catching mice or (hopefully) defending. I'm delighted to have you by my side as my paranymph. Dear Evi & Marijn, thank you for being awesome friends. Hanging out with you two always feels like a warm bath. It's been a joy watching your lives unfold and I cannot wait to be at your wedding. Meeke, you are and will always be my roomie, watching series together during the pandemic was one of the things that kept me (moderately) sane. Snowboarding together with you, Esmée, Evi, Marijn and Hailey, was an absolute blast.

Jeannette, Kevin, Tyler and Kelsey, thank you for having me on the camping trip in Oregon, and for showing me what a real American holiday season looks like. I hope to be there for many more of those! And Jeannette, backpacking together was amazing! It was a well-deserved treat after handing in my thesis.

I have been really blessed to work with some amazing people during my PhD. Sierd, getting the chance to work with you has felt like winning the lottery. I couldn't have asked for a better supervisor. I really appreciate that you try to listen and learn, and that you have a well-developed sense of self-awareness. These characteristics make you a great ally to anyone that needs support. Your way of supervising will have a lasting effect on my career and my own supervision approach. I want to thank you for consistently checking in during the pandemic, and sharing your network and many opportunities with me after. I think we work together really well and I look forward to our future collaborations.

Caroline, you have had such an enormous influence on my work and development in the past years. You're passion about research is infectious. Of course, I wish we could have seen each other more in-person, but I honestly think we have made the best of a complicated situation. Seeing you in your natural environment in Sweden was a joy and I have thoroughly enjoyed all the adventures that came after (including some dance moves in Sydney).

Ad, in the past few years I have come to dread your comments in the most positive of ways. There will always only be a few, but those few will have me thinking for days. Your insights and your way of working with students have made me a better academic.

Many thanks to the whole DuneForce team! This includes our colleagues at Wageningen, Jan-Markus, Juul, Michel and Aaron. I have enjoyed working with you and I have learned a lot from the more ecological perspective that you all bring. I also want to thank the DuneForce users that were involved in our research project. The user meetings were always inspiring and constructive. I am thankful to have been able build my professional network around such an energetic group of people.

A big thanks to the AeoLiS Development Team for their enthusiasm and support! I loved working and travelling with you all. Highlights include the amazing contributions of Niket and Manuel, the success of the AeoLiS short course, climbing in Sweden, and our competitiveness in the arcade. A special thank you to Nick for welcoming me in

Duck for fieldwork during confusing covid times and for being extraordinarily supportive while I was figuring out future job options.

There are many people at the TU Delft that have contributed to my PhD being a really positive experience. Thanks to Anne, Anna and Matthijs for being great office mates. Sander, thank you for collaborating with me on some very interesting projects. A big thank you to my other colleagues: Ana, Bart, Camilo, Floris, Gijs, Jakob, Jill, Mario, Marion, Marlies, Matthieu, Paul B., Paul van W., Stuart, Su, Tosca and many others. I also want to thank the BSc and MSc students that I got to work with during my PhD. Their work was inspiring and collaborating with them has shown me how much I enjoy supervision.

Thank you to all the people at or related to Oregon State University that made me feel very welcome in San Diego, Corvallis and New Orleans: Meredith, Reggie, Joey, Tessa, Meghan, Liz, Alex, Jeremy, Meagan, Peter, Rob, Jeff, Quentin, Hannah, Carson and many others. I'm so excited to collaborate and hang out with you all more soon!

More broadly, I want to thank coastal researchers, engineers and professionals for being awesome. This particular field has a great atmosphere and I hope to collaborate with many of you and to contribute to the field for many years to come.

To close, there are two beings that I love most in this world and they both deserve the biggest hug for getting me through the pandemic and finishing my dissertation. Julius, you are the best covid cat one could wish for. The amount of cat hair on my keyboard is a testament to you keeping an eye on my work-life balance. I hope I have deleted all of your contributions to this dissertation, and I apologize in advance for putting you on a plane to the US.

Lieve Hailey, your unconditional support has helped tremendously while going through the many ups and downs that come with finishing a PhD. I really like how your brain works and our many interesting work-related conversations have had a huge influence on my development as a coastal researcher. I am very thankful that you are so communicative and that we have been able to, not only, navigate a professional-private balance, but also the many changing covid regulations and three years of long distance. In the past years, we have been having some crazy adventures, but I am so ready for it to be us at home with a cat.

Bibliography

Aagaard, T., & Greenwood, B. (2008). Infragravity wave contribution to surf zone sediment transport - The role of advection. *Marine Geology*, *251*(1-2), 1–14. doi: 10.1016/j.margeo.2008.01.017

Abuodha, J. O. (2003). Grain size distribution and composition of modern dune and beach sediments, Malindi Bay coast, Kenya. *Journal of African Earth Sciences*, *36*(1-2), 41–54. doi: 10.1016/S0899-5362(03)00016-2

AeoLiS Development Team. (2023). *AeoLiS (Version v2.1.0). [Software]*. 4TU Repository. doi: 10.4121/22215562

Anderson, R. S., & Haff, P. K. (1988). Simulation of Eolian Saltation. *Science*, *241*(4867), 820–823. doi: 10.1126/SCIENCE.241.4867.820

Anfuso, G. (2005). Sediment-activation depth values for gentle and steep beaches. *Marine Geology*, *220*(1-4), 101–112. doi: 10.1016/J.MARGEO.2005.06.027

Arens, S. M., & Wiersma, J. (1994). The Dutch foredunes: inventory and classification. *Journal of Coastal Research*.

Atkinson, A. L., Baldock, T. E., Birrien, F., Callaghan, D. P., Nielsen, P., Beuzen, T., … Ranasinghe, R. (2018). Laboratory investigation of the Bruun Rule and beach response to sea level rise. *Coastal Engineering*, *136*, 183–202. doi: 10.1016/j.coastaleng.2018.03.003

Baas, A. C. (2006). Wavelet power spectra of aeolian sand transport by boundary layer turbulence. *Geophysical Research Letters*, *33*(5), 5403. doi: 10.1029/2005GL025547

Bagnold, R. A. (1937a). The size-grading of sand by wind. *Proceedings of the Royal Society of London. Series A - Mathematical and Physical Sciences*, *163*(913), 250–264. doi: 10.1098/rspa.1937.0225

Bagnold, R. A. (1937b). The Transport of Sand by Wind. *The Geographical Journal*, *89*(5), 409. doi: 10.2307/1786411

Bagnold, R. A. (1941). The Physics of Blown Sand and Desert Dunes. *The Geographical Journal*. doi: 10.2307/1787211

Barbero-García, I., Kuschnerus, M., Vos, S., & Lindenbergh, R. (2023). Automatic detection of bulldozer-induced changes on a sandy beach from video using YOLO algorithm. *International Journal of Applied Earth Observation and Geoinformation*, *117*. doi: 10.1016/j.jag.2023.103185

Barbour, S. L., & Krahn, J. (2004). Numerical modelling - Prediction or process? *Geotechnical News*, *22*(4), 44–52.

Barchyn, T. E., Martin, R. L., Kok, J. F., & Hugenholtz, C. H. (2014). Fundamental mismatches between measurements and models in aeolian sediment transport prediction: The role of small-scale variability. *Aeolian Research*, *15*, 245–251. doi: 10.1016/J.AEOLIA.2014.07.002

Barnard, P. L., Rubin, D. M., Harney, J., & Mustain, N. (2007). Field test comparison of an autocorrelation technique for determining grain size using a digital 'beachball' camera versus traditional methods. *Sedimentary Geology*, *201*(1-2), 180–195. doi: 10.1016/J.SEDGEO.2007.05.016

Bascom, W. N. (1951). The relationship between sand size and beach-face slope. *Eos, Transactions American Geophysical Union*, *32*(6), 866–874. doi: 10.1029/TR032I006P00866

Bauer, B. (1991). Aeolian Decoupling of Beach Sediments. *Annals of the Association of American Geographers*, *81*(2), 290–303. doi: 10.1111/j.1467-8306.1991.tb01691.x

Bauer, B., & Davidson-Arnott, R. G. (2002). A general framework for modeling sediment supply to coastal dunes including wind angle, beach geometry, and fetch effects. *Geomorphology*, *49*(1), 89–108. doi: 10.1016/S0169-555X(02)00165-4

Bauer, B., Davidson-Arnott, R. G., Hesp, P. A., Namikas, S. L., Ollerhead, J., & Walker, I. J. (2009). Aeolian sediment transport on a beach: Surface moisture, wind fetch, and mean transport. *Geomorphology*. doi: 10.1016/j.geomorph.2008.02.016

Bauer, B., & Wakes, S. J. (2022). CFD simulations of wind flow across scarped foredunes: Implications for sediment pathways and beach–dune recovery after storms. *Earth Surface Processes and Landforms*, *47*(12), 2989–3015. doi: 10.1002/ESP.5439

Beaucage, P., Glazer, A., Choisnard, J., Yu, W., Bernier, M., Benoit, R., & Lafrance, G. (2007). Wind assessment in a coastal environment using synthetic aperture radar satellite imagery and a numerical weather prediction model. *Canadian Journal of Remote Sensing*, *33*(5), 368–377. doi: 10.5589/M07-043

Beets, D. J., van der Valk, L., & Stive, M. J. (1992). Holocene evolution of the coast of Holland. *Marine Geology*, *103*(1-3), 423–443. doi: 10.1016/0025-3227(92)90030-L

Bemmelen, C. v. (1988). *De korrelgrootte-samenstelling van het strandzand langs de Nederlandse Noordzee-kust - Rijkswaterstaat Rapportendatabank* (Tech. Rep.). Utrecht: Geografisch Instituut, Vakgroep Fysische Geografie, Rijksuniv. Utrecht.

Beuzen, T., Simmons, J., Harley, M., Plant, N. G., Stockdon, H. F., Beuzen, T., … Stockdon, H. F. (2019). A machine learning approach for identifying dune toes on beach profile transects. *AGUFM*, *2019*, EP54C-06.

Beven, J. L., Hagen, A., & Berg, R. (2022). *Tropical Cyclone Report Hurricane Ida* (Tech. Rep.). Miami: National Hurricane Center.

Biel, R. G., Hacker, S. D., Ruggiero, P., Cohn, N., Seabloom, E. W., Biel, C. ., … Seabloom, E. W. (2017). Coastal protection and conservation on sandy beaches and dunes: context-dependent tradeoffs in ecosystem service supply. *Ecosphere*, *8*(4), e01791. doi: 10.1002/ECS2.1791

Brakenhoff, L., Ruessink, B. G., & van der Vegt, M. (2017). Saw-Tooth Bar Dynamics on the Ameland Ebb-Tidal Delta. *Coastal Dynamics*(076), 198–199.

Brand, E., De Sloover, L., De Wulf, A., Montreuil, A. L., Vos, S., & Chen, M. (2019). Cross-Shore Suspended Sediment Transport in Relation to Topographic Changes in the Intertidal Zone of a Macro-Tidal Beach (Mariakerke, Belgium). *Journal of Marine Science and Engineering 2019, Vol. 7, Page 172*, *7*(6), 172. doi: 10.3390/

JMSE7060172

Breedveld, R. (2022). *Modelling of the cross-shore grain size distribution in the intertidal zone*.

Bristow, N. R., Best, J., Wiggs, G. F., Nield, J. M., Baddock, M. C., Delorme, P., & Christensen, K. T. (2022). Topographic perturbation of turbulent boundary layers by low-angle, early-stage aeolian dunes. *Earth Surface Processes and Landforms*, *47*(6), 1439–1454. doi: 10.1002/ESP.5326

Bruun, P. (1962). Sea-Level Rise as a Cause of Shore Erosion. *Journal of the Waterways and Harbors Division*, *88*(1).

BS1377-2. (1990). Part 2: Classification tests. In *Methods of tests for soils for civil engineering purposes*. London: British Standard.

Burland, J. (1987). The teaching of soil mechanics - a personal view. In *Proc. 9th ercsmfe, dublin* (pp. 1427–1447).

Buscombe, D., Rubin, D. M., & Warrick, J. A. (2010). A universal approximation of grain size from images of noncohesive sediment. *Journal of Geophysical Research: Earth Surface*, *115*(F2), 2015. doi: 10.1029/2009JF001477

Carson, M., Köhl, A., Stammer, D., A. Slangen, A. B., Katsman, C. A., W. van de Wal, R. S., … White, N. (2016). Coastal sea level changes, observed and projected during the 20th and 21st century. *Climatic Change*, *134*(1-2), 269–281. doi: 10.1007/S10584-015-1520-1/FIGURES/6

Carter, R. W., & Rihan, C. L. (1978). Shell and pebble pavements on beaches: Examples from the north coast of Ireland. *CATENA*, *5*(3-4), 365–374. doi: 10.1016/0341-8162(78)90019-X

Castelle, B., Bujan, S., Ferreira, S., & Dodet, G. (2017). Foredune morphological changes and beach recovery from the extreme 2013/2014 winter at a high-energy sandy coast. *Marine Geology*, *385*, 41–55. doi: 10.1016/J.MARGEO.2016.12.006

Castelle, B., Marieu, V., Bujan, S., Splinter, K. D., Robinet, A., Sénéchal, N., & Ferreira, S. (2015). Impact of the winter 2013-2014 series of severe Western Europe storms on a double-barred sandy coast: Beach and dune erosion and megacusp embayments. *Geomorphology*, *238*, 135–148. doi: 10.1016/j.geomorph.2015.03.006

Cazenave, A., & Cozannet, G. L. (2014). Sea level rise and its coastal impacts. *Earth's Future*, *2*(2), 15–34. doi: 10.1002/2013EF000188

CBS; PBL; RIVM; WUR. (2016). *Sea level: Dutch coast and worldwide, 1890-2014*. Statistics Netherlands (CBS), The Hague; PBL Netherlands Environmental Assessment Agency, The Hague; RIVM National Institute for Public Health and the Environment, Bilthoven; and Wageningen University and Research, Wageningen.

Çelikoglu, Y., Yüksel, Y., & Sedat Kabdaşli, M. (2006). Cross-Shore Sorting on a Beach under Wave Action. *Journal of Coastal Research*, *22*(3 (223)), 487–501. doi: 10.2112/05-0567.1

Chakrabarti, A. (1981). Burrow patterns of Ocypode ceratophthalma (Pallas) and their environmental significance. *Journal of Paleontology*.

Cheng, H., He, J., Zou, X., Li, J., Liu, C., Liu, B., … Kang, L. (2015). Characteristics of particle size for creeping and saltating sand grains in aeolian transport.

Sedimentology, *62*(5), 1497–1511. doi: 10.1111/SED.12191

Clifton, H. E. (1969). Beach lamination: Nature and origin. *Marine Geology*, *7*(6), 553–559. doi: 10.1016/0025-3227(69)90023-1

Coch, N. K., & Wolff, M. P. (1992). Effects of Hurricane Hugo storm surge in coastal South Carolina. *Journal of Coastal Research, Special Issue*, *8*, 201–226.

Cohn, N., Dickhudt, P., & Brodie, K. (2022). Remote Observations of Aeolian Saltation. *Geophysical Research Letters*, *49*(16), e2022GL100066. doi: 10.1029/2022GL100066

Cohn, N., Dickhudt, P., & Marshall, J. (2022). In-situ measurement of grain size characteristics within the aeolian saltation layer on a coastal beach. *Earth Surface Processes and Landforms*, *47*(9), 2230–2244. doi: 10.1002/ESP.5373

Cohn, N., Hoonhout, B., Goldstein, E., de Vries, S., Moore, L., Durán Vinent, O., & Ruggiero, P. (2019). Exploring Marine and Aeolian Controls on Coastal Foredune Growth Using a Coupled Numerical Model. *Journal of Marine Science and Engineering*, *7*(1), 13. doi: 10.3390/jmse7010013

Cohn, N., Ruggiero, P., de Vries, S., & Kaminsky, G. M. (2018). New Insights on Coastal Foredune Growth: The Relative Contributions of Marine and Aeolian Processes. *Geophysical Research Letters*, *45*(10), 4965–4973. doi: 10.1029/2018GL077836

Cohn, N., Ruggiero, P., García-Medina, G., Anderson, D., Serafin, K. A., & Biel, R. (2019). Environmental and morphologic controls on wave-induced dune response. *Geomorphology*, *329*, 108–128. doi: 10.1016/j.geomorph.2018.12.023

Costas, S., Ferreira, Ó., Plomaritis, T. A., & Leorri, E. (2016). Coastal barrier stratigraphy for Holocene high-resolution sea-level reconstruction. *Scientific Reports*, *6*(1), 1–12. doi: 10.1038/srep38726

Darke, I. B., Walker, I. J., & Hesp, P. A. (2016). Beach–dune sediment budgets and dune morphodynamics following coastal dune restoration, Wickaninnish Dunes, Canada. *Earth Surface Processes and Landforms*, *41*(10), 1370–1385. doi: 10.1002/ESP.3910

Davidson, M. A., & Turner, I. L. (2009). A behavioral template beach profile model for predicting seasonal to interannual shoreline evolution. *Journal of Geophysical Research: Earth Surface*, *114*(1). doi: 10.1029/2007JF000888

Davidson, S. G., Hesp, P. A., & da Silva, G. M. (2020). Controls on dune scarping. *Progress in Physical Geography*, *44*(6), 923–947. doi: 10.1177/0309133320932880

Davidson-Arnott, R. G. D. (2005). Conceptual model of the effects of sea level rise on sandy coasts. *Journal of Coastal Research*, *21*(6), 1166–1172. doi: 10.2112/03-0051.1

Davidson-Arnott, R. G. D., & Law, M. (1990). Seasonal patterns and controls on sediment supply to coastal foredunes, Long Point, Lake Erie. *Coastal Dunes: Form and Process*, 177–200.

Davidson-Arnott, R. G. D., Yang, Y., Ollerhead, J., Hesp, P. A., & Walker, I. J. (2008). The effects of surface moisture on aeolian sediment transport threshold and mass flux on a beach. *Earth Surf. Process. Landforms*, *33*, 55–74. doi: 10.1002/esp

Dean, R. G., & Houston, J. R. (2016). Determining shoreline response to sea level rise. *Coastal Engineering*, *114*, 1–8. doi: 10.1016/j.coastaleng.2016.03.009

De Bakker, A. T., Tissier, M. F., & Ruessink, B. G. (2016). Beach steepness effects on nonlinear infragravity-wave interactions: A numerical study. *Journal of Geophysical Research: Oceans*, *121*(1), 554–570. doi: 10.1002/2015JC011268

Defeo, O., McLachlan, A., Schoeman, D. S., Schlacher, T. A., Dugan, J., Jones, A., … Scapini, F. (2009). Threats to sandy beach ecosystems: A review. *Estuarine, Coastal and Shelf Science*, *81*(1), 1–12. doi: 10.1016/J.ECSS.2008.09.022

Delgado-Fernandez, I. (2010). A review of the application of the fetch effect to modelling sand supply to coastal foredunes. *Aeolian Research*, *2*(2-3), 61–70. doi: 10.1016/j.aeolia.2010.04.001

Delgado-Fernandez, I. (2011). Meso-scale modelling of aeolian sediment input to coastal dunes. *Geomorphology*, *130*(3-4), 230–243. doi: 10.1016/j.geomorph.2011.04.001

Delgado-Fernandez, I., Davidson-Arnott, R. G., & Hesp, P. A. (2019). Is 're-mobilisation' nature restoration or nature destruction? A commentary. *Journal of Coastal Conservation*, *23*(6), 1093–1103. doi: 10.1007/S11852-019-00716-9/FIGURES/2

Delgado-Fernandez, I., O'Keeffe, N., & Davidson-Arnott, R. G. (2019). Natural and human controls on dune vegetation cover and disturbance. *Science of The Total Environment*, *672*, 643–656. doi: 10.1016/J.SCITOTENV.2019.03.494

De Ruig, J. H. (1998). Coastline management in The Netherlands: Human use versus natural dynamics. *Journal of Coastal Conservation*, *4*(2), 127–134. doi: 10.1007/BF02806504

De Ruyck, M. C., Soares, A. G., & McLachlan, A. (1997). Social carrying capacity as a management tool for sandy beaches. *Journal of Coastal Research*, *13*(3).

De Vriend, H. J. (1991). Mathematical modelling and large-scale coastal behaviour - Part 1: Physical Processes. *Journal of Hydraulic Research*, *29*(6).

de Vriend, H. J., van Koningsveld, M., Aarninkhof, S. G., de Vries, M. B., & Baptist, M. J. (2015). Sustainable hydraulic engineering through building with nature. *Journal of Hydro-environment Research*, *9*(2), 159–171. doi: 10.1016/J.JHER.2014.06.004

de Vries, S., Arens, S. M., de Schipper, M. A., & Ranasinghe, R. (2014). Aeolian sediment transport on a beach with a varying sediment supply. *Aeolian Research*. doi: 10.1016/j.aeolia.2014.08.001

de Vries, S., Southgate, H. N., Kanning, W., & Ranasinghe, R. (2012). Dune behavior and aeolian transport on decadal timescales. *Coastal Engineering*. doi: 10.1016/j.coastaleng.2012.04.002

de Vries, S., van Thiel de Vries, J. S., van Rijn, L. C., Arens, S. M., & Ranasinghe, R. (2014). Aeolian sediment transport in supply limited situations. *Aeolian Research*, *12*, 75–85. doi: 10.1016/j.aeolia.2013.11.005

de Vries, S., Verheijen, A. ., Hoonhout, B. ., Vos, S. ., Cohn, N. ., & Ruggiero, P. (2017). Measured spatial variability of beach erosion due to aeolian processes. In T. Aagaard, R. Deigaard, & D. Fuhrman (Eds.), *Proceedings of coastal dynamics 2017*. Helsingør, Denmark.

de Winter, W., Donker, J., Sterk, G., van Beem, J., & Ruessink, G. (2020). Regional versus local wind speed and direction at a narrow beach with a high and steep foredune. *PLOS ONE*, *15*(1), e0226983. doi: 10.1371/JOURNAL.PONE.0226983

Diamantidou, E. (2019). *Dune foot position, accompanying data on the research of Assessment of the effects of nourishments on coastal state indicators, using a Bayesian modelling approach [Data set]*. 4TU. Centre for Research Data. doi: https://doi.org/10.4121/uuid:0a5237ec-8ccc-4bbe-8d41-01716d835471

Diamantidou, E., Santinelli, G., Giardino, A., Stronkhorst, J., & de Vries, S. (2020). An Automatic Procedure for Dune Foot Position Detection: Application to the Dutch Coast. *Journal of Coastal Research*, *36*(3), 668. doi: 10.2112/jcoastres-d-19-00056.1

Dickey, J., Wengrove, M., Cohn, N., Ruggiero, P., & Hacker, S. D. (2023). Observations and modeling of shear stress reduction and sediment flux within sparse dune grass canopies on managed coastal dunes. *Earth Surface Processes and Landforms*, 1–16. doi: 10.1002/esp.5526

Dodet, G., Castelle, B., Masselink, G., Scott, T., Davidson, M., Floc'h, F., … Suanez, S. (2019). Beach recovery from extreme storm activity during the 2013-14 winter along the Atlantic coast of Europe. *Earth Surface Processes and Landforms*, *44*(1), 393–401. doi: 10.1002/esp.4500

Dong, Z., Wang, H., Liu, X., & Wang, X. (2004). A wind tunnel investigation of the influences of fetch length on the flux profile of a sand cloud blowing over a gravel surface. *Earth Surf. Process. Landforms*, *29*, 1613–1626. doi: 10.1002/esp.1116

Doran, K., Long, J., & Overbeck, J. (2015). *A method for determining average beach slope and beach slope variability for US sandy coastlines* (Tech. Rep.). USGS. doi: 10.3133/ofr20151053

Doyle, T. B., Short, A. D., Ruggiero, P., & Woodroffe, C. D. (2019). Interdecadal Foredune Changes along the Southeast Australian Coastline: 1942–2014. *Journal of Marine Science and Engineering*, *7*(6), 177. doi: 10.3390/jmse7060177

Durán, O., Claudin, P., & Andreotti, B. (2011). On aeolian transport: Grain-scale interactions, dynamical mechanisms and scaling laws. *Aeolian Research*, *3*(3), 243–270. doi: 10.1016/J.AEOLIA.2011.07.006

Durán, O., & Herrmann, H. J. (2006). Vegetation against dune mobility. *Physical Review Letters*, *97*(18), 1–4. doi: 10.1103/PhysRevLett.97.188001

Durán, O., & Moore, L. J. (2013). Vegetation controls on the maximum size of coastal dunes. *Proceedings of the National Academy of Sciences of the United States of America*. doi: 10.1073/pnas.1307580110

Edwards, A. C. (2001). Grain size and sorting in modern beach sands. *Journal of Coastal Research*, *17*(1).

Elko, N. A., Sallenger, A. H., Guy, K., & Morgan, K. L. M. (2002). *Barrier island elevations relevant to potential storm impacts; 2. South Atlantic* (Tech. Rep. No. 02-0288). St. Petersburg: U.S. Geological Survey.

Emery, K. O. (1978). Grain size in laminae of beach sand. *Journal of Sedimentary Research*, *48*(4), 1203–1212. doi: 10.1306/212F7630-2B24-11D7

-8648000102C1865D

Everard, M., Jones, L., & Watts, B. (2010). Have we neglected the societal importance of sand dunes? An ecosystem services perspective. *Aquatic Conservation: Marine and Freshwater Ecosystems*, *20*(4), 476–487. doi: 10.1002/AQC.1114

Field, J. P., & Pelletier, J. D. (2018). Controls on the aerodynamic roughness length and the grain-size dependence of aeolian sediment transport. *Earth Surface Processes and Landforms*, *43*(12), 2616–2626. doi: 10.1002/ESP.4420

Gallagher, E. L., MacMahan, J., Reniers, A., Brown, J., & Thornton, E. (2011). Grain size variability on a rip-channeled beach. *Marine Geology*. doi: 10.1016/j.margeo .2011.06.010

Gallagher, E. L., Wadman, H., McNinch, J., Reniers, A., & Koktas, M. (2016). A Conceptual Model for Spatial Grain Size Variability on the Surface of and within Beaches. *Journal of Marine Science and Engineering 2016, Vol. 4, Page 38*, *4*(2), 38. doi: 10.3390/JMSE4020038

Gao, X., Narteau, C., & Rozier, O. (2016). Controls on and effects of armoring and vertical sorting in aeolian dune fields: A numerical simulation study. *Geophysical Research Letters*, *43*(6), 2614–2622. doi: 10.1002/2016GL068416

George, E., Lunardi, B., Smith, A., Lehner, J., Wernette, P., & Houser, C. (2021). Short communication: Storm impact and recovery of a beach-dune system in Prince Edward Island. *Geomorphology*, *384*, 107721. doi: 10.1016/J.GEOMORPH .2021.107721

Giardino, A., Santinelli, G., & Vuik, V. (2014). Coastal state indicators to assess the morphological development of the Holland coast due to natural and anthropogenic pressure factors. *Ocean and Coastal Management*, *87*, 93–101. doi: 10.1016/j.ocecoaman.2013.09.015

Gillette, D. A., Herbert, G., Stockton, P. H., & Owen, P. (1996). Causes of the fetch effect in wind erosion. *Earth Surface Processes and Landforms*, *21*, 641–659. doi: 10.1002/(SICI)1096-9837(199607)21:7

Goldstein, E. B., Stasiewicz, J., Mieras, R., & Mohanty, S. (2022). *Instagrain: A camera for instant sediment grain size measurements*. Zenodo. doi: https://doi.org/ 10.5281/zenodo.7041151

Guillén, J., Stive, M. J., & Capobianco, M. (1999). Shoreline evolution of the Holland coast on a decadal scale. *Earth Surface Processes and Landforms*, *24*(6), 517–536. doi: 10.1002/(SICI)1096-9837(199906)24:6<517::AID-ESP974>3 .0.CO;2-A

Gunaratna, T., Suzuki, T., & Yanagishima, S. (2019). Cross-shore grain size and sorting patterns for the bed profile variation at a dissipative beach: Hasaki Coast, Japan. *Marine Geology*, *407*, 111–120. doi: 10.1016/J.MARGEO.2018.10.008

Hage, P. M., Ruessink, B. G., & Donker, J. J. (2018, 8). Determining sand strip characteristics using Argus video monitoring. *Aeolian Research*, *33*, 1–11. doi: 10.1016/j.aeolia.2018.03.007

Hallin, C., Almström, B., Larson, M., & Hanson, H. (2019). Longshore Transport Variability of Beach Face Grain Size: Implications for Dune Evolution. *Journal of Coastal Research*, *35*(4), 751–764. doi: 10.2112/JCOASTRES-D-18-00153.1

Hallin, C., Huisman, B. J., Larson, M., Walstra, D. J. R., & Hanson, H. (2019). Impact

of sediment supply on decadal-scale dune evolution — Analysis and modelling of the Kennemer dunes in the Netherlands. *Geomorphology*, *337*, 94–110. doi: 10.1016/j.geomorph.2019.04.003

Hallin, C., Larson, M., & Hanson, H. (2019). Simulating beach and dune evolution at decadal to centennial scale under rising sea levels. *PLOS ONE*, *14*(4), e0215651. doi: 10.1371/journal.pone.0215651

Hallin, C., van IJzendoorn, C. O., Homberger, J.-M., & de Vries, S. (2023). Simulating surface soil moisture on sandy beaches. *Submitted to Coastal Engineering*.

Hardin, E., Kurum, M. O., Mitasova, H., & Overton, M. F. (2012). Least cost path extraction of topographic features for storm impact scale mapping. *Journal of Coastal Research*, *28*(4), 970–978. doi: 10.2112/JCOASTRES-D-11-00126.1

Hemer, M. A., Fan, Y., Mori, N., Semedo, A., & Wang, X. L. (2013). Projected changes in wave climate from a multi-model ensemble. *Nature Climate Change 2013 3:5*, *3*(5), 471–476. doi: 10.1038/nclimate1791

Hesp, P. A. (2013). A 34 year record of foredune evolution, Dark Point, NSW, Australia. *Journal of Coastal Research*, *165*(65 (10065)), 1295–1300. doi: 10.2112/si65-219.1

Hinton, C., & Nicholls, R. J. (1998). Spatial and Temporal Behaviour of Depth of Closure along the Holland Coast. *Proceedings of the Coastal Engineering Conference*, *3*, 2913–2925. doi: 10.1061/9780784404119.221

Hoonhout, B., & de Vries, S. (2016). A process-based model for aeolian sediment transport and spatiotemporal varying sediment availability. *Journal of Geophysical Research: Earth Surface*, *121*(8), 1555–1575. doi: 10.1002/2015JF003692

Hoonhout, B., & de Vries, S. (2017). Field measurements on spatial variations in aeolian sediment availability at the Sand Motor mega nourishment. *Aeolian Research*. doi: 10.1016/j.aeolia.2016.12.003

Hoonhout, B., & de Vries, S. (2019). Simulating spatiotemporal aeolian sediment supply at a mega nourishment. *Coastal Engineering*, *145*, 21–35. doi: 10.1016/j.coastaleng.2018.12.007

Houser, C. (2009). Synchronization of transport and supply in beach-dune interaction. *Progress in Physical Geography*, *33*(6), 733–746. doi: 10.1177/0309133309350120

Houser, C. (2013). Alongshore variation in the morphology of coastal dunes: Implications for storm response. *Geomorphology*, *199*, 48–61. doi: 10.1016/j.geomorph.2012.10.035

Houser, C., Wernette, P., Rentschlar, E., Jones, H., Hammond, B., & Trimble, S. (2015). Post-storm beach and dune recovery: Implications for barrier island resilience. *Geomorphology*, *234*, 54–63. doi: 10.1016/J.GEOMORPH.2014.12.044

Houston, J. R. (2015). Shoreline Response to Sea-Level Rise on the Southwest Coast of Florida. *Journal of Coastal Research*, *31*(4), 777–789. doi: 10.2112/JCOASTRES-D-14-00161.1

Hovenga, P. A., Ruggiero, P., Goldstein, E. B., Hacker, S. D., & Moore, L. J. (2021). The relative role of constructive and destructive processes in dune evolution on Cape Lookout National Seashore, North Carolina, USA. *Earth Surface Processes and Landforms*, *46*(14), 2824–2840. doi: 10.1002/ESP.5210

Huisman, B. J., de Schipper, M. A., & Ruessink, B. G. (2016). Sediment sorting at the Sand Motor at storm and annual time scales. *Marine Geology*, *381*, 209–226. doi: 10.1016/J.MARGEO.2016.09.005

Itzkin, M., Moore, L. J., Ruggiero, P., & Hacker, S. D. (2020). The effect of sand fencing on the morphology of natural dune systems. *Geomorphology*, *352*. doi: 10 .1016/j.geomorph.2019.106995

Itzkin, M., Moore, L. J., Ruggiero, P., Hovenga, P. A., & Hacker, S. D. (2022). Combining process-based and data-driven approaches to forecast beach and dune change. *Environmental Modelling and Software*, *153*, 105404. doi: 10.1016/j.envsoft .2022.105404

Jackson, N. L., Masselink, G., & Nordstrom, K. F. (2004). The role of bore collapse and local shear stresses on the spatial distribution of sediment load in the uprush of an intermediate-state beach. *Marine Geology*, *203*(1-2), 109–118. doi: 10.1016/ S0025-3227(03)00328-1

Jackson, N. L., & Nordstrom, K. F. (1993). Depth of activation of sediment by plunging breakers on a steep sand beach. *Marine Geology*, *115*(1-2), 143–151. doi: 10.1016/0025-3227(93)90079-B

Jackson, N. L., Sherman, D., & Hesp, P. (2006). Small-scale spatial variations in aeolian sediment transport on a fine-sand beach. *Journal of Coastal Research - Special Issue 39*, *I*(39), 379–383.

Katsman, C. A., Sterl, A., Beersma, J. J., Van Den Brink, H. W., Church, J. A., Hazeleger, W., … Kopp, R. E. (2011). Exploring high-end scenarios for local sea level rise to develop flood protection strategies for a low-lying delta-the Netherlands as an example. *Climatic Change*, *109*, 617–645. doi: 10.1007/s10584-011-0037-5

Kawamura, R. (1951). Study on sand movement by wind. *Rept. Inst. Sci. Technol.*(5), 95–112.

Keijsers, J. G., De Groot, A. V., & Riksen, M. J. (2015). Vegetation and sedimentation on coastal foredunes. *Geomorphology*. doi: 10.1016/j.geomorph.2014.10.027

Keijsers, J. G., Poortinga, A., Riksen, M. J., & Maroulis, J. (2014). Spatio-temporal variability in accretion and erosion of coastal foredunes in the Netherlands: Regional climate and local topography. *PLoS ONE*. doi: 10.1371/journal.pone.0091115

Kriebel, D. L., & Dean, R. G. (1985). Numerical simulation of time-dependent beach and dune erosion. *Coastal Engineering*, *9*(3), 221–245. doi: 10.1016/0378 -3839(85)90009-2

Kroon, A., de Schipper, M., de Vries, S., & Aarninkhof, S. (2022). Subaqueous and Subaerial Beach Changes after Implementation of a Mega Nourishment in Front of a Sea Dike. *Journal of Marine Science and Engineering 2022, Vol. 10, Page 1152*, *10*(8), 1152. doi: 10.3390/JMSE10081152

Kroy, K., Sauermann, G., & Herrmann, H. J. (2002). Minimal model for sand dunes. *Physical Review Letters*, *88*(5), 543011–543014. doi: 10.1103/PhysRevLett.88 .054301

Krumbein, W. C. (1934). Size frequency distributions of sediments. *Journal of Sedimentary Research*, *4*(2), 65–77. doi: 10.1306/D4268EB9-2B26-11D7 -8648000102C1865D

Kurtböke, D. I., Neller, R. J., & Bellgard, S. E. (2007). Mesophilic actinomycetes in the

natural and reconstructed sand dune vegetation zones of Fraser Island, Australia. *Microbial Ecology*, *54*(2), 332–340. doi: 10.1007/s00248-007-9207-4

Laporte-Fauret, Q., Lubac, B., Castelle, B., Michalet, R., Marieu, V., Bombrun, L., … Rosebery, D. (2020). Classification of Atlantic coastal sand dune vegetation using in situ, UAV, and airborne hyperspectral data. *Remote Sensing*, *12*(14). doi: 10.3390/rs12142222

Larson, M., & Kraus, N. C. (1994). Temporal and spatial scales of beach profile change, Duck, North Carolina. *Marine Geology*, *117*(1-4), 75–94. doi: 10.1016/0025-3227(94)90007-8

Lettau, K., & Lettau, H. (1978). Experimental and micrometeorological field studies of dune migration. In K. Lettau & H. Lettau (Eds.), *Exploring the world's driest climate* (pp. 110–147). Center for Climatic Research, University of Wisconsin-Madison.

Li, S. H., & Hong, H. P. (2015). Observations on a Hurricane Wind Hazard Model Used to Map Extreme Hurricane Wind Speed. *Journal of Structural Engineering*, *141*(10). doi: 10.1061/(ASCE)ST.1943-541X.0001217

Liu, Y., Liu, X., & Sun, Y. (2021). QGrain: An open-source and easy-to-use software for the comprehensive analysis of grain size distributions. *Sedimentary Geology*, *423*, 105980. doi: 10.1016/J.SEDGEO.2021.105980

Martínez, M. L., Hesp, P. A., & Gallego-Fernández, J. B. (2013). Coastal Dune Restoration: Trends and Perspectives. In *Restoration of coastal dunes* (pp. 323–339). Springer, Berlin, Heidelberg. doi: 10.1007/978-3-642-33445-0{_}20

Martínez, M. L., Maun, M. A., & Psuty, N. P. (2008). The Fragility and Conservation of the World's Coastal Dunes: Geomorphological, Ecological and Socioeconomic Perspectives. In M. L. Martínez & N. Psuty (Eds.), *Coastal dunes ecology and conservation* (pp. 355–369). Springer-Verlag Berlin Heidelberg. doi: 10.1007/978-3-540-74002-5{_}21

Martinho, C. T., Hesp, P. A., & Dillenburg, S. R. (2010). Morphological and temporal variations of transgressive dunefields of the northern and mid-littoral Rio Grande do Sul coast, Southern Brazil. *Geomorphology*, *117*(1-2), 14–32. doi: 10.1016/j.geomorph.2009.11.002

Masselink, G., Auger, N., Russell, P., & O'Hare, T. (2007). Short-term morphological change and sediment dynamics in the intertidal zone of a macrotidal beach. *Sedimentology*, *54*(1), 39–53. doi: 10.1111/j.1365-3091.2006.00825.x

Masselink, G., & Puleo, J. A. (2006). *Swash-zone morphodynamics* (Vol. 26) (No. 5). Pergamon. doi: 10.1016/j.csr.2006.01.015

McCarroll, R. J., Masselink, G., Valiente, N. G., King, E. V., Scott, T., Stokes, C., & Wiggins, M. (2021). An XBeach derived parametric expression for headland bypassing. *Coastal Engineering*, *165*, 103860. doi: 10.1016/J.COASTALENG.2021.103860

McKenna Neuman, C., & Bédard, O. (2017). A wind tunnel investigation of particle segregation, ripple formation and armouring within sand beds of systematically varied texture. *Earth Surface Processes and Landforms*, *42*(5), 749–762. doi: 10.1002/ESP.4019

McKenna Neuman, C., Li, B., & Nash, D. (2012). Micro-topographic analysis of shell pavements formed by aeolian transport in a wind tunnel simulation.

Journal of Geophysical Research: Earth Surface, *117*(F4), 4003. doi: 10.1029/2012JF002381

Medina, R., Losada, M. A., Losada, I. J., & Vidal, C. (1994). Temporal and spatial relationship between sediment grain size and beach profile. *Marine Geology*, *118*(3-4), 195–206. doi: 10.1016/0025-3227(94)90083-3

Mehrtens, B., Lojek, O., Kosmalla, V., Bölker, T., & Goseberg, N. (2023). Foredune growth and storm surge protection potential at the Eiderstedt Peninsula, Germany. *Frontiers in Marine Science*, *9*, 1–21. doi: 10.3389/fmars.2022.1020351

Melvin, S. M., Griffin, C. R., & Macivor, L. H. (1991). Recovery strategies for piping plovers in managed coastal landscapes. *Coastal Management*, *19*(1). doi: 10.1080/08920759109362129

Miot da Silva, G., & Hesp, P. (2010). Coastline orientation, aeolian sediment transport and foredune and dunefield dynamics of Moçambique Beach, Southern Brazil. *Geomorphology*, *120*(3-4), 258–278. doi: 10.1016/j.geomorph.2010.03.039

Mitasova, H., Hardin, E., Starek, M. J., Harmon, R. S., Overton, M. F., & Carolina, N. (2011). Landscape dynamics from LiDAR data time series. *Geomorphometry*, 3–6.

Mitasova, H., Overton, M. F., Recalde, J. J., Bernstein, D. J., & Freeman, C. W. (2009). Raster-Based Analysis of Coastal Terrain Dynamics from Multitemporal Lidar Data. *Journal of Coastal Research*, *252*, 507–514. doi: 10.2112/07-0976.1

Moayeri, V., Miri, A., Shahriari, A., Rahdari, V., & Gill, T. E. (2023). A field study of the surface disturbance effects of animals and motor vehicles on aeolian sediment emission from a silty playa surface. *Environmental Research*, *216*, 114606. doi: 10.1016/J.ENVRES.2022.114606

Muller, J., Figlus, J., & Vries, S. d. (2018). XBeach simulation of hybrid coastal protection: a Galveston seawall test case. *Coastal Engineering Proceedings*, *1*(36), papers.100. doi: 10.9753/icce.v36.papers.100

Nield, J. M., & Wiggs, G. F. (2011, 2). The application of terrestrial laser scanning to aeolian saltation cloud measurement and its response to changing surface moisture. *Earth Surface Processes and Landforms*, *36*(2), 273–278. doi: 10.1002/ESP.2102

Nield, J. M., Wiggs, G. F., & Squirrell, R. S. (2011). Aeolian sand strip mobility and protodune development on a drying beach: Examining surface moisture and surface roughness patterns measured by terrestrial laser scanning. *Earth Surface Processes and Landforms*, *36*(4), 513–522. doi: 10.1002/esp.2071

Nordstrom, K. F., Lampe, R., & Vandemark, L. M. (2000). Reestablishing naturally functioning dunes on developed coasts. *Environmental Management*, *25*(1), 37–51. doi: 10.1007/S002679910004/METRICS

O'Dea, A., Brodie, K. L., & Hartzell, P. (2019). Continuous coastal monitoring with an automated terrestrial lidar scanner. *Journal of Marine Science and Engineering*, *7*(2). doi: 10.3390/jmse7020037

Ojeda, E., Ruessink, B. G., & Guillen, J. (2008). Morphodynamic response of a two-barred beach to a shoreface nourishment. *Coastal Engineering*, *55*(12), 1185–1196. doi: 10.1016/j.coastaleng.2008.05.006

Okin, G. S. (2008). A new model of wind erosion in the presence of vegetation.

Journal of Geophysical Research: Earth Surface, *113*(F2), 2–10. doi: 10.1029/2007JF000758

Osborne, P. D., & Rooker, G. A. (1999). Sand re-suspension events in a high energy infragravity swash zone. *Journal of Coastal Research*, *15*(1), 74–86.

Owen, P. R. (1964). Saltation of uniform grains in air. *Journal of Fluid Mechanics*, *20*(2), 225–242. doi: 10.1017/S0022112064001173

Palmsten, M. L., & Holman, R. A. (2012). Laboratory investigation of dune erosion using stereo video. *Coastal Engineering*, *60*(1), 123–135. doi: 10.1016/J.COASTALENG.2011.09.003

Pellón, E., de Almeida, L. R., González, M., & Medina, R. (2020). Relationship between foredune profile morphology and aeolian and marine dynamics: A conceptual model. *Geomorphology*, *351*, 106984. doi: 10.1016/j.geomorph.2019.106984

Phillips, M. S., Blenkinsopp, C. E., Splinter, K. D., Harley, M. D., & Turner, I. L. (2019). Modes of Berm and Beachface Recovery Following Storm Reset: Observations Using a Continuously Scanning Lidar. *Journal of Geophysical Research: Earth Surface*, *124*(3), 720–736. doi: 10.1029/2018JF004895

Pickart, A. J., Maslach, W. R., Parsons, L. S., Jules, E. S., Reynolds, C. M., & Goldsmith, L. M. (2021). Comparing Restoration Treatments and Time Intervals to Determine the Success of Invasive Species Removal at Three Coastal Dune Sites in Northern California, U.S.A. *Journal of Coastal Research*, *37*(3), 557–567. doi: 10.2112/JCOASTRES-D-20-00085.1

Pontee, N. (2013). Defining coastal squeeze: A discussion. *Ocean & Coastal Management*, *84*, 204–207. doi: 10.1016/J.OCECOAMAN.2013.07.010

Poppema, D. W., Wijnberg, K. M., Mulder, J. P., Vos, S. E., & Hulscher, S. J. (2021). The effect of building geometry on the size of aeolian deposition patterns: Scale model experiments at the beach. *Coastal Engineering*, *168*, 103866. doi: 10.1016/J.COASTALENG.2021.103866

Prodger, S., Russell, P., & Davidson, M. (2017). Grain-size distributions on high-energy sandy beaches and their relation to wave dissipation. *Sedimentology*, *64*(5), 1289–1302. doi: 10.1111/sed.12353

Ranasinghe, R. (2016). Assessing climate change impacts on open sandy coasts: A review. *Earth-Science Reviews*, *160*, 320–332. doi: 10.1016/J.EARSCIREV.2016.07.011

Ranasinghe, R., Callaghan, D., & Stive, M. J. (2012, 2). Estimating coastal recession due to sea level rise: Beyond the Bruun rule. *Climatic Change*, *110*(3-4), 561–574. doi: 10.1007/s10584-011-0107-8

Reeves, I. R., Moore, L. J., Murray, A. B., Anarde, K. A., & Goldstein, E. B. (2021). Dune Dynamics Drive Discontinuous Barrier Retreat. *Geophysical Research Letters*, *48*(13), e2021GL092958. doi: 10.1029/2021GL092958

Reniers, A. J. H. M., Gallagher, E. L., MacMahan, J. H., Brown, J. A., van Rooijen, A. A., van Thiel de Vries, J. S. M., & van Prooijen, B. C. (2013). Observations and modeling of steep-beach grain-size variability. *Journal of Geophysical Research: Oceans*, *118*(2), 577–591. doi: 10.1029/2012JC008073

Reyes-Martínez, M. J., Ruíz-Delgado, M. C., Sánchez-Moyano, J. E., & García-García,

F. J. (2015). Response of intertidal sandy-beach macrofauna to human trampling: An urban vs. natural beach system approach. *Marine Environmental Research*, *103*, 36–45. doi: 10.1016/J.MARENVRES.2014.11.005

Rodriguez, A. B., & Meyer, C. T. (2006). Sea-level variation during the holocene deduced from the morphologic and stratigraphic evolution of Morgan Peninsula, Alabama, U.S.A. *Journal of Sedimentary Research*, *76*(2), 257–269. doi: 10.2110/jsr.2006.018

Roelvink, D., & Costas, S. (2019). Coupling nearshore and aeolian processes: XBeach and duna process-based models. *Environmental Modelling and Software*, *115*, 98–112. doi: 10.1016/j.envsoft.2019.02.010

Roelvink, D., Reniers, A., van Dongeren, A., van Thiel de Vries, J., McCall, R., & Lescinski, J. (2009). Modelling storm impacts on beaches, dunes and barrier islands. *Coastal Engineering*. doi: 10.1016/j.coastaleng.2009.08.006

Rosati, J. D., Dean, R. G., & Walton, T. L. (2013). The modified Bruun Rule extended for landward transport. *Marine Geology*, *340*, 71–81. doi: 10.1016/j.margeo.2013.04.018

Rozé, F., & Lemauviel, S. (2004). Sand Dune Restoration in North Brittany, France: A 10-Year Monitoring Study. *Restoration Ecology*, *12*(1), 29–35. doi: 10.1111/J.1061-2971.2004.00264.X

Rubin, D. M. (2004). A Simple Autocorrelation Algorithm for Determining Grain Size from Digital Images of Sediment. *Journal of Sedimentary Research*, *74*(1), 160–165. doi: 10.1306/052203740160

Ruessink, B. G., Arens, S. M., Kuipers, M., & Donker, J. J. (2018). Coastal dune dynamics in response to excavated foredune notches. *Aeolian Research*, *31*, 3–17. doi: 10.1016/j.aeolia.2017.07.002

Ruessink, B. G., & Jeuken, M. C. (2002). Dunefoot dynamics along the Dutch coast. *Earth Surface Processes and Landforms*, *27*(10), 1043–1056. doi: 10.1002/esp.391

Ruggiero, P., Komar, P. D., & Allan, J. C. (2010). Increasing wave heights and extreme value projections: The wave climate of the U.S. Pacific Northwest. *Coastal Engineering*, *57*(5), 539–552. doi: 10.1016/J.COASTALENG.2009.12.005

Ruggiero, P., Komar, P. D., Mcdougal, W. G., & Beach, R. A. (1996). Chapter 216 Extreme Water Levels , Wave Runup and. *Coastal Engineering*, 2793–2805.

Sallenger, A. H. (1979). Inverse grading and hydraulic equivalence in grain-flow deposits. *Journal of Sedimentary Research*, *49*(2), 553–562. doi: 10.1306/212F7789-2B24-11D7-8648000102C1865D

Sarre, R. D. (1987). Aeolian sand transport. *Progress in Physical Geography*, *11*(2), 157–182. doi: 10.1177/030913338701100201/ASSET/030913338701100201.FP.PNG{_}V03

Sauermann, G., Kroy, K., & Herrmann, H. J. (2001). Continuum saltation model for sand dunes. *Physical Review E - Statistical Physics, Plasmas, Fluids, and Related Interdisciplinary Topics*, *64*(3), 10. doi: 10.1103/PhysRevE.64.031305

Schlacher, T. A., Lucrezi, S., Connolly, R. M., Peterson, C. H., Gilby, B. L., Maslo, B., … Schoeman, D. S. (2016). Human threats to sandy beaches: A meta-analysis of ghost crabs illustrates global anthropogenic impacts. *Estuarine, Coastal and*

Shelf Science, *169*, 56–73. doi: 10.1016/J.ECSS.2015.11.025

Semedo, A., Weisse, R., Behrens, A., Sterl, A., Bengtsson, L., & Günther, H. (2012). Projection of Global Wave Climate Change toward the End of the Twenty-First Century. *Journal of Climate*, *26*(21), 8269–8288. doi: 10.1175/JCLI-D-12-00658.1

Sherman, D. J. (1992). An equilibrium relationship for shear velocity and apparent roughness length in aeolian saltation. *Geomorphology*, *5*, 419–431.

Sherman, D. J., & Li, B. (2012). Predicting aeolian sand transport rates: A reevaluation of models. *Aeolian Research*. doi: 10.1016/j.aeolia.2011.06.002

Sherman, D. J., Short, A., & Takeda, I. (1993). Sediment mixing-depth and bedform migration in rip channels. *Journal of coastal research*, *15*, 39–48.

Slangen, A. B. A., Carson, M., Katsman, C. A., van de Wal, R. S. W., Köhl, A., Vermeersen, L. L. A., & Stammer, D. (2014). Projecting twenty-first century regional sea-level changes. *Climatic Change*, *124*(1-2), 317–332. doi: 10.1007/S10584-014-1080-9

Slinger, J., Stive, M., & Luijendijk, A. (2021). Nature-Based Solutions for Coastal Engineering and Management. *Water 2021, Vol. 13, Page 976*, *13*(7), 976. doi: 10.3390/W13070976

Smit, Y., Ruessink, G., Brakenhoff, L. B., & Donker, J. J. (2018). Measuring spatial and temporal variation in surface moisture on a coastal beach with a near-infrared terrestrial laser scanner. *Aeolian Research*, *31*, 19–27. doi: 10.1016/j.aeolia.2017.07.004

Smith, A., Houser, C., Lehner, J., George, E., & Lunardi, B. (2020). Crowd-sourced identification of the beach-dune interface. *Geomorphology*, *367*, 107321. doi: 10.1016/j.geomorph.2020.107321

Sonu, C. J. (1972). Bimodal Composition and Cyclic Characteristics of Beach Sediment in Continuously Changing Profiles. *SEPM Journal of Sedimentary Research*, *42*(4), 852–857. doi: 10.1306/74d72653-2b21-11d7-8648000102c1865d

Splinter, K. D., Kearney, E. T., & Turner, I. L. (2018). Drivers of alongshore variable dune erosion during a storm event: Observations and modelling. *Coastal Engineering*, *131*, 31–41. doi: 10.1016/J.COASTALENG.2017.10.011

Srisuwan, C., Work, P. A., Karasu, S., & Özölçer, I. H. (2015). Beach Profile Model with Size-Selective Sediment Transport. I: Laboratory Experiment and Sensitivity Study. *Journal of Waterway, Port, Coastal, and Ocean Engineering*, *141*(2), 04014032. doi: 10.1061/(ASCE)WW.1943-5460.0000255

Stauble, D. K., & Cialone, M. A. (1997). Sediment Dynamics and Profile Interactions: DUCK94. *Proceedings of the Coastal Engineering Conference*, *4*, 3921–3934. doi: 10.1061/9780784402429.303

Stive, M. J., & de Vriend, H. J. (1995). Modelling shoreface profile evolution. *Marine Geology*, *126*(1-4), 235–248. doi: 10.1016/0025-3227(95)00080-I

Stockdon, H. F., Sallenger, A. H., Holman, R. A., & Howd, P. A. (2007). A simple model for the spatially-variable coastal response to hurricanes. *Marine Geology*, *238*(1-4), 1–20. doi: 10.1016/j.margeo.2006.11.004

Strypsteen, G., Houthuys, R., & Rauwoens, P. (2019). Dune Volume Changes at Decadal Timescales and Its Relation with Potential Aeolian Transport. *Journal of Marine Science and Engineering 2019, Vol. 7, Page 357*, *7*(10), 357. doi: 10.3390/

JMSE7100357

Strypsteen, G., van Rijn, L. C., Hoogland, M. D., Rauwoens, P., Fordeyn, J., Hijma, M. P., & Lodder, Q. J. (2021). Reducing aeolian sand transport and beach erosion by using armour layer of coarse materials. *Coastal Engineering*, *166*, 378–3839. doi: 10.1016/J.COASTALENG.2021.103871

Swann, C., Lee, D., Trimble, S., & Key, C. (2021). Aeolian sand transport over a wet, sandy beach. *Aeolian Research*, *51*, 100712. doi: 10.1016/J.AEOLIA.2021.100712

Sytnik, O., & Stecchi, F. (2015). Disappearing coastal dunes: tourism development and future challenges, a case-study from Ravenna, Italy. *Journal of Coastal Conservation*, *19*(5), 715–727. doi: 10.1007/S11852-014-0353-9/TABLES/3

Thieler, E. R., Pilkey, O. H., Young, R. S., Bush, D. M., & Chai, F. (2000). The use of mathematical models to predict beach behavior for U.S. coastal engineering: A critical review. *Journal of Coastal Research*, *16*(1), 48–70.

Tillotson, K., & Komar, P. D. (1997). The wave climate of the Pacific Northwest (Oregon and Washington): A comparison of data sources. *Journal of Coastal Research*, *13*(2), 440–452.

Twenhofel, W. H. (1946). *Mineralogical and physical composition of the sands of the Oregon coast from Coos Bay to the mouth of the Columbia River* (Tech. Rep.). Portland: State of Oregon, Department of Geology and Mineral Industrie.

Uphues, C. F. K., IJzendoorn, C. O. v., Hallin, C., Pearson, S. G., Prooijen, B. C. v., Silva, G. M. d., & de Vries, S. (2022). Coastal aeolian sediment transport in an Active Bed Surface Layer: tracer study and conceptual model. *Earth Surface Processes and Landforms*. doi: 10.1002/ESP.5449

Van Der Meulen, F., & Udo De Haes, H. A. (1996). Nature conservation and integrated coastal zone management in Europe: Present and future. *Landscape and Urban Planning*, *34*(3-4), 401–410. doi: 10.1016/0169-2046(95)00234-0

Van Der Spek, A. J., & Lodder, Q. (2015). A New Sediment Budget for the Netherlands; the Effects of 15 Years of Nourishing (1991-2005). In J. Cheng, J. Rosati, & P. Wang (Eds.), *The proceedings of the coastal sediments 2015* (pp. 1–12). San Diego, California, USA: World Scientific Pub Co Pte Lt. doi: 10.1142/9789814689977{_}0074

van der Wal, D. (2000a). Grain-size-selective aeolian sand transport on a nourished beach. *Journal of Coastal Research*, *16*(3).

van der Wal, D. (2000b). Modelling aeolian sand transport and morphological development in two beach nourishment areas. *Earth Surface Processes and Landforms*, *25*(1), 77–92. doi: 10.1002/(SICI)1096-9837(200001)25:1<77::AID-ESP49>3.0.CO;2-M

Van der Zanden, J., Van der A, D. A., Hurther, D., Cáceres, I., O'Donoghue, T., Hulscher, S. J., & Ribberink, J. S. (2017). Bedload and suspended load contributions to breaker bar morphodynamics. *Coastal Engineering*, *129*, 74–92. doi: 10.1016/J.COASTALENG.2017.09.005

Van Dijk, P. M., Arens, S. M., & Van Boxel, J. H. (1999). Aeolian processes across transverse dunes. II: Modelling the sediment transport and profile development. *Earth Surface Processes and Landforms*, *24*, 319–333.

van IJzendoorn, C. O. (2023). *Python code for the analysis of AeoLiS grain size scenarios (Version 1.1.0) [Software]*. 4TU Repository. doi: 10.4121/22220134

van IJzendoorn, C. O., Hallin, C., Cohn, N., Reniers, A. J., & de Vries, S. (2022). Novel sediment sampling method provides new insights into vertical grain size variability due to marine and aeolian beach processes. *Earth Surface Processes and Landforms*. doi: 10.1002/ESP.5518

Van Rijn, L. C. (2014). A simple general expression for longshore transport of sand, gravel and shingle. *Coastal Engineering*, *90*, 23–39. doi: 10.1016/J.COASTALENG.2014.04.008

van Rijn, L. C., & Strypsteen, G. (2020). A fully predictive model for aeolian sand transport. *Coastal Engineering*, *156*, 103600. doi: 10.1016/J.COASTALENG.2019.103600

Vellinga, P. (1982). Beach and dune erosion during storm surges. *Coastal Engineering*, *6*(4), 361–387. doi: 10.1016/0378-3839(82)90007-2

Vitousek, S., Barnard, P. L., Limber, P., Erikson, L., & Cole, B. (2017). A model integrating longshore and cross-shore processes for predicting long-term shoreline response to climate change. *Journal of Geophysical Research: Earth Surface*, *122*(4), 782–806. doi: 10.1002/2016JF004065

Vos, S., Anders, K., Kuschnerus, M., Lindenbergh, R., Höfle, B., Aarninkhof, S., & de Vries, S. (2022). A high-resolution 4D terrestrial laser scan dataset of the Kijkduin beach-dune system, The Netherlands. *Scientific Data 2022 9:1*, *9*(1), 1–11. doi: 10.1038/s41597-022-01291-9

Voulgaris, G., & Collins, M. B. (2000). Sediment resuspension on beaches: response to breaking waves. *Marine Geology*, *167*(1-2), 167–187. doi: 10.1016/S0025-3227(00)00025-6

Vousdoukas, M. I., Almeida, L. P., & Ferreira, Ó. (2011). Modelling storm-induced beach morphological change in a meso-tidal, reflective beach using XBeach. *Journal of Coastal Research*(64), 1916–1920.

Vousdoukas, M. I., Ranasinghe, R., Mentaschi, L., Plomaritis, T. A., Athanasiou, P., Luijendijk, A., & Feyen, L. (2020). Sandy coastlines under threat of erosion. *Nature Climate Change*, *10*(3), 260–263. doi: 10.1038/s41558-020-0697-0

Walker, I. J., Davidson-Arnott, R. G., Bauer, B., Hesp, P. A., Delgado-Fernandez, I., Ollerhead, J., & Smyth, T. A. (2017). *Scale-dependent perspectives on the geomorphology and evolution of beach-dune systems* (Vol. 171). doi: 10.1016/j.earscirev.2017.04.011

Walker, I. J., Hesp, P. A., Davidson-Arnott, R. G., & Ollerhead, J. (2006). Topographic steering of alongshore airflow over a vegetated foredune: Greenwich Dunes, Prince Edward Island, Canada. *Journal of Coastal Research*, *22*(5), 1278–1291. doi: 10.2112/06A-0010.1

Weng, W. S., Hunt, J. C. R., Carruthers, D. J., Warren, A., Wiggs, G. F. S., Livingstone, I., & Castro, I. (1991). Air flow and sand transport over sand-dunes. In *Aeolian grain transport: The erosional environment* (Vol. 2, pp. 1–22). Vienna: Springer. doi: 10.1007/978-3-7091-6703-8{_}1

Wernette, P., Houser, C., & Bishop, M. P. (2016). An automated approach for extracting Barrier Island morphology from digital elevation models. *Geomorphology*, *262*,

1–7. doi: 10.1016/j.geomorph.2016.02.024

Wernette, P., Thompson, S., Eyler, R., Taylor, H., Taube, C., Medlin, A., … Houser, C. (2018). Defining Dunes: Evaluating How Dune Feature Definitions Affect Dune Interpretations from Remote Sensing. *Journal of Coastal Research*, *34*(6), 1460–1470. doi: 10.2112/JCOASTRES-D-17-00082.1

Wiggs, G. F., Baird, A. J., & Atherton, R. J. (2004). The dynamic effects of moisture on the entrainment and transport of sand by wind. *Geomorphology*. doi: 10.1016/j.geomorph.2003.09.002

Wiggs, G. F., & Weaver, C. M. (2012). Turbulent flow structures and aeolian sediment transport over a barchan sand dune. *Geophysical Research Letters*, *39*(5), 5404. doi: 10.1029/2012GL050847

Wijnberg, K. M., & Terwindt, J. H. (1995). Extracting decadal morphological behaviour from high-resolution, long-term bathymetric surveys along the Holland coast using eigenfunction analysis. *Marine Geology*, *126*(1-4), 301–330. doi: 10.1016/0025-3227(95)00084-C

Wright, L. D., & Short, A. D. (1984). Morphodynamic variability of surf zones and beaches: A synthesis. *Marine Geology*, *56*(1-4), 93–118. doi: 10.1016/0025-3227(84)90008-2

Yasso, W. E., & Hartman, E. M. (1972). Rapid field technique using spray adhesive to obtain peels of unconsolidated sediment. *Sedimentology*, *19*(3-4), 295–298. doi: 10.1111/j.1365-3091.1972.tb00026.x

Yokokawa, M., & Masuda, F. (1991). Tidal influence on foreshore deposits, Pacific coast of Japan. *Clastic tidal sedimentology*.

Zhang, P., Sherman, D. J., & Li, B. (2021). Aeolian creep transport: A review. *Aeolian Research*, *51*, 100711. doi: 10.1016/J.AEOLIA.2021.100711

Zhang, W., Zhao, J., Chen, M., Chen, Y., Yan, K., Li, L., … Chu, Q. (2015). Registration of optical imagery and LiDAR data using an inherent geometrical constraint. *Optics Express*, *23*(6), 7694. doi: 10.1364/OE.23.007694

Zhenlin Li, M., & Komar, P. D. (1992). Longshore grain sorting and beach placer formation adjacent to the Columbia River. *Journal of Sedimentary Research*, *62*(3), 429–441. doi: 10.1306/D426791A-2B26-11D7-8648000102C1865D

A

Supplementary Figure for "Sea level rise outpaced by vertical dune toe translation"

This appendix was published as supplementary information for the following article (Chapter 3):

C.O. van IJzendoorn, S. de Vries, C. Hallin, P.A. Hesp. Sea level rise outpaced by vertical dune toe translation on prograding coasts. *Scientific Reports* 11, 12792 (2021).

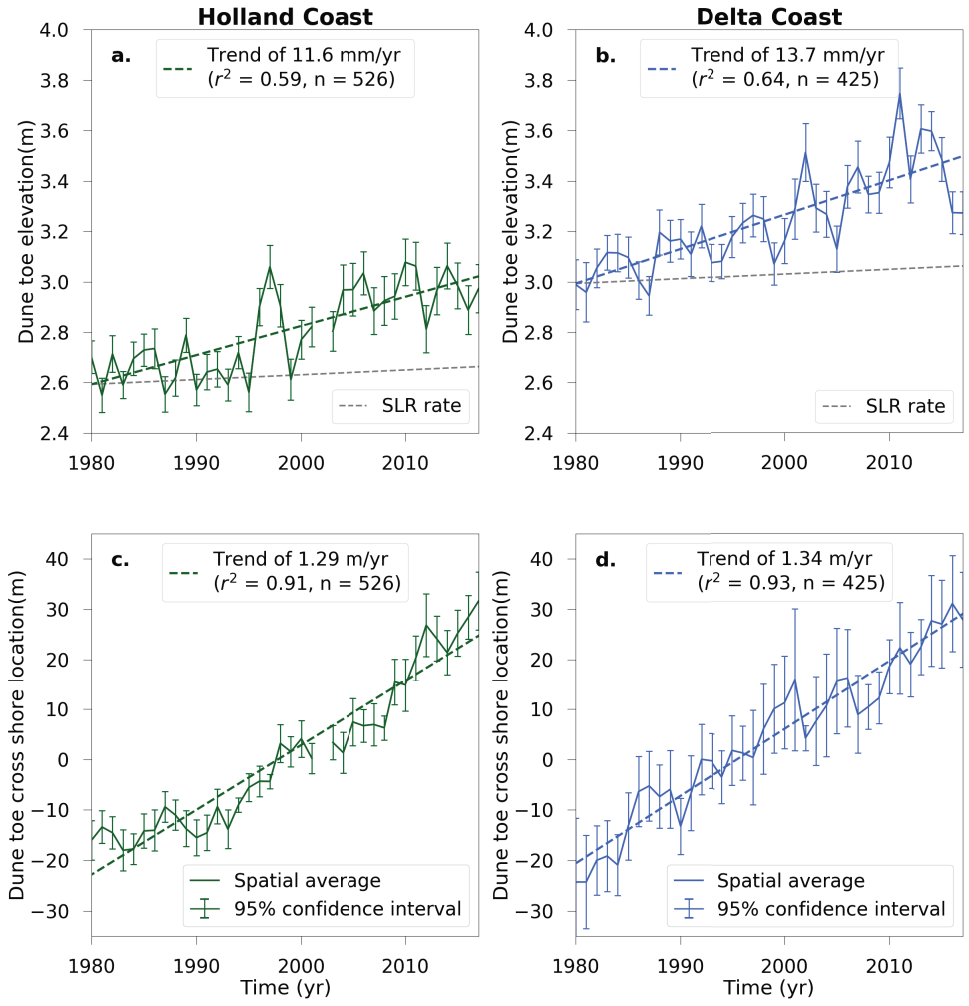

Figure A.1: **Trends in the dune toe position along the Holland coast (a and c) and Delta coast (b and d) extracted using the machine learning method of pybeach.** The trend in dune toe elevation (a and b), and the trend in cross-shore dune toe location (c and d) are shown. In each subplot, the spatial average of all transects along the coast is represented by the solid line. The vertical bars along this line show the 95% confidence interval for each year. The overall trend in the spatial average is represented by the dashed line. In each subplot, the rate (in m/yr), r-squared value and number of transect locations (n) of this trend are given in the upper left corner. The grey dashed lines in subplots a and b show the development of the dune toe elevation if it had increased at the same rate as sea level rise (SLR).

About the author

Christa van IJzendoorn was born on the 18th of June 1995. Her interest in coasts and rivers might have already started before her birth, when her parents needed to evacuate during a high water event in January of 1995. Throughout her youth, Christa and her family moved several times, although they did stick to the provinces of Utrecht and Gelderland in the Netherlands. Towards the end of high school in Gorinchem, her interest in earth system processes was cemented. Through a BSc and MSc degree from Utrecht University, she specialized in physical geography and came in first contact with the coastal field. After working at the Flood Risk Management department of Deltares for nine months, she started a PhD in coastal engineering at Delft University of Technology. She is now proud to call herself a coastal researcher, and studies aeolian sand transport to better understand coastal dune development and to improve the implementation of nature based solutions. In the Fall of 2023, she will start a postdoc at Oregon State University in the United States.

Personalia

Christa Ottie van IJzendoorn
18 June 1995, 's-Hertogenbosch, the Netherlands

Education

2016-2018 MSc Physical Geography (*cum laude*), Utrecht University
Thesis: Monitoring the bathymetry of the Ameland ebb-tidal delta using X-band radar data

2013-2016 BSc Earth Sciences (*cum laude*), Utrecht University
Thesis: The control of beach and dune characteristics on local coastal dune erosion and accretion

2007-2013 VWO N&T (*cum laude*), Gymnasium Camphusianum, Gorinchem

Employment

2018-2019 Junior advisor/researcher, Deltares

List of Publications

Peer-reviewed journal articles

First author

4. **van IJzendoorn, C.O.**, Boomaars, K., Vos, S.E., Reniers, A.J.H.M., Kuschnerus, M. & Lindenberg, R. (in preparation). Detection of aeolian sand strips and their characteristics using terrestrial laser scanning.

3. **van IJzendoorn, C.O.**, Hallin, C., Reniers, A.J.H.M. & de Vries, S. (submitted). Modeling multi-fraction coastal aeolian sediment transport with horizontal and vertical grain size variability. Authorea Preprints. https://doi.org/10.22541/essoar.167898491.19162099/v1

2. **van IJzendoorn, C.O.**, Hallin, C., Cohn, N., Reniers, A.J.H.M. & de Vries, S. (2022). Novel sediment sampling method provides new insights into vertical grain size variability due to marine and aeolian beach processes. Earth Surface Processes and Landforms. https://doi.org/10.1002/esp.5518

1. **van IJzendoorn, C.O.**, de Vries, S., Hallin, C., & Hesp, P.A. (2021). Sea level rise outpaced by vertical dune toe translation on prograding coasts. Nature Scientific reports, 11(1), 1-8. https://doi.org/10.1038/s41598-021-92150-x

Co-author

4. de Vries, S., van Westen, B., **van IJzendoorn, C.O.**, Hallin, C., Rauwoens, P. & Cohn. N. (in preparation). AeoLiS – A new model for predicting aeolian sediment transport processes and coastal dune development.

3. Vos, S. & **van IJzendoorn, C.O.** (in preparation). The influence of beach buildings on dune development from small to large spatio-temporal scales.

2. Hallin, C., **van IJzendoorn, C.O.**, Homberger, J.M. & de Vries, S. (in review). Simulating soil moisture on sandy beaches. Submitted to Coastal Engineering.

1. Uphues, C.F.K., **van IJzendoorn, C.O.**, Hallin, C., Pearson, S.G., van Prooijen, B.C., Miot da Silva, G. & de Vries, S. (2022). Coastal aeolian sediment transport in an active bed surface layer: Tracer study and conceptual model. Earth Surface Processes and Landforms, 47(13), 3147-3162. https://doi.org/10.1002/esp.5449

Conference papers

First author

1. **van IJzendoorn, C.O.**, Hallin, & de Vries, S. (2023). Integration of short and long-term

marine and aeolian processes in quantitative coastal dune development predictions. In Coastal Sediments 2023: The Proceedings of the Coastal Sediments 2023 (pp. 753-759).

Co-author

1. Hallin, C., **van IJzendoorn, C.O.**, Skaden, J., de Vries, S. (2023). Evaluation of threshold-based models to account for surface moisture in meso-scale aeolian sediment transport simulations. In Coastal Sediments 2023: The Proceedings of the Coastal Sediments 2023 (pp. 670-683).

Conference contributions and presentations

First author

9. **van IJzendoorn, C.O.**, Hallin, C. & de Vries, S. (2023). Integration of short and long-term marine and aeolian processes in quantitative coastal dune development predictions. 13 April 2023, Coastal Sediments 2023, New Orleans, USA.

8. **van IJzendoorn, C.O.**, Hallin, C., Reniers, A.J.H.N. & de Vries, S. (2023). A framework to unify academic and applied approaches in coastal research and engineering. 31 March 2023, NCK Days, Delft, the Netherlands.

7. **van IJzendoorn, C.O.**, Hallin, C. & de Vries, S. (2022). Implications of spatial grain size variability for aeolian transport. 8 December 2022, International Conference on Coastal Engineering, Sydney, Australia.

6. **van IJzendoorn, C.O.**, Hallin, C. & de Vries, S. (2022). How vertical grain size layering at the beach surface affects aeolian sediment transport, 17 March 2022, NCK Days, Enschede, the Netherlands.

5. **van IJzendoorn, C.O.**, Hallin, C., Vos, S.E., Cohn, N. & de Vries, S. (2021). The effect of marine and aeolian processes on vertical grain size variability in the intertidal area. 1 December 2021, AGU Fall Meeting, New Orleans, USA, virtual.

4. **van IJzendoorn, C.O.**, Hallin, C., Vos, S.E., & de Vries, S. (2021). Grain size dynamics in the intertidal zone: vertical variability due to marine and aeolian processes. Coastal Dynamics 2021, Delft, the Netherlands, virtual.

3. **van IJzendoorn, C.O.**, de Vries, S., & Hallin, C. (2021). Dune toe elevation increase outpaces sea level rise. 25 March 2021, NCK Days, virtual.

2. **van IJzendoorn, C.O.**, de Vries, S., & Hallin, C. (2020). Are the Dutch dunes keeping up with sea level rise? March 2020, NCK Days, canceled due to COVID-19.

1. **van IJzendoorn, C.O.**, de Vries, S., & Hallin, C. (2020). The contribution of aeolian and marine processes to decadal coastal dune evolution along the Dutch coast. 18 February 2020, Ocean Sciences Meeting, San Diego, US.

Co-author

6. Hallin, C., **van IJzendoorn, C.O.**, Skaden, J., de Vries, S. (2023). Evaluation of threshold-based models to account for surface moisture in meso-scale aeolian sediment transport simulations. 14 April 2023, Coastal Sediments 2023, New Orleans, USA.

5. Vos, S., **van IJzendoorn, C.O.**, Kuschnerus, M. & de Vries, S. (2022). The influence of dune pavilions on longer term dune development. 13 April 2022, Building Coastal Resilience 2022, Brugge, Belgium.

4. Uphues, C.F.K., **van IJzendoorn, C.O.**, Miot da Silva, G., Pearson, S.G., & de Vries, S. (2021). Observations of Coastal Aeolian Sediment Transport in an Active Surface Layer using Tracers. 1 December 2021, AGU Fall Meeting New Orleans, USA, virtual.

3. Hallin, C., de Vries, S., & **van IJzendoorn, C.O.** (2020). Enhance dune-building processes with nature-based nourishment design. October 2020, International Conference on Coastal Engineering, virtual.

2. Vos, S., Kuschnerus, K., **van IJzendoorn, C.O.**, di Biase, V., & Breedveld, R. (2020). Scan Experiment 2020. March 2020, NCK Days, canceled due to COVID-19.

1. Hallin, C., de Vries, S., & **van IJzendoorn, C.O.** (2020). Enhance dune-building processes with nature-based nourishment design. Coastal Engineering Proceedings, (36v), 34-34. https://doi.org/10.9753/icce.v36v.management.34

Web-based publications

2. de Vries, S., **van IJzendoorn, C.O.**, Delgado-Fernandez, I., Hesp, P., Ruessink, G. & Wijnberg, K. (28 June 2021). Dune Dynamics Short Course. Zenodo. https://doi.org/10.5281/zenodo.5592230

1. **van IJzendoorn, C.O.** (2021). JAT - Jarkus Analysis Toolbox. https://doi.org/10.4121/14514213

Other publications

2. **van IJzendoorn, C.O.**, Van losse korrel to stevig duin, Geo.Brief, July 2021.

1. **van IJzendoorn, C.O.**, Zijn de Nederlandse stranden en duinen nog te redden? Klimaathelpdesk, 13 March 2021.


THERE
IS
STRENGTH
IN
NUMBERS